Synthesis and Performance Evaluation of Chitosan Based Adsorbent for CO_2 Capture

Keren Osler

A dissertation submitted to the Faculty of Engineering and the Built Environment, University of the Witwatersrand, Johannesburg, in fulfilment of the requirements for the degree of Master of Science in Engineering

Supervisor: Prof M.O. Daramola

Co-supervisor: Dr. O.O. Oluwasina

July 2017

Declaration

I declare that this dissertation is my own unaided work. It is being submitted for the degree of Master of Science in Engineering to the University of the Witwatersrand, Johannesburg, South Africa. It has not been submitted before for any degree or examination to any other University.

……...

(Signature of Candidate)

……day of……2017

(Day) (Month) (Year)

Abstract

Carbon dioxide capture is essential to reducing CO_2 emissions in an attempt to mitigate climate change. Absorption via amine based solvents is currently the mature technology that is applied for the capture of CO_2. However, amines can pose health and environmental risks when emitted into the air from CO_2 capture plants. Furthermore, the efficiency penalty caused by CO_2 capture via absorption and the huge costs associated with the regeneration of the spent amine based solvent poses a threat to the economic viability of CO_2 capture by the absorption process. Adsorption technology is an alternative to absorption technology. Adsorption technology seems promising due to its moderate energy consumption (which stems from the ability to operate at moderate temperatures and pressures) as well as being health and environmentally benign. Recently, extensive research has been conducted on designing adsorbents that have the ability to adsorb large quantities of CO_2 with a low energy consumption. The challenge in CO_2 adsorption technology is to design an adsorbent that is not only non-toxic, biodegradable and cost effective but also has the ability to selectively and efficiently remove CO_2 gas from a mixed gas stream. This study proposes chitosan, a biodegradable, non-toxic polymer, as one such adsorbent. Chitosan has the potential to be a suitable adsorbent for CO_2 capture because it contains the desired amine groups which act as CO_2 adsorption sites.

In this study, chitosan was studied as an adsorbent in order to confirm that it is suitable for CO_2 capture. Chitosan and chitosan impregnated carbon nanotubes (CNTs) (chitosan/MWCNTs) composite adsorbents were synthesized. Chitosan was impregnated onto MWCNTs in order to enhance the physical properties (surface area, pore size and pore volume), CO_2 adsorption capacity and CO_2 affinity of the composite adsorbent. The synthesized materials (chitosan and chitosan/MWCNTs) were characterized and evaluated for CO_2 adsorption.

Chitosan was successfully synthesised from chitin. This was confirmed using FTIR spectroscopy. The synthesised chitosan had desirable properties for CO_2 capture. This was confirmed using TGA and custom built CO_2 adsorption equipment. The synthesised chitosan samples were inexpensive, had the desired amine groups and were thermally suitable at industrial CO_2 capture operational temperatures. The CO_2 adsorption capacity of the synthesised chitosan was generally low when compared with literature. The highest CO_2 adsorption capacity achieved by the synthesised chitosan in this study was 11 gCO_2/kg adsorbent. However, it is important to consider that the polymer is derived from a waste material and as such it is possible to cost effectively utilize a large amount. The amount of CO_2 adsorbed by the synthesised chitosan is dependent on the number of amine groups present.

Against this background this study aimed to increase the number of amine groups present. This was done using response surface methodology (RSM) to develop a polynomial regression model. The developed

polynomial regression model is able to predict the DDA of the synthesised chitosan based on the synthesis variables used. The polynomial model was validated using chitosan from literature and found to be statistically significant. The polynomial model showed the optimum synthesis conditions to yield the highest DDA.

Chitosan was successfully impregnated onto MWCNTs. This was confirmed using FTIR spectroscopy. The synthesised chitosan/MWCNT adsorbent was not suitable for CO_2 capture. This was confirmed using Raman spectroscopy, N_2 physisorption, SEM TGA and custom built CO_2 adsorption equipment. The CO_2 adsorption capacity of the synthesised chitosan/MWCNTs was low when compared to literature. This is attributed to the fact that the MWCNTs used in this study are not suitable as adsorbents for CO_2 capture as they showed a low CO_2 adsorption capacity before chitosan impregnation. However, the CO_2 adsorption capacity of the MWCNTs was improved by 650 % after chitosan impregnation. Reports from literature, where CNTs were impregnated with other amines did not show such a significant increase in CO_2 adsorption capacity. It is hypothesized that if chitosan were impregnated onto more suitable CNTs for CO_2 capture is would improve the CO_2 adsorption capacity of that CNT by 650 %. Thus, yielding a suitable non-toxic, biodegradable adsorbent for CO_2 capture. It is concluded that chitosan possesses properties that make the polymer suitable for use as an adsorbent for CO_2 capture.

Acknowledgments

I would like to acknowledge the efforts of my supervisors, Prof. M. O. Daramola and Dr. O. O. Oluwasina. Thank you for your tremendous knowledge, support and effort during the course of this project. I am truly grateful. I would also like to acknowledge Mr. W. Augustyn from Chemvak for his continuous availability to assist with training and servicing of equipment used in this project. Many thanks go out to Mr. Osler and ABB South Africa for making an ABB gas analyser available for the project.

I would like acknowledge the financial support of the EnPe-NORAD agreement between the University of the Witwatersrand (Wits) and the Norwegian University of Science and Technology, Trondheim (NTNU) for the CO_2 capture project. Furthermore, the financial assistance of the South African Centre for Carbon Capture and Storage towards this research is hereby acknowledged. Opinions expressed and conclusions arrived at, are those of the author and are not necessarily to be attributed to SACCCS.

I would like to send a very warm thanks to my Mom and Dad. They started me on this long academic journey – from pre-school to postgraduate studies. You have given me the freedom and ability to achieve anything I set my mind to. Your love for me and pride in my academic achievements is overwhelming. While I am on the subject of family, I would also like to thank my siblings and friends who are family. You have kept me sane through this study by giving me a welcome distraction when I needed. I love you all for the reasons that I have mentioned and many more.

Lastly, I would like to acknowledge all those that I can't name individually who contributed to this project materially or otherwise. Without you all, this project would not have been a success.

Publications from the Study

A few conference papers and journal have emanated from this research project and are as listed below:

Publications

1. **K.Osler**, D. Dheda, J. Noy, N. Wagner, M.O. Daramola. (2017). Synthesis and Evaluation of Carbon Nanotube Composite Adsorbent for CO_2 Capture: A Comparative Study of CO_2 Adsorption Capacity of Single-Walled and Multi-Walled Carbon Nanotubes. Int. J of Coal Science and Technology. 4(1), 41 - 49. DOI 10.1007/s40789-017-0157-2.

2. **K. Osler**, N. Twala, O. O. Oluwasina, M.O. Daramola, (2017). Synthesis and Performance Evaluation of Chitosan/Carbon nanotube (Chitosan/MWCNT) Composite Adsorbent Carbon Dioxide Capture. Energy Procedia.

3. **K. Osler**, O. O. Oluwasina, M.O. Daramola. Application of Response Surface Methodology (RSM) to the Synthesis of Chitosan Based Adsorbent for Post Combustion CO_2 Capture. *Manuscript in preparation*

Presentations

1. **K. Osler**, D. Dheda, J. Noy, N. Wagner, M.O. Daramola. Synthesis and Evaluation of Carbon Nanotube Composite Adsorbent for CO_2 Capture: A Comparative Study of CO_2 Adsorption Capacity of Single-Walled and Multi-Walled Carbon Nanotubes. **Oral Presentation**. Carbon Capture Workshop, University of the Western Cape, Cape Town, South Africa. March 2015
2. **K. Osler**, D. Dheda, J. Ngoy, N. Wagner, M.O. Daramola. Synthesis and Evaluation of Carbon Nanotube Composite Adsorbent for CO_2 Capture: A Comparative Study of CO_2 Adsorption Capacity of Single-Walled and Multi-Walled Carbon Nanotubes. **Poster Presentation**. Trondheim Carbon Capture and Storage Conference – 8 (TCCS-8), Norwegian University of Science and Technology, Trondheim, Norway. June 2015
3. **K. Osler**, O. O. Oluwasina, M.O. Daramola. Synthesis and Performance Evaluation of a Chitosan Based Adsorbent for Post-Combustion CO_2 Capture. **Oral Presentation**. Cross-Faculty Symposium. University of the Witwatersrand, Johannesburg, South Africa. March 2016.
4. **K. Osler**, O. O. Oluwasina, M.O. Daramola. Synthesis and Performance Evaluation of a Chitosan Based Adsorbent for Post-Combustion CO_2 Capture. **Oral Presentation.** Reps 2016. University of Fort Hare, Fort Hare, South Africa. September 2016

5. **K. Osler**, O. O. Oluwasina, M.O. Daramola. Synthesis and Performance Evaluation of Chitosan/Carbon nanotube (Chitosan/MWCNT) Composite Adsorbent Carbon Dioxide Capture. **Poster Presentation**. GHGT-13. Lausanne, Switzerland. November 2016
6. **K. Osler**, O. O. Oluwasina, M.O. Daramola. Characterisation and Performance Evaluation of a Chitosan Based Adsorbent for CO_2 Capture. **Oral Presentation**. CREW 2016. Vaal University of Technology, Vaal, South Africa. November 2016

Contents

List of Figures

List of Tables

Nomenclature

ANOVA – Analysis of Variance

ASU – Air Separation Unit

BET – Brunauer-Emmett-Teller

CCS – Carbon Capture and Storage

CCD – Central Composite Designs

CMS – Carbon Molecular Sieves

CNT(s) – Carbon Nanotube(s)

CO – Carbon Monoxide

CO_2 – Carbon Dioxide

DDA – Degree of Deacetylation

DF – Degrees of Freedom

DOE – Design of Experiments

EBR – Enhanced Coal Bed Methane Recovery

EOR – Enhanced Oil Recovery

EPA – Environmental Protection Agency

ESA – Electric Swing Adsorption

FTIR – Fourier Transform Infrared Spectroscopy

GHG(s) – Green House Gas(es)

HCl – Hydrochloric Acid

H_2 – Hydrogen

H_2O – Water

H_2S – Hydrogen Sulphide

IEA – International Energy Agency

IPCC – Intergovernmental Panel on Climate Change

MEA – Monoethanol Amine

MOF(s) – Metal Organic Framework(s)

MS – Mean Squares

MWCNT(s) – Multi-Walled Carbon Nanotube(s)

NASA – National Aeronautics and Space Administration

NaOH – Sodium Hydroxide

NH_2 – Amine Functional Group

N_2 - Nitrogen

NOAA – National Oceanic and Atmospheric Administration

O_2 – Oxygen

NO_x – Nitrous Oxides

PEI - Polyethyeneimine

PM – Particulate Matter

PSA – Pressure Swing Adsorption

RSM – Response Surface Methodology

SACCCS – South African Center for Carbon Capture and Storage

SEM – Scanning Electron Microscopy

SO_x – Sulphur Oxides

SO_2 – Sulphur Dioxide

SS – Sum of Squares

SWCNT(s) – Single-Walled Carbon Nanotube(s)

TGA – Thermogravimetric Analysis

TSA – Temperature Swing Adsorption

UN – United Nations

UNFCCC – United Nations Frameworks Convention on Climate Change

USA – United States of America

VSA – Vacuum Swing Adsorption

WGS – Water Gas Shift (Reaction)

Chapter 1 Introduction

1.1. Background and Motivation

The industrial revolution which began in the 18th century and was the start of a global energy dependence. Since then there has been an ever-increasing demand for cheap and reliable energy and energy generation methods. Historically, this method has been the combustion of fossil fuels. Modern methods of energy production that do not utilize fossil fuels, such as nuclear electric power and various types of renewable energy such as solar and wind power have been developed since the industrial revolution. Figure 1.1, produced by the International Energy Agency (IEA) in 2015 and covers a period of 1971 to 2013, compares the energy supplied by fossil fuels to non-fossil fuels worldwide (International Energy Agency, 2015). Non-fossil fuel energy generation methods still do not feature significantly for energy generation. Consider that in 1971, 86 % of energy was produced from fossil fuels and in 2013 this decreased only slightly by 1 % to 82 % (International Energy Agency, 2015). Despite the development of non-fossil fuel energy generation methods, there has not been a significant reduction in the proportion of energy supplied by fossil fuels.

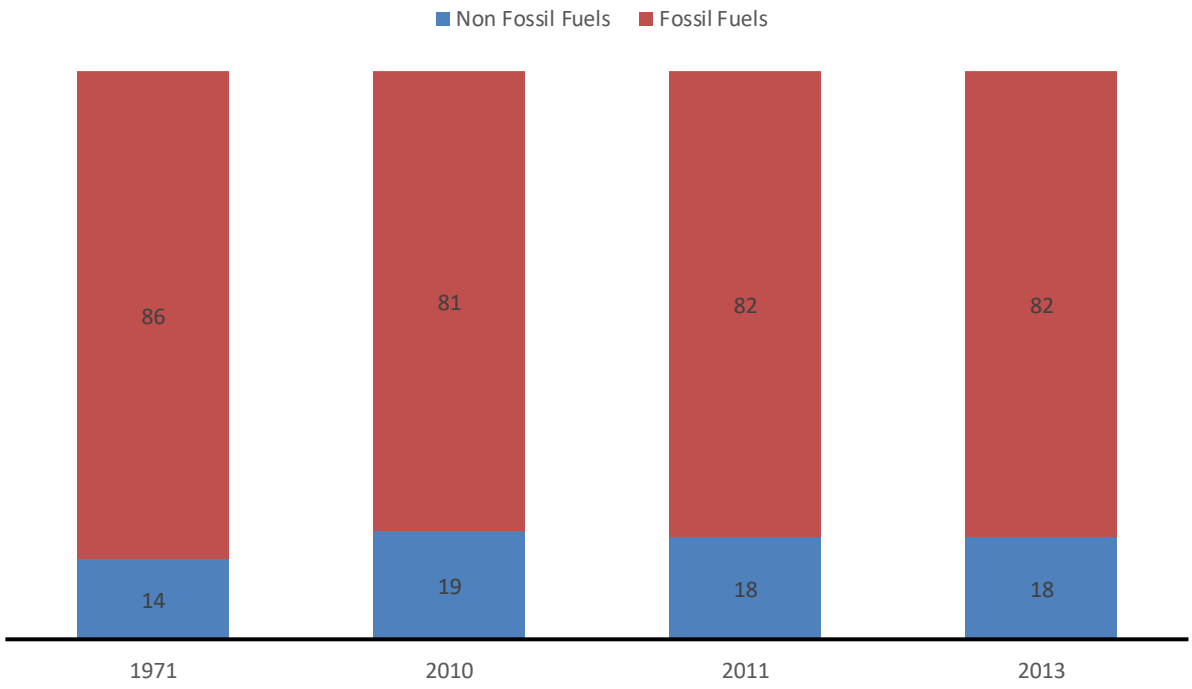

Figure 1.1: World energy supply proportions (Adapted from (International Energy Agency, 2015))

Fossil fuels are currently and are predicted to continue as a major energy generation method for future decades because of their substantial advantages. These advantages include, the ability to produce cheap, reliable energy, grid stability and abundant fossil fuel supply. The biggest disadvantage of fossil fuels for

energy production is that their combustion produces heat and gases such as water vapour (H_2O) and carbon dioxide (CO_2) as the main products (EPA, 2015). In some cases, sulphur dioxide (SO_2) and hydrogen sulphide (H_2S) are also produced. These gases are harmful to the environment. CO_2 and H_2O are greenhouse gases (GHGs) and contribute significantly to the greenhouse effect. The greenhouse effect is caused when GHGs trap the heat radiated by the earth's surface (Bolland, 2014). The rate of contained heat is directly proportional to the quantity of GHGs. Energy generation by the combustion of fossil fuels is causing the surface temperature of the earth to increase by increasing the atmospheric concentration of GHGs (International Energy Agency, 2015). This is a phenomenon termed as climate change. While, both H_2O and CO_2 are GHGs, only the atmospheric concentration of CO_2 is considered with regards to climate change. This is because the atmospheric concentration of H_2O is not significantly influenced by human activities.

Figure 1.2 was produced by the National Oceanic and Atmospheric Administration (NOAA), a division of NASA and shows the average atmospheric CO_2 concentration from 1958 to January 2017. (NASA, 2016). The atmospheric CO_2 concentration reached 406.13 ppm in January 2017. The trend shows that there is an increase in atmospheric CO_2 concentration. If business continues as usual a further increase will be seen.

Figure 1.2: Atmospheric CO_2 concentration per year (Adapted from (NASA, 2016))

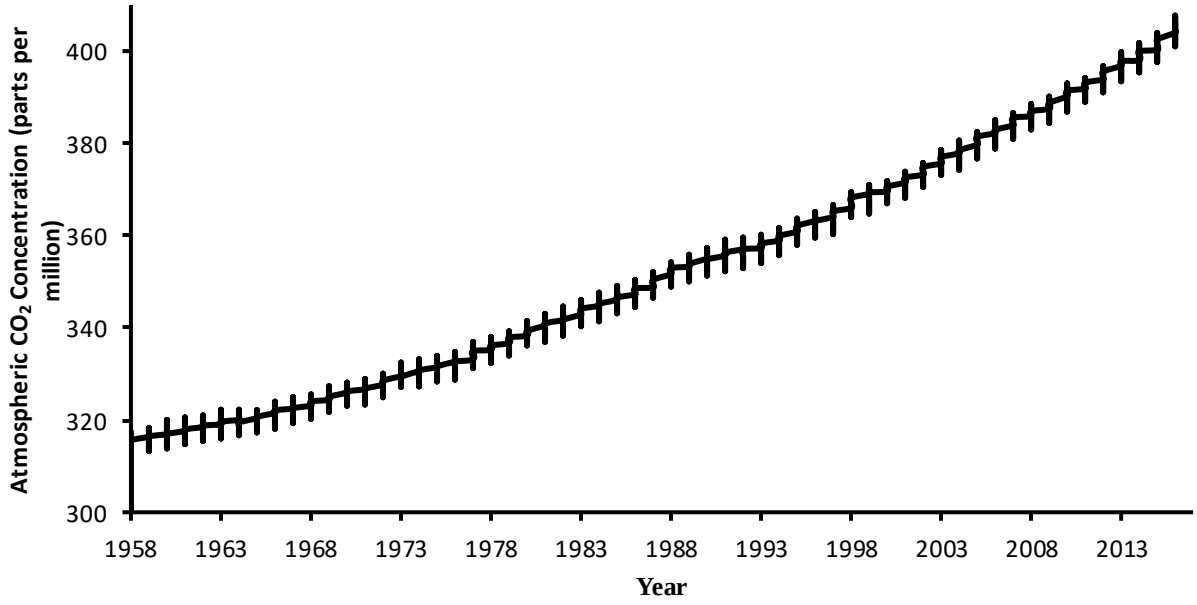

In an attempt to quantify the rise of global mean surface temperatures the NASA Goddard Institute for Space Studies has been extensively recording the surface temperature of the Earth in the years since 1880. Figure 1.3 shows the recorded mean global surface temperature from 1880 to present relevant to 1951 –

1980 average temperatures (NASA, 2016). The trend shows that there is a definite increase in the global mean surface temperature. If business continues as usual a further increase will be seen. The most recent measurement shows that in 2016 the global mean surface temperature was 0.99 ºC warmer than the average temperature between 1951 – 1980. The Intergovernmental Panel on Climate Change (IPCC) reports that if business proceeds as usual, anthropogenic GHG emissions will increase the mean global surface temperature by 6.4 ^{0}C during the 21st century (Shao et al., 2009).

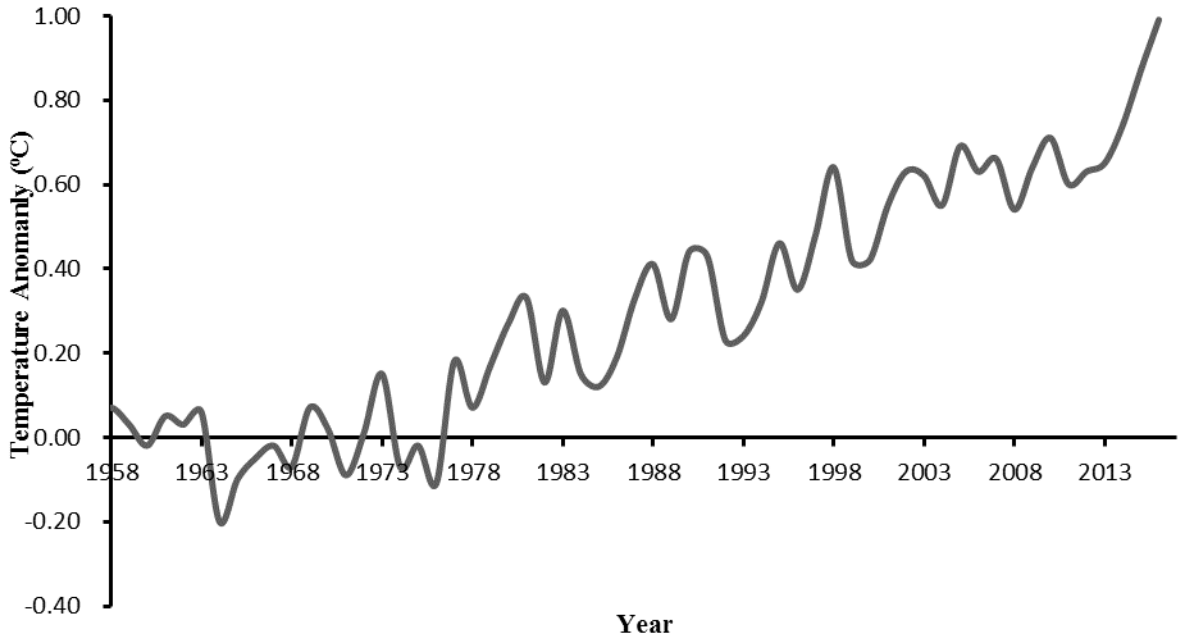

Figure 1.3: The change in global surface temperature relative to 1951-1980 average temperatures (Adapted from (NASA, 2016))

The rise in global mean temperature will cause changes to hydrological cycles, higher occurrences of harsh weather conditions (storms, heavy precipitation, heat waves etc.), ocean acidification, and a rise in sea levels (Maroto-Valer, 2010).

1.2. Mitigation of Climate Change

The increase in mean global surface temperature was discussed at the United Nations Frameworks Convention on Climate Change (UNFCCC) in Cancún in 2010. The conclusion from this conference was that it is necessary to avoid such dire climate change consequences and to sustain our current life style. To do this, required to stabilise the global mean surface temperature increase at 2 °C. The Paris Agreement, from COP 21 in Paris 2015 raised this agreement to 1.5 °C. In order to have at least a 50 % chance of meeting this target, it is necessary to keep the atmospheric CO_2 concentration below 450 ppm (UNFCC,

2010). Recall Figure 1.3 which showed that the atmospheric CO_2 concentration reached 405.25 ppm in January 2017. If target of maintaining the atmospheric CO_2 concentration to below 450 ppm is to be realised it is crucial to implement a plan of action to combat CO_2 emissions immediately.

The IEA has laid out an energy deployment system which is published in Energy Technology Perspectives 2015. That gives a pathway and emissions trajectory that will allow this target to be reached. The perspective only allows for a cumulative emissions level of approximately 1 000 Gt CO_2 from 2013 to 2050. The perspective identifies changes that need to be made to reduce emissions and

Figure 1.4 graphically depicts this energy deployment system. These changes show that switching to renewables could be used to reduce emissions by 32 %, increasing power generation efficiency and fuel switching could be used to reduce emissions by 1 %, end use fuel switching could be used to reduce emissions by 10 %, end use efficiency could be used to reduce emissions by 38 %, nuclear power generation methods could be used to reduce emissions by 7 %. With all these changes in place it is still not possible to reduce emissions enough to reach target of maintain the atmospheric CO_2 concentration below 450 ppm, particularly for developing countries who lack the financial support.

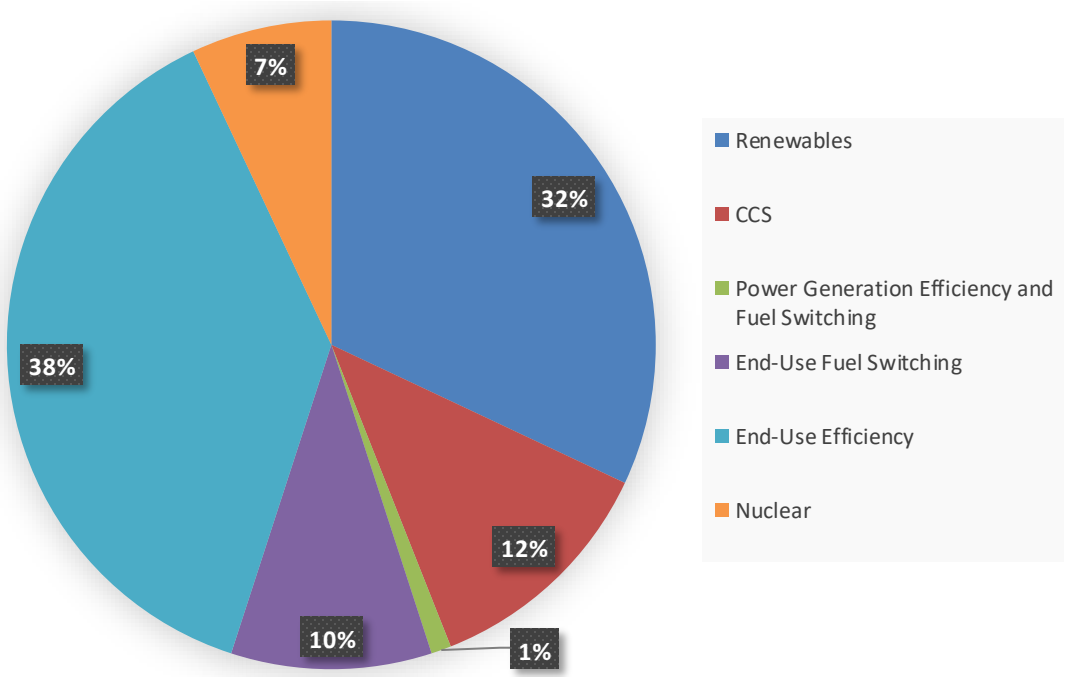

Figure 1.4: IEA Strategy to reduce CO_2 emissions (Adapted from (International Energy Agency, 2015))

Coal has dominated the South African energy supply sector from as early as 1800, when coal was utilized in the Kimberly Diamond Fields. Eskom reports that 77 % of the country's primary energy needs are met by the combustion of coal in the 16 Coal fired power plants that the country operates. Eskom is the seventh largest electricity generator in the world (Eskom, 2015).

To put this into a worldwide CO_2 emissions perspective, in 2014 South Africa was reported to be the 12th most significant CO_2 emitter worldwide and is responsible for almost half of Africa's CO_2 emissions (Florini et al. 2014). Clearly, South Africa is heavily dependent on fossil fuels to meet energy requirements. With two new coal fired power plants (Medupi and Kusile) under construction, it is not likely that the country will be able to economically move away fossil fuels for energy generation soon enough to meet the target of maintaining CO_2 emissions.

In order to meet the CO_2 emissions target, the practice of venting anthropogenic CO_2 gas into the atmosphere needs to cease. With a lifestyle so dependent on energy and all the necessary infrastructure already in place to produce this from fossil fuels, this seems an impossible task. The Energy Deployment System creates a problematic situation for not only South Africa but also for other developing as well as developed countries. There becomes a need for a method of energy generation from fossil fuels that is able to avoid CO_2 emissions while still providing the advantages of fossil fuels. One proposed method is carbon capture and storage (CSS). In this process CO_2 is captured from large point sources, such as electricity generation power stations, and then stored for many years. CCS is widely considered the solution to this CO_2 emissions problem (International Energy Agency, 2016). The Energy Technology Perspectives 2015 laid out by the IEA and shown in Figure 1.4, thus incorporates CCS to reduce CO_2 emissions by a further 12 % which will allow for the 450 ppm atmospheric CO_2 concentration target to be reached.

1.3. Problem Identification and Problem Statement

CO_2 emissions need to be reduced. South Africa has made governmental commitments to decreasing its CO_2 emissions through CCS. The South African Centre for Carbon Capture and Storage (SACCCS) has been put in place to develop and implement the application of CCS in South Africa. Currently CCS has not been developed in large scale in South Africa but is at the research stage with a particular emphasis on storage. This research is largely managed by SACCCS along with the Council for Geosciences and a few academic institutions. There is a need to place more focus on the capture component as CO_2 must be captured before it can be stored.

There are currently many different capture technologies being researched worldwide. Many of these technologies have low CO_2 capture efficiencies, are costly and have been shown to give health risks (Pires et al., 2011). Resulting in CCS being economically unviable, especially for developing countries. For CCS

to be implemented on a global industrial scale, it is of paramount importance that more suitable capture technologies that are both cost effective and efficient are developed

CCS will only gain public acceptance and implementation in industry once it has been confirmed to be viable economically. There are many factors that affect the economic viability of CCS. One of these factors is the lack of inexpensive technology and high performance materials for selective removal of CO_2 from flue gas. For this reason, various novel materials for the post combustion CO_2 capture have been developed and studied (Bolland, 2014), (International Energy Agency, 2016). Examples of these are solvents for absorption, solid adsorbents for adsorption, materials for cryogenic separation and membranes for membrane separation. The most mature and established of the proposed technologies for CO_2 capture is chemical absorption using liquid amine based solvents (e.g. monoethanolamine (MEA)). The use of amines can pose health risks when released into air from CO_2 capture plants. There is also an efficiency penalty and the huge costs associated with the regeneration of the spent amine based liquid solvent. This has led to the proposal of a range of potentially more efficient and less energy-intensive second and third generation capture technologies (Pires et al., 2011). One such technology is adsorption, which seems promising due to its moderate energy consumption as well as its improved health and environmentally benign properties. This stems from the ability to operate at moderate temperatures and pressures. Recently, extensive research has been conducted on designing adsorbents that have the ability to adsorb large amounts of CO_2 with low energy consumption while not posing additional health and environmental risks (Pires et al., 2011). This study proposes chitosan, a biodegradable non-toxic polymer as an adsorbent that has the potential to be one such material. The advantages of using chitosan is that is has the desired amine functional groups and is derived from shrimp shells, a material that would otherwise be considered as a waste product. The disadvantages to using chitosan as an adsorbent for CO_2 capture is that chitosan samples differ widely based on the degree of deacetylation (DDA). DDA gives an indication of the amount of amine groups present. However, there is little information in open literature concerning the use of chitosan for CO_2 capture. Against this background this study aims at developing a chitosan based novel adsorbent material for the selective post combustion capture of CO_2 and to study the DDA of chitosan samples.

1.4. Research Aims, Objectives and Expected Outcomes

The main aim of this study was to successfully synthesis chitosan from chitin and to impregnate chitosan onto carbon nanotubes (CNTs) to produce a composite adsorbent named chitosan/MWCNTs. Then characterize and evaluate the CO_2 adsorption performance of these materials (both chitosan and chitosan/MWCNTs) for use as adsorbents for post combustion CO_2 capture. To achieve the aforementioned aims, the questions below were expected to be answered in the course of the study.

i. Can chitosan, with desirable properties for CO_2 capture, be synthesised from chitin?
ii. What is the effect of independent variables during the synthesis stage on the degree of deacetylation of chitosan derived from chitin?
iii. Can chitosan be impregnated onto CNTs to produce a composite adsorbent with desirable properties for CO_2 capture?
iv. What is the CO_2 adsorption performance of this composite adsorbent material in the presence of impurities?

The main objective of this study was to develop a chitosan based adsorbent for post combustion CO_2 capture. Other objectives are:

i. To synthesize chitosan, with desirable properties for CO_2 capture from chitin.
ii. To study the effect of synthesis variables on degree of deacetylation of chitosan synthesised from chitin by using a statistical approach.
iii. To impregnate chitosan onto CNTs to produce a composite adsorbent with desirable properties for CO_2 capture.
iv. To evaluate the CO_2 adsorption performance of chitosan and chitosan/MWCNTS.

The following outcomes resulted from this research effort:

i. Synthesized chitosan with desirable properties for CO_2 capture.
ii. Information on the effect of synthesis variables on the synthesis of chitosan from chitin and the optimum synthesis conditions possible for the material.
iii. A synthesized chitosan/MWCNTs composite adsorbent with more desirable properties for CO_2 capture relative to the base material (MWCNTs).
iv. Peer reviewed paper publications and conference presentations
v. A well-documented report in the form of a dissertation and an award.

1.5. Dissertation structure:

The structure of this dissertation is presented as follows:

- Chapter 2: Literature review

The details of CCS are discussed in chapter 2. The history of CCS is considered and its current application. The concepts of CO_2 capture, compression, transports and storage are considered with the focus being on CO_2 capture. Within the concept of CO_2 capture, different capture technologies are considered with an emphasis on post-combustion CO_2 capture via adsorption. The chapter then considers the factors that

influence post-combustion CO_2 capture and the various types of adsorbents in the context of adsorption. Lastly, chapter proposes chitosan as an alternative non-toxic biodegradable polymer as a potential adsorbent for post-combustion CO_2 capture and explores this interesting polymer.

- Chapter 3: Materials and experimental procedure

The details of the materials, equipment and experimental procedure that was utilized are discussed in chapter 3.

- Chapter 4: Synthesis of chitosan and effect of the synthesis variables on the degree of deacetylation of chitosan

The results pertaining to the synthesis and characterisation of the synthesised chitosan samples are discussed in chapter 4. The influence of the synthesis variables on the degree of deacetylation of the synthesised chitosan samples is also discussed in this chapter.

- Chapter 5: Evaluation of the CO_2 adsorption capacity of the synthesised chitosan

The results obtained from the evaluation if the CO_2 adsorption capacity of the synthesised chitosan is discussed chapter 5.

- Chapter 6: Synthesis, characterisation and evaluation of the CO_2 adsorption capacity of the synthesised chitosan/MWCNTs

The results pertaining to the synthesis and characterisation of the chitosan/MWCNTs are discussed in chapter 6. The results obtained from the evaluation if the CO_2 adsorption capacity of the chitosan/MWCNTs are also discussed chapter 6.

- Chapter 7: General conclusions and recommendations

The general conclusions and recommendations are discussed in chapter 7.

Chapter 2 Literature Review

2.1. Introduction

This chapter discusses the details of CCS. The history of CCS is considered first, followed by its current applications. The concepts of CO_2 compression, transport and storage are explained with the main focus being on CO_2 capture. Within the concept of CO_2 capture, different capture technologies are considered with an emphasis on post-combustion CO_2 capture via adsorption. The chapter then considers the factors that influence post-combustion CO_2 capture and the various types of adsorbents in the context of adsorption. Lastly, chapter proposes chitosan as an alternative non-toxic biodegradable polymer as a potential adsorbent for post-combustion CO_2 capture and explores this interesting polymer.

2.2. Carbon Dioxide Capture and Storage (CCS)

CSS is a series of processes where the aim is to reduce CO_2 emissions to the atmosphere by removing CO_2 from sources where it is emitted, such as the flue gas of power stations and storing the CO_2 where is it not able to enter the atmosphere (Intergovernmental Panel on Climate Change, 2005). The series of processes of CCS are the separation of CO_2 from large industrial sources of CO_2 (section 2.2.2), the compression and transport of the CO_2 to suitable storage sites (section 2.2.1) and finally the injection and long-term storage of the CO_2 (section 2.2).

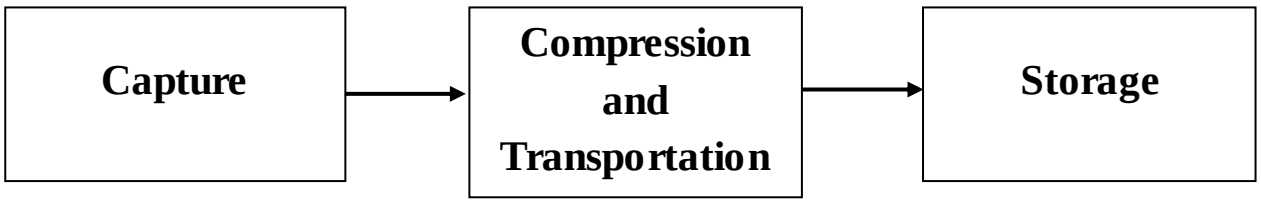

Figure 2.1: Schematic showing the stages in carbon capture and storage (CCS)

The sub-surface of the Earth has been a carbon reservoir for millions of years. CO_2 derived from biological activities and chemical reactions between rocks and fluids accumulates naturally in the earth's subsurface. These accumulations are in the form of coal, oil, organic rich gas shales, carbonate rock or in a gaseous or supercritical form either as a gas mixture of pure CO_2. The idea of engineered CO_2 injection takes advantage of this naturally occurring geographical process.

The first occurrence of engineered CO_2 injection was for Enhanced Oil Recovery (EOR) during the early 1970s in Texas USA. This process has been found to be beneficial to mining and not harmful to the environment. EOR is still ongoing in both Texas and numerous locations worldwide (Intergovernmental

Panel on Climate Change, 2005). Around the same time as EOR, the idea of injecting CO_2 for geographical storage was proposed but little research was done until the early 1990s. In 1996 the world's first large scale storage project was started by Norway in the North Sea by Statoil and its partners at the Sleipner Gas Field (Sleipner Project) (Intergovernmental Panel on Climate Change, 2005). It is reported that approximately 1 Million Tonnes of CO_2 is stored annually by this project. In the years following this project, there was a global interest in geological storage as a CO_2 emissions mitigation option (International Energy Agency, 2016). Successful projects include In Salah in Algeria and Gorgon in Australia (International Energy Agency, 2016).

The first industrial scale CCS project in which CO_2 was separated from the flue gas of power stations commenced in 2014 in Saskatchewan, Canada. This project is known as the Boundary Dam CCS Project. In this project an existing 115 megawatt coal-fired power station was rebuilt with carbon capture technology. This technology is capable of capturing 1 Million tonnes of CO_2 per year. Once captured, the CO_2 is piped to oil fields in Southern Saskatchewan where it is utilized for EOR or stored in the Aquistore Project (International Energy Agency, 2016). The Aquistore Project aims to research and monitor the effects of CO_2 storage in a layer of brine-filled standstone. As of August 2016, this project has surpassed the 1 Million tonnes of CO_2 stored (International Energy Agency, 2016). The success of these projects have promoted both public and private investment into CCS (International Energy Agency, 2016).

The aforementioned stages of CCS (Storage, Transport and Capture) will now be discussed. Capture is the first stage in CCS, but it will be discussed last as it is the main focus of this chapter.

2.2.1. CO_2 Compression and Transport

CO_2 compression involves increasing the density of CO_2 gas by decreasing its volume. CO_2 needs to be compressed to a dense or supercritical fluid prior to transportation and storage. By compressing CO_2, the transportation process will be simplified and more economical (Intergovernmental Panel on Climate Change, 2005).

CO_2 transport involves moving the captured CO_2 from the capture site to the geological storage site. CO_2 can be transported in three phases, gas, liquid or solid. However, CO_2 in the gas phase occupies a large volume and will requires very large transport and storage facilities. Gas occupies less volume when compressed to a liquid and can be transported via pipeline. It is possible to further compress CO_2 to the solid phase where it will occupy the least volume, however by doing this compression costs will increase substantially. Due to energy use and size constraints, CO_2 transport predominantly occurs in the liquid phase via pipelines. Transport of CO_2 and other gases via pipelines is a mature technology, with decades of

practical experience, mostly in North America. Most of this experience is as a result of the EOR that is undertaken in North America, where there have been extensive CO_2 pipeline networks since the 1980s. The knowledge on pipeline transport of CO_2 is well regulated safe, mature and has been extensively documented. The transport of gas via pipeline is also applied in South Africa, since 2004 Sasol has piped natural gas from Mozambique to Secunda Mpumalanga.

The compression and transport of CO_2 is an important aspect of CCS however it is beyond the scope of this study and will not be discussed in further detail in this report.

2.2.2. CO_2 Storage

CO_2 storage involves the isolation of anthropogenic CO_2. The isolation of CO_2 is achieved by the injection of the CO_2 into the sub-surface of the earth. The time period of isolation needs to be long-term, approximately 1000 years. The first step in CO_2 storage is to characterise geological formations to determine if they are suitable for long-term storage of CO_2. The characterisation process includes studies on permeability, thickness, storage capacity, geological structures and lithology of the storage site (EPA, 2013). This extensive study aims to determine is the storage site has adequate storage capacity, is suitable for injection, has a suitable seal, and whether the environment storage site is geologically suitable (Intergovernmental Panel on Climate Change, 2005).

Geological storage of CO_2 can be undertaken in a variety of geological settings in sedimentary basins. Potentially suitable geological storage sites for CO_2 include depleted oil and gas reservoirs, use of CO_2 in EOR, deep unused saline water-saturated reservoir rocks, deep unmineable coal seams, use of CO_2 in enhanced coal bed methane recovery (EBR) and other suggested options such as basalts, oil shales and cavities (Global CCS institute, 2014).

The IEA consider depleted oil and gas reservoirs to be ideal for storage locations because they have many advantages (International Energy Agency, 2016). Oil and gas reservoirs were able to contain the oil and gas for millions of years which indicates storage security. Information on these reservoirs was gathered during the original mining process and as such they have already been well characterized. Lastly, oil and gas have already been or is currently being extracted, so the infrastructure is already in place and it has been proven that the sites are suitable for injection. CO_2 injections could potentially aid oil and gas recovery thus allowing for the extraction of oil and gas that was previously considered unmineable.

Saline formations are deep sedimentary rocks with formation water that contains a high concentration of dissolved salts (brine). Saline formations have the potential to be geological storage sites for CO_2 because the brine solution absorbs CO_2 into the bulk of the fluid. The Sleipner Project in the North Sea is an example

of CO_2 storage in a saline formation. Studies from the Sleipner Project have shown that the dissolved CO_2 will eventually sink to the bottom of the reservoir. This is beneficial to ensuring that there are no CO_2 leaks from the formation (Liebscher & Munch, 2015).

Deep unminable coal seams can be used for CO_2 storage. Coal beds contain natural fractures, known as cleats (Rodrigues et al., 2014). These cleats will allow for the movement of the injected CO_2 through the coal bed, enabling the adsorption of the gas onto the coal bed (Laubach et al., 1998). Adsorption onto the coal bed is beneficial in ensuring that there are no CO_2 leaks from the formation. The adsorption of CO_2 onto the coal bed will lead to Enhanced Coal Bed Methane Recovery (EBR). Coal has a greater affinity for CO_2 than methane (White et al., 2005). As the coal bed adsorbs CO_2, it will desorb methane. There is some financial gain in this process as methane is a valuable product.

In addition to these mentioned potential storage sites, there are suggested options such as basalts, oil shales and cavities that are currently being researched. Currently in South Africa research is underway to determine the country's potential for CO_2 storage, this research is facilitated by SACCCS (see section 2.3). The SACCCS published a storage atlas in 2010 to review which showed the potential CO_2 storage sites in South Africa. SACCCS estimates that the geological storage capacity in South Africa is 150 Gt of CO_2. About 98 % of this storage volume is offshore and along the coast in the saline formations of the Mesozoic basins (SACCCS, 2010). South Africa is committed to reducing her CO_2 emissions, but the general overview is that there is limited storage capacity. Whilst this is a very important aspect, it is beyond the scope of this study and will not be discussed in further detail in this report.

2.2.3. CO_2 Capture

CO_2 capture involves the separation of CO_2 from other gases at industrial process facilities that produce CO_2. An example of an industrial process facility where CO_2 would be captured is power station. Flue/exhaust gas from power stations is commonly vented to the atmosphere. Flue gas consists of mainly N_2 and O_2 but also CO_2 at an approximate concentration of 10-15% (Saha et al., 2012). It is imperative to separate the CO_2 from the gases for storage as it would be impossible to store all of the flue gas due to legislation and compression, transport and storage costs.

Three main capture technological pathways are being considered for CO_2 capture. These are, pre-combustion capture, post-combustion capture and oxy-combustion capture.

2.2.3.1. Pre-combustion Capture

Pre-combustion capture is the capture of CO_2 before the electricity generation stage in a power plant. CO_2 is captured from enriched syngas produced from the water gas-shift reaction. Pre-combustion capture

involves the reaction of fuel (commonly in the form of coal or natural gas) and O_2 in a gasifier or reformer in order to yield synthesis gas. Synthesis gas consists hydrogen (H_2) gas and carbon monoxide (CO) by definition. This syngas is further subjected to a water gas-shift reaction (WGS) (Equation 2.1) for the purpose of converting the CO to CO_2.

$$CO\ (g) + H_2O\ (g) \leftrightarrow CO_2\ (g) + H_2\ (g) \quad (2.1)$$

The CO_2 is separated from the H_2. The H_2 enters a combustion or oxidation process. Whereas the CO_2 is captured in the capture plant (The Linde Group, 2014). Figure 2.2 gives a schematic of pre-combustion capture.

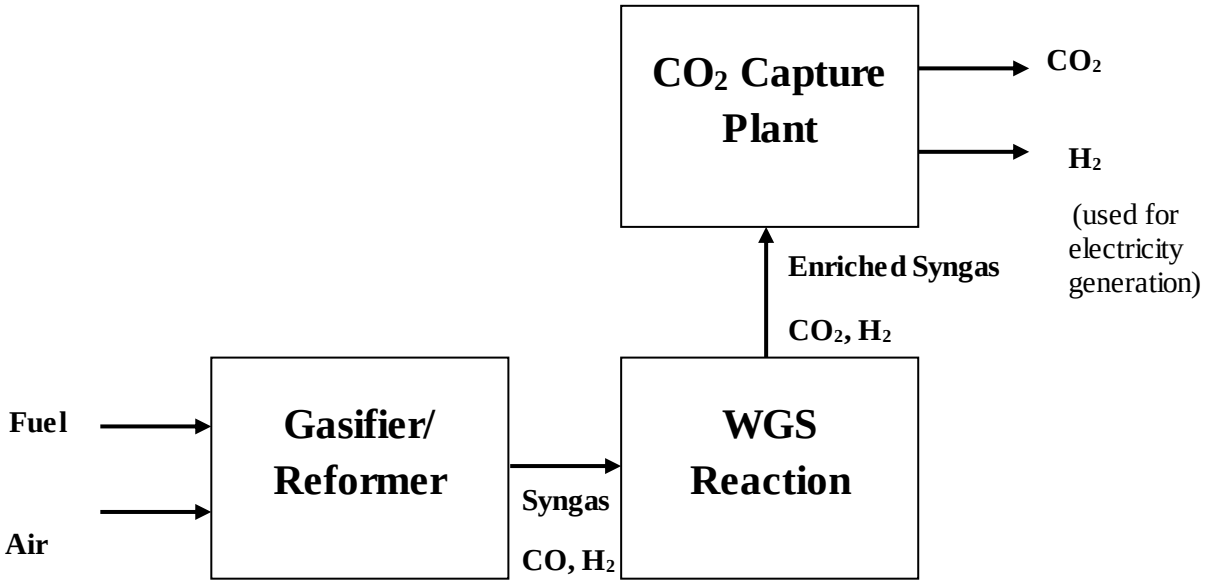

Figure 2.2: Pre-combustion CO_2 capture

2.2.3.2. Post-combustion Capture

Post-combustion is the capture of CO_2 from the flue/exhaust gases produced during the combustion of fossil fuels using O_2 from air (Global CCS institute, 2014). The fuel is fed with excess air into a combustor and combustion occurs. An example of a possible reaction of fuel and oxygen is given by Equation 2.2, which is the reaction of coal and oxygen.

$$C\ (s) + O_2(g) \rightarrow CO_2(g) \quad (2.2)$$

The CO_2 gas that is produced mixes the remaining components of air, the result of this is a gas mixture that has a dilute concentration of CO_2. This gas is known as the flue gas and is vented to atmosphere. During the capture stage the CO_2 gas is needs to be separated from flue gas prior to being vented to atmosphere. The use of air instead of pure O_2 complicates the separation in the capture stage because the CO_2 is more diluted. Figure 2.3 gives a schematic of post-combustion capture.

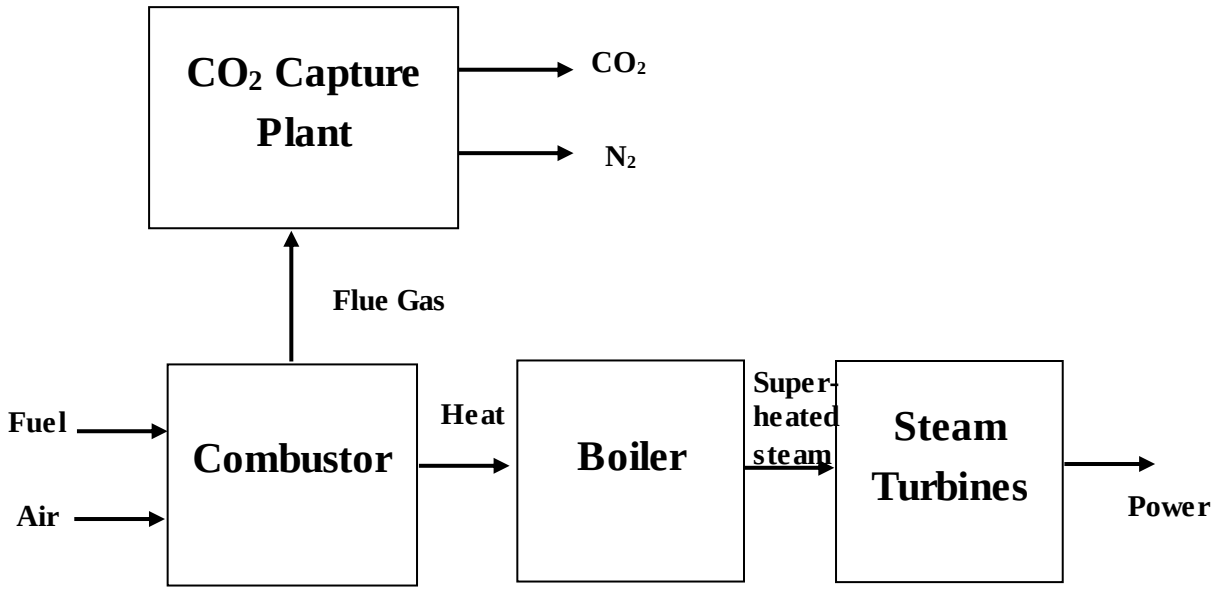

Figure 2.3: Post-combustion CO_2 capture

A substantial amount of the energy generation related anthropogenic CO_2 emissions come from post combustion systems such as, power plants, cement kilns, steel and iron production plants. It is possible to retrofit these with post-combustion capture plants. Therefore, the practical importance of the post-combustion capture systems becomes evident when confronted with the reality of today's CO_2 emission sources. This has resulted in post-combustion CO_2 capture being a commonly practiced method of CO_2 capture. South Africa has a heavy dependence on the combustion of fossil fuels in the power plants that Eskom operates (Eskom, 2015). It is possible to retrofit these power plants with post-combustion CO_2 capture plants (Herzog et al., 2009).

2.2.3.3. Oxy- Fuel Combustion

Oxy-fuel combustion is almost the same process as post-combustion, but fuel is combusted with pure and limited O_2 rather than excess air. This ensures that the flue gas stream is not diluted with the impurities found in air. The use of pure and limited O_2 simplifies the separation in the capture stage because the CO_2

is less diluted (Bolland, 2014). Figure 2.4 gives a schematic of oxy-combustion. Although combusting with pure O_2 simplifies the capture stage the air separation unit (ASU) that separates O_2 from air complicates the oxy-fuel combustion process.

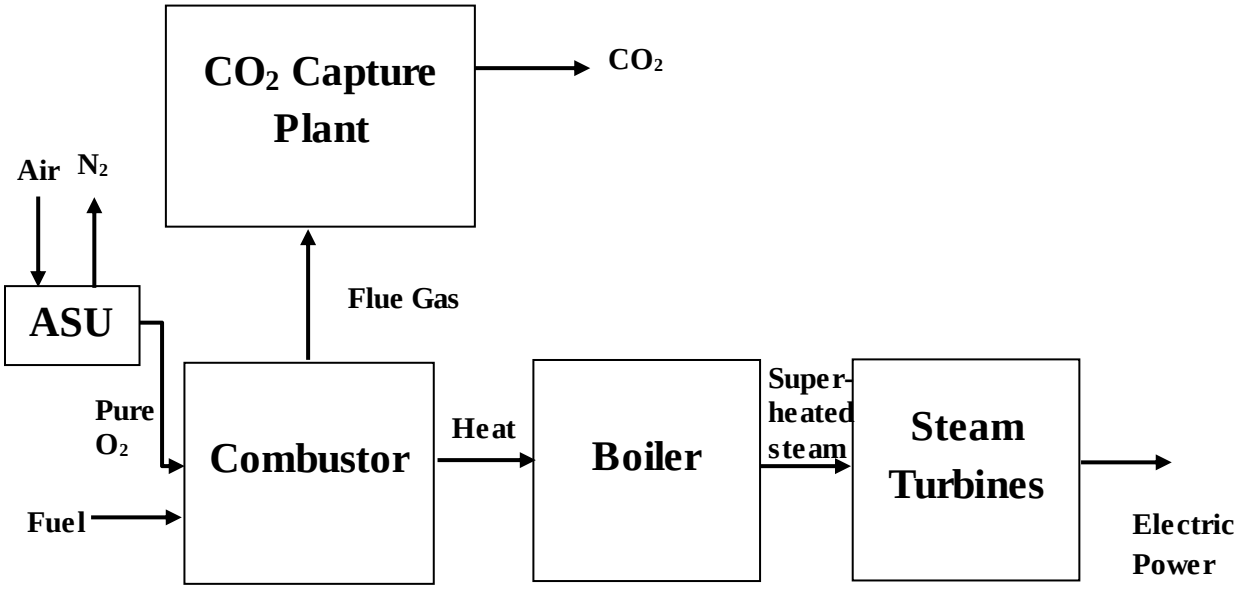

Figure 2.4: Oxy-combustion CO_2 capture

There are emerging technologies such as chemical looping combustion for solid fuels, post-combustion calcium looping systems and CO_2 capture from air (International Energy Agency, 2016). Whilst this is a very important aspect, it is beyond the scope of this study and will not be discussed in further detail in this report.

2.3. Coal, CO_2 Emissions and CCS in South Africa

As mentioned in Chapter 1, South Africa is a significant emitter of CO_2 and is committed to reducing her CO_2 emissions. However, as was also mentioned in Chapter 1, South Africa is heavily dependent on the use of coal to meets its energy needs.

In 2014 South Africa was reported to be the 12th largest emitter of CO_2 worldwide and is solely responsible for nearly half of Africa's CO_2 emissions (Florini et al., 2014). South Africa has made governmental commitments to decreasing its CO_2 emissions through CCS. The South African Centre for Carbon Capture and Storage (SACCCS) has been put in place for the purpose of developing and implementing the

commercial application of CCS in South Africa. The SACCCS was established on the 30 of March 2009. The SACCCS has put into place a five-stage plan, known as a CCS roadmap. The first stage was to verify whether the country has CO_2 rich streams where CO_2 can be captured. The second stage involved developing a geological storage atlas. Both of these stages have been successfully completed and have shown promising results for the possibility of implementing CCS (SACCCS, 2014). The third stage of the road map is a pilot CO_2 storage project experiment and is currently being undertaken (SACCCS, 2014). The fourth and fifth stages of the CCS road map are to facilitate the commencement of a CCS demonstration plant that can capture 100 kt of CO_2 per year (by 2020) and coordinate the implementation of commercial CCS deployment respectively (by 2025).

Figure 2.5 shows the companies in South Africa that are the highest direct emitters of CO_2. Eskom is the most significant of the CO_2 emitters out of the companies considered. This is due to the use of coal for energy production. This study and much of the research currently being undertaken in South Africa is aimed at reducing the CO_2 emissions from these sources.

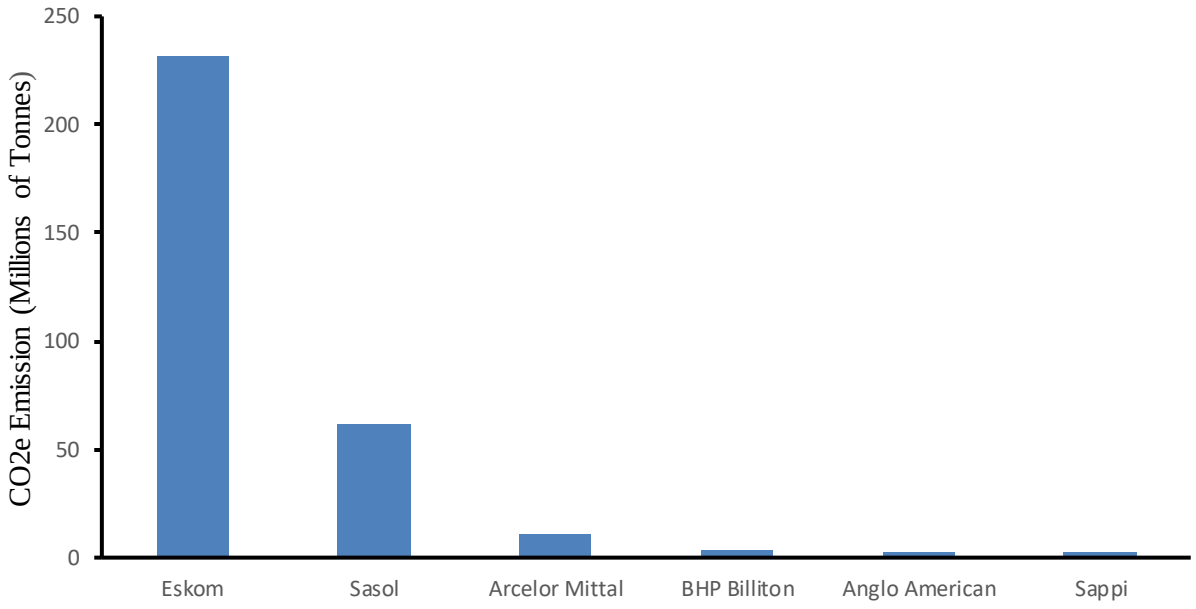

Figure 2.5: South Africa's highest CO_2 emitters (Adapted from (Urban Earth, 2012))

2.4. Techniques for CO_2 Capture in Existing Coal-Fired Power Plants

In order to define techniques to capture CO_2 from coal fired power plants it is necessary to understand their means of operation. Figure 2.6 gives the schematic of a typical coal fired power plant. Fuel, in the form of coal, is fed to a combustor and combusted where heat and exhaust gas are produced. The produced heat heats up water to steam in a boiler. The steam is used to turn turbines which produce electrical energy. The produced flue/exhaust gas is made up of N_2, water vapour, CO_2, O_2, particulate matter (PM), nitrous oxides (NO_x) and sulphur oxides (SO_x). In a typical coal fired power plant the PM, NO_x and SO_x are removed and the gas that remains, known as flue gas, is emitted to the atmosphere. CCS proposes to add another stage onto the flow process in order to remove CO_2.

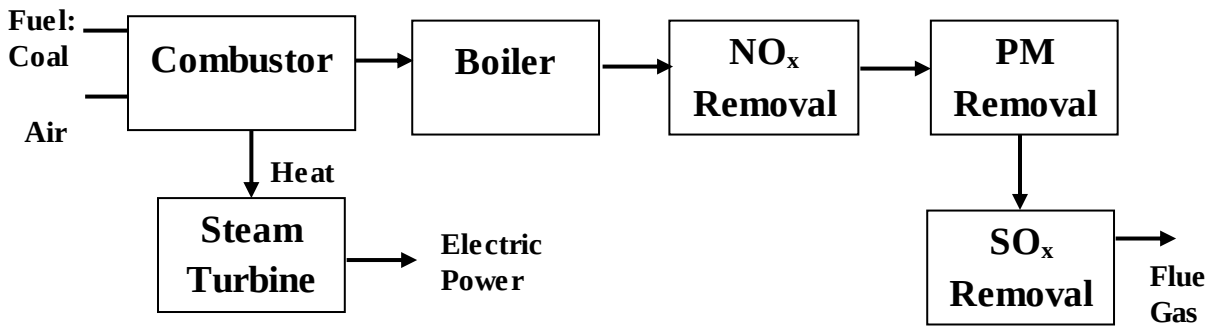

Figure 2.6: Flow diagram illustrating the structure of a coal-fired power plant

It is possible to retrofit typical coal-fired power station with post-combustion capture plants. There are several technologies that can be used for post-combustion CO_2 capture plants. Some of these technologies are mature and are currently being used in industry whereas others are still in the research stages. Possible capture technologies include but are not limited to, membrane separation, cryogenic distillation and sorption techniques such as absorption techniques and adsorption techniques. Absorption and adsorption technologies are explained below.

2.4.1. Sorption

Sorption is one of the techniques employed in post-combustion CO_2 capture. The sorption process involves contacting a free fluid phase with a durable sorbent phase, with the purpose of the sorbent phase taking up and holding the free fluid phase. The chosen sorbent needs to have the ability to take up and hold the fluid phase (Perry & Chilton, 2008). The free fluid phase is commonly known as the solute or adsorbate and the sorbent phase is commonly known as the solvent or adsorbent. The principle of CO_2 capture via sorption involves a two-step process. The first being the sorption of the CO_2 and then the other being the release of

the CO_2. This second step is usually referred to as solvent regeneration or desorption. The solvent is retrieved in this stage so that absorption can occur again.

There are two types of sorption processes namely, absorption and adsorption. The difference between the two stems from how the substance is retained. Absorption technology is more mature than adsorption. Absorption is currently the technology that is applied to the capture of CO_2. This technology is also used to separate various other gases in applications outside of CO_2 capture. However, the efficiency penalty caused by carbon capture via absorption and the huge costs associated with desorption of the spent solvents pose a threat to the economic viability of the absorption of CO_2 and CCS as a whole. On the other hand, adsorption technology seems promising due to its moderate energy consumption (which stems from the ability to operate at moderate temperatures and pressures) as well as having less negative effects on health and the environment. The process of post combustion capture via both absorption and adsorption are explained below.

2.2.4.1. Absorption

CO_2 capture via gas absorption is the process in which CO_2 (the solute) from the flue gas mixture is dissolved into a liquid (the solvent) (Perry & Chilton, 2008). In the absorption process CO_2 will physically enter into the bulk phase of the solvent and dissolves into it. This process is illustrated in Figure 2.7. From Figure 2.7 it is apparent that the solute has entered 'inside' of the bulk of the solvent.

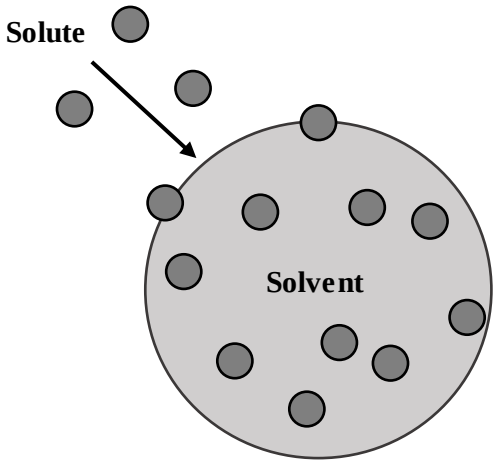

Figure 2.7: Schematic of absorption process

The absorption process can be physical or chemical, where there is a reaction between the solute and solvent. Physical absorption involves a physical process and follows Henry's Law. CO_2 is absorbed at high pressures and low temperatures and desorption occurs at low pressures and high temperatures. In physical absorption the absorbent molecules dissolve into the solvent and there is no chemical reaction. The properties of the solvent and solute remaining unchanged. Due to the physical nature of the process there is a lower energy requirement to desorb the solute. This process is widely used in industry where the typical solvents are Selexol (dimethyl ethers of polyethylene glycol) and Rectisol (methanol) (Wang et al., 2011) and (Lurgi, 2010).

Chemical absorption involves a reaction between the solute and solvent. Chemical absorption results in the formation of a new species that is soluble in the solvent, making it a chemical process whereby the absorbent and the absorbate are separated using a larger energy input. Chemical absorbents have two main advantages over physical absorbents. The first advantage is the high selectivity to CO_2 while not co-absorbing hydrocarbons and other chemical species. Physical absorbents have been shown to absorb hydrocarbons and other chemical species which are often the desired product. The second advantage of using a chemical absorption process is its good absorption behaviour at low partial pressures. The most significant drawbacks to the use of chemical solvents is the high energy requirements for desorption, limitation of the absorption process due to stoichiometry, and degradation of the solvent. The use of a hybrid solvent which possess the advantages of both physical and chemical absorption properties have been developed to overcome the disadvantages of each solvent type described (Lurgi, 2010).

At industrial scale, packed bed columns are used to remove CO_2. Examples of packed columns are an absorber and a stripper. The CO_2 rich flue gas is fed to the bottom of the absorber while lean amine solvent is fed at the top of the column (counter current flow pattern). The CO_2 and solvent thus make contact and the CO_2 moves from the flue gas phase to the solvent phase. The CO_2 rich amine solvent exits from the bottom of the absorber column and enters the stripper column, where the absorbed CO_2 is desorbed by adjusting operating conditions in the stripper. In this way the amine solvent is recovered (Perry & Chilton, 2008). This process has numerous disadvantages. These include high equipment corrosion due to the corrosive nature of the amine solvents used and the high energy requirement for solvent recovery which renders the absorption process undesirably expensive (Pires et al., 2011).

2.2.4.2. Adsorption

While adsorption is not as commonly utilized as absorption for separation processes it is estimated that 90% of chemicals produced by heterogeneously catalyzed processes are adsorption processes. For this reason, adsorption is important in today's industries. While adsorption is not extensively used for gas

separation Pires et. al. (2011) states that adsorption seems promising due to its moderate energy consumption as well as its improved health and environmentally benign properties.

CO_2 capture via gas adsorption is the process in which CO_2 (the adsorbate) from the flue gas is collected on the surface of a solid (the adsorbent) (Perry & Chilton, 2008). During the adsorption process molecules are attracted to and will adhere to the surface of another substance. Adsorption differs from absorption because the molecules do not enter the bulk of that substance. This process is illustrated in Figure 2.8, and it is apparent that the adsorbate adheres to the outside of the adsorbent.

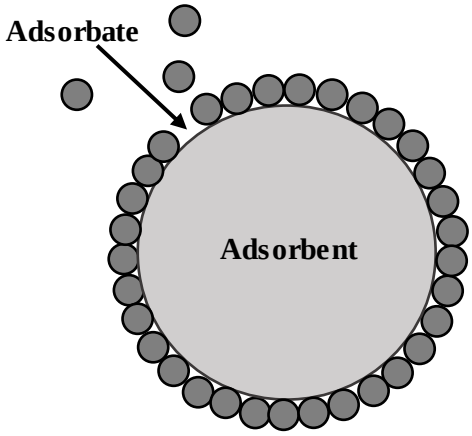

Figure 2.8: Schematic of adsorption process

The adsorption process is driven by the presence of interactive forces between the surface of the adsorbent and the adsorbate. A difference in surface energy causes the adsorbate to adhere to the surface of the adsorbent. This is an electrostatic force of attraction. Electrostatic forces are weak forces and as such the molecules are weakly held on the adsorbent's surface and can thus be easily desorbed and the adsorbent can be easily regenerated. This is different from absorption where it is more difficult and energy intensive to regenerate the solvent (Diffen, 2014). The adsorption process can be a purely physical in nature, known as physisorption, or chemical in nature and involve a reaction between the adsorbate and adsorbent, known as chemisorption. The nature of the adsorption process is determined by the electrostatic forces present.

Physisorption is a physical process where the properties of the adsorbates and adsorbents remains unchanged. During the physisorption process, the adsorbate approaches the adsorbent surface where repulsive and attractive forces become balanced and adsorption occurs. The type of forces present are called van der Waals forces. Before adsorption occurs the adsorbate has three degrees of translational freedom. After adsorption occurs the adsorbate loses one degree of translational freedom. The decrease in the degree

of translational freedom results in a decrease in both the entropy and Gibbs free energy (Crittenden & Thomas, 1998). This causes an increase in the enthalpy, which means that the adsorption process is exothermic as shown in Equation 2.3 (Crittenden & Thomas, 1998).

$$\Delta G = \Delta H - T\Delta S \quad (2.3)$$

$$\Delta G < 0, \Delta S < 0 \ \therefore \ \Delta H > 0$$

Thus, due to the exothermic nature of adsorption, the amount of adsorption that occurs during physisorption decreases with an increase in temperature.

Chemisorption is a chemical process where the properties of both the adsorbent and adsorbate change due to the formation of covalent chemical bonds (IUPAC, 2002). During chemisorption there is a transfer of electrons between the adsorbent and adsorbate which results in the formation of covalent bonds. Chemisorption does not follow the same thermodynamic structure as physisorption and is thus possible at a larger range of temperature, notwithstanding, chemisorption is still an exothermic process. With physisorption under the optimum operating conditions (temperature and pressure), it is possible to achieve multilayer adsorption. In contrast, chemisorption is limited by the number of sites where chemical bonding can occur. Another draw-back to chemisorption is that due to the chemical bonds, the regeneration of the adsorbent is often difficult or impossible due to the high energy requirement to break the bonds (Fletcher, 2008).

In physisorption, it has been found that the adsorption capacity decreases substantially with increasing temperature and reduced partial pressures because of the nature of van der Waals forces. Chemisorption has been shown to give better CO_2 adsorption at lower CO_2 concentrations (Berger & Bhown, 2011) and shows better CO_2 adsorption at higher temperatures than physisorption. Chemisorption has been adopted for CO_2 capture and optimised by manipulating and enhancing the surfaces of the adsorbents. For the purpose of understanding adsorbent behaviour and equipment design, it is important to be able to distinguish between physisorption and chemisorption. The heat of adsorption can be used as an indicator to determine whether physisorption or chemisorption occurs. The heat of adsorption for physisorption of CO_2 ranges from -25 to -50 kJ/mol. The heat of adsorption for chemisorption of CO_2 ranges from -60 to -100 kJ/mol depending on the adsorbent used (Berger & Bhown, 2011). The nature of the adsorption is dependent on the heat of adsorption, temperature pressure and the nature of the adsorbate and adsorbent.

Table 2.1: Characteristics associated with physisorption and chemisorption (Adapted from (Fletcher, 2008) and (Berger & Bhown, 2011))

	Physisorption	Chemisorption
Heat of Adsorption (kJ/mol)	- 25 to -50	60 to -100
Rate of Adsorption (273 K)	Fast	Slow
Effect of temperature increase on adsorbate uptake	Decreases	Increases
Desorption	Easy- by reduced pressure or increased temperature	Difficult - high temperature required to break bonds
Desorbed Species	Adsorbate unchanged	May be different to original adsorptive
Specificity to gases	Non-specific	Very Specific
Monolayer Coverage	Mono or multilayer condition dependent	Monolayer

a) Adsorption Isotherms and Adsorption Equilibria

The adsorption process is commonly described through adsorption isotherms. Adsorption isotherms are the function of gas adsorbed onto an adsorbent at a constant temperature and equilibrium partial pressure. The quantity of gas that is adsorbed is nearly always given relative to the mass of the adsorbent used; the purpose of this being to allow for a comparison of different materials. Adsorption isotherms can be used to predict the behaviour of adsorption systems because they are governed by the type of adsorption that occurs. Adsorption isotherms represent the equilibrium relationship between the adsorbent and adsorbate at any given temperature. Fletcher reported six types of adsorption isotherms according to Brunauer, Emmett and Teller (BET) theory. Fletcher states that all adsorption isotherms should fit one or a combination of the six recognised types classified (Fletcher, 2008).

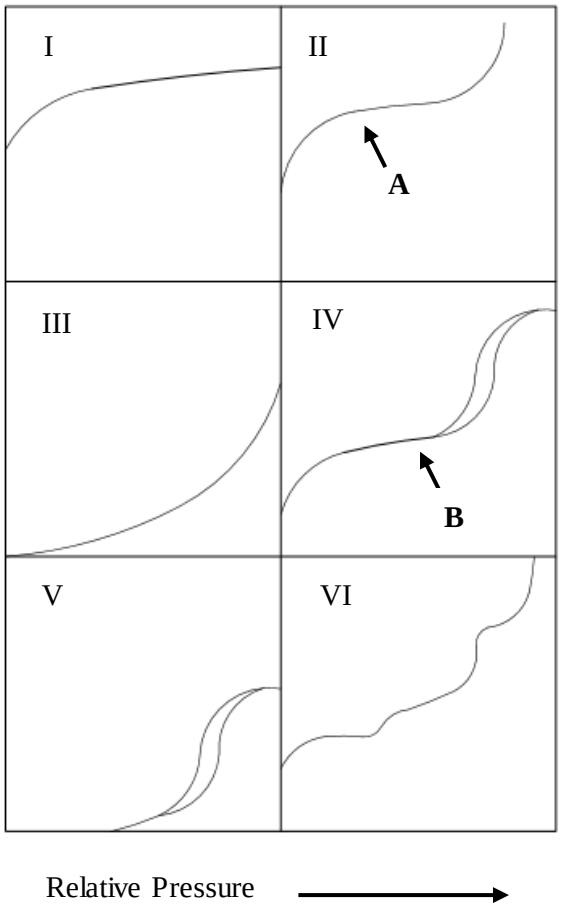

Figure 2.9: Possible adsorption isotherms according to the BET theory (Adapted from (Fletcher, 2008))

Type I: This adsorption isotherm is typical to monolayer adsorption. Adsorbents that give Type I adsorption isotherms are microporous (having predominantly micropores). In this type of adsorption, a single layer of adsorbate forms on the surface of the adsorbent.

Type II: This adsorption isotherm is typical to multilayer adsorption. Adsorbents that give Type II adsorption isotherms can be both micro and macroporous (having both micropores and macropores). Single layer coverage is followed by multilayering of the adsorbate on the surface of the adsorbent. The inflection point (see point A on Figure 2.9) is a result of the completion of the single layer and the initiation of the multilayer adsorption.

Type III: This adsorption isotherm is typical to weak interactions between the adsorbent and adsorbate. Adsorbents that give Type III adsorption isotherms are non-porous or microporous. Type III adsorption isotherms are unfavourable as they are caused by weak interactions between the adsorbent and adsorbate which leads to slow adsorption.

Type IV: This adsorption isotherm is typical to adsorption where the adsorbate condenses inside the adsorbent pores. Adsorbents that give Type IV adsorption isotherms are mesoporous (having predominantly mesopores). As with Type II adsorption isotherms, the inflection point (see point B in Figure 2.9) confirms that monolayer adsorption is followed by multilayer adsorption. The difference is that type IV adsorption isotherms show a hysteresis loop which is due to the condensation that occurs inside the pores of the adsorbent.

Type V: This adsorption isotherm is typical to adsorption that is a combination of both Type III and Type IV. Adsorbents that give type V isotherms are microporous.

Type VI: This adsorption isotherm is typical to adsorption where a double phase transition occurs, for example, the adsorbate changes from a gas to liquid and liquid to solid during adsorption. This type of isotherm was introduced primarily as hypothetical with very few known examples. The shape of this isotherm is due to the formation of single layers of adsorption before progressing to subsequent layers. Each point of inflection indicates the completion of a single layer of adsorption (Fletcher, 2008, Berger & Bhown, 2011 and Crittenden & Thomas, 1998).

When the adsorbent and adsorbate are contacted for long enough an equilibrium will be established and no more adsorbate will be adsorbed. Adsorption equilibrium is an important aspect to consider when designing adsorption systems and is represented by adsorption isotherms. There are several adsorption equilibria theories and these include the Langmuir theory, the BET theory, the Freundlich theory, the Polanyi Potential theory and the Temkin theory amongst others. This study will focus on the Langmuir and BET theories as they are the most relevant to this study.

The Langmuir Theory: Type I adsorption isotherms are characteristic of the Langmuir theory, and in other literature are described as Langmuir isotherms. This isotherm can describe adsorption systems in which there is only a single layer of adsorbate covering at or before the relative pressure of unity is reached (Fletcher, 2008). The single layer coverage means that this adsorption isotherm can used to describe chemisorption and can be extended to describe binary adsorbate systems (Crittenden & Thomas, 1998). This theory assumes a dynamic equilibrium between the adsorbed phase and the gas phase. The rate at which the adsorbate strikes the adsorbent surface is proportional to the product of the partial pressure (P)

of the gas and a fraction $(1-\theta)$ of the adsorbent surface remaining uncovered and therefore available as adsorption sites. An important assumption of the Langmuir theory is that it assumes that all sites are probable for adsorption to occur. The Langmuir theory also covers desorption. Langmuir theory predicts that the rate of desorption of adsorbate from the adsorbent surface is directly proportional to the fractional surface coverage (θ) and that the adsorption and desorption rates are equal at equilibrium (Crittenden & Thomas, 1998).

$$k_a P(1-\theta) = k_d \theta \qquad (2.4)$$

Where k_a and k_d are the adsorption and desorption constants respectively.

The more common form of equation 2.4 is:

$$\theta = \frac{q}{q_m} = \frac{bP}{(1+bP)} \qquad (2.5)$$

Where, q is the adsorbate adsorbed, q_m is the total quantity (q) of adsorbate that could potentially be adsorbed in a single monolayer and $b = ka/kd$

The BET theory: Type II and Type IV isotherms are characteristics of BET theory. The BET theory is an extension of Langmuir theory in that it accounts for the existence of multilayer adsorption. Accounting for the existence of multilayer coverage means that this adsorption isotherm can be used to describe physisorption of gas molecules onto adsorbent surface. This theory is also commonly used to determine the specific surface areas of different porous materials. This theory uses the same assumptions of the Langmuir theory as well as assumes that there can be infinite multilayers, each layer is independent of other layers, there is no interaction between layers and the Langmuir theory can be applied to each layer. Based on these assumptions the equations used in Langmuir theory have been extended for BET theory:

$$\frac{1}{v\left[\left(\frac{P_s}{P}\right)-1\right]} = \frac{c-1}{v_m c}\left(\frac{P_s}{P}\right) + \frac{1}{v_m c} \qquad (2.6)$$

Where, P_s and P are the saturation pressure and equilibrium pressure of the adsorbate molecules at the adsorption temperature respectively. v is the adsorbed quantity of gas in volume units. v_m is the single layer of adsorbed gas and c is the BET constant and is given by $c = \exp\left[\frac{E_1 - E_L}{RT}\right]$ where E_1 is the heat of adsorption of the first layer and E_L is the heat of adsorption for the second layer and higher layers and is equal to the heat of liquefaction. R is the gas constant and T is the temperature.

b) Adsorption – Desorption Cycles

Desorption is the process whereby the adsorbent is regenerated by rendering it adsorbate free, and ready for the next adsorption cycle. In CO_2 capture both the adsorption and desorption processes should be studied as they are both important in the separation of CO_2. Regeneration of the adsorbent allows for the CO_2 capture process to be cyclic. Several desorption methods which can be used for CO_2 adsorption exist. The various adsorption desorption cycles are pressure swing adsorption (PSA), temperature swing adsorption (TSA), electric swing adsorption (ESA) and vacuum swing adsorption (VSA). PSA and TSA are the two main methods and will be discussed below.

Pressure Swing Adsorption: Pressure swing adsorption is dependent on the variation of pressure inside the adsorption column. Increasing pressure results in the adsorbate molecules interacting more with the adsorbent surface. At higher partial pressures the kinetic energy of the adsorbate molecules is increased and favours the adsorption of the adsorbate onto the adsorbent. The adsorption takes place at high pressures and low temperatures. Once equilibrium has been reached the adsorbent is then regenerated by stopping the gas flow and reducing the pressure (Monoj & Mondal, 2012). The decrease in pressure leads to the decrease in the partial pressure of the adsorbate which favours desorption. Adsorption desorption cycles can thus be controlled by controlling the pressure inside the packed column.

Temperature Swing Adsorption: Temperature swing adsorption is dependent on the variation of temperature inside the adsorption column. Decreasing temperature results in the adsorbate molecules adsorbing to the surface of the adsorbent due to the exothermic nature of adsorption. The adsorption takes place at low temperature and low/ambient pressure. Once equilibrium has been reached the adsorbent is then regenerate by stopping the gas flow and increasing the temperature (Monoj & Mondal, 2012). The increase in temperature leads to the endothermic process being favoured based on Le Chatlier's principle. The endothermic process is the desorption of the adsorbate. The adsorption desorption cycles can thus be controlled by controlling the temperature inside the packed column.

PSA is more commonly used than TSA because the PSA process gives shorter time periods of cycles and has a slightly lower operational cost. The shorter time periods of cycles associated with PSA is since TSA requires more time to heat up and cool down the adsorbent bed. This heating of the adsorbent bed increases the energy requirements and thus makes TSA more expensive than PSA (Thomas & Crittenden, 1998). However, PSA is not always more favourable than TSA. TSA is preferred when the adsorbate is strongly fixed to the adsorbent surface or if there only need be slight temperature change between adsorption and desorption cycles as the energy requirements will not be as significant (Thomas & Crittenden, 1998). Thus,

the choice between the use of TSA and PSA should be made after taking the entire system and its requirements into consideration.

At industrial scale, packed bed columns are used to remove CO_2. The solid adsorbent material is used to pack the column. The CO_2 rich flue gas is fed at the bottom of the packed column and flows up contacting the adsorbent. The CO_2 moves from the gas phase to the solid phase. Numerous packed columns are used and are arranged adjacently to enable a continuous process. One packed column will adsorb CO_2 and when that adsorbent has reached equilibrium the flue gas will be rerouted to the next packed column and first packed bed will be desorbed and the adsorbent regenerated.

2.4.2. Factors influencing Post Combustion CO_2 Capture via Adsorption

The efficiency of the adsorption capture process is influenced by several factors. These factors are temperature, pressure, flue gas composition and the nature of the adsorbent used. These factors influence the adsorption and determine the magnitude of the adsorption that occurs. These factors will be discussed in the following paragraphs.

The temperature of the flue gas stream is an important factor for post-combustion CO_2 capture via adsorption. The temperature will influence the type of adsorption that occurs, be it physisorption or chemisorption. Recall that chemisorption has a higher heat of adsorption and thus occurs at higher temperatures than physisorption (Thomas & Crittenden, 1998). At equilibrium, a temperature increase will result in a decrease in the magnitude of CO_2 adsorbed. Conversely, a decrease in temperature will increase the magnitude of CO_2 adsorbed. This is due to the exothermic nature of adsorption. Le Chatlier's principle explains this, with an exothermic process an increase in temperature will decrease the rate of exothermic reaction. Fogler states that with chemisorption the magnitude of the adsorption will initially increase to a maximum with an increase in temperature and will decrease thereafter (Fogler, 2010). Fogler suggests that this is because with chemisorption the activation energy must be achieved first, thereafter the reaction occurs and the subsequent decrease is attributed to exothermic nature of the reaction (Fogler, 2010).

The pressure of the flue gas stream is an important factor for post-combustion CO_2 capture via adsorption. The pressure will influence the magnitude of the CO_2 adsorbed. The magnitude of the CO_2 adsorbed and the pressure of the flue gas are directly proportional. The higher the partial pressure of the CO_2 adsorbed the more CO_2 adsorbed. Conversely, the lower the partial of the CO_2, the less CO_2 adsorbed (Keller & Staudt, 2005).

The flue gas composition is an important factor for post-combustion CO_2 capture via adsorption. The higher the CO_2 concentration the easier adsorption will be. The converse is true, the lower the CO_2 concentration

the more difficult the adsorption will be. It is possible for impurities to be present in the flue gas which will also affect the magnitude of the CO_2 adsorbed.

The nature of the adsorbents is an important factor for post-combustion CO_2 capture via adsorption. The nature of the adsorbents refers to all the properties of the adsorbent such as surface geometry, chemistry of the adsorbent and the physical form of the adsorbent (Thomas & Crittenden, 1998). The more favourable these properties are for adsorption, the greater the magnitude of adsorption. For example, for physisorption, the greater the surface area the greater the magnitude of adsorption (Ngoy et al., 2014). For chemisorption, the chemistry of the adsorbent refers to the functional groups and affects the adsorption because different functional groups have affinity for different components of the flue gas.

2.4.3. Types of Adsorbents for CO_2 Capture

An adsorbent is the solid material that is used to target and remove adsorbate molecules from the bulk fluid in an adsorption process. It is important that the adsorbate be effectively removed from the bulk fluid as this is the target of any separation process. The efficiency and economic viability of the adsorption process is dependent on the adsorbent used. Recently, extensive research has been conducted on designing adsorbents that would be suitable to use for CO_2 capture. For an adsorbent to be effective it must be cost effective, can adsorb CO_2 efficiently at moderate operating conditions, have no adverse effects on the environment and be moisture and impurity (SO_x and NO_x). In addition, the following properties are expected of a good adsorbent.

High surface area: A large surface area is a desirable characteristic of an adsorbent because it implies the more space there is for the adsorbate to adsorb to.

High pore volume: Pore volume is the ratio of air volume to the total volume of a porous material and is an indication of the free space available inside the porous material. A high pore volume is a desirable property of an adsorbent because it implies that there is more space available for adsorption to occur.

Good pore size: Porosity is the collective term that is given to these pores and their distribution in the structure of a solid. Pores are the minute openings in solids that are accessible to gases. Pore size refers to the diameter of the pores (Mosher, 2011). Pore size is an important characteristic for adsorption for two reasons, the first being that different gases display different particle sizes based on the intramolecular forces and bond strengths experienced. For adsorption to take place it is necessary for the gas particles to be able to enter into the pores of the adsorbent. If the gas particle is too large for the pores, then adsorption is less likely to occur. The second reason that pore size is important for the determination of a good adsorbent is that different pore sizes have been shown to behave differently during adsorption. For example, micropores

(width not exceeding 2 nm) will primarily experience physisorption at a pore-filing stage only. This differs to mesopores (width between 2 nm and 50 nm) and macropores (width exceeding 50 nm) which show multilayer adsorption. Mesopores have been shown to be the best for CO_2 gas adsorption (Mosher, 2011). Surface area, internal volume and pore size are referred to as the surface geometry of the adsorbent and are commonly measured using N_2 physisorption at 77 K.

High adsorption capacity***:*** Gray et al. suggests that for adsorbents to be competitive with conventional amine-based adsorbents they should achieve a CO_2 adsorption capacity of 3 – 6 mol CO_2/kg adsorbent (or 132 – 264 g CO_2/kg adsorbent) (Gray et al., 2008).

High selectivity for CO_2**:** Flue gas contains only 10 – 15 % CO_2 gas, with O_2, N_2, moisture and various other impurities making up the remainder (Saha et al., 2012). An ideal adsorbent should selectively adsorb CO_2 over other flue gas components. The degree of selectivity achieved has a direct impact on the purity of the CO_2 and thus subsequent pumping and storage processes.

Fast adsorption/desorption kinetics**:** The adsorption/desorption kinetics give a measure of the rate at which the adsorbent will adsorb and desorb CO_2. This gives an indication of the overall separation performance of the adsorbent at the specific working conditions. For fixed-bed reactors, faster kinetics can reduce cyclic operation time as well as reduce the amount of adsorbent required for per volume of flue gas (Zhao , 2012).

Sufficient recyclability and cyclic stability: It is important that the adsorbent can be regenerated and recycled. The recycled adsorbent should maintain its adsorption capacity. The adsorbent must be able to be used for many cyclic operations without noticeable deteriorations in performance.

Mechanical strength**:** The adsorbent must have suitable microstructure and morphology under several different operating conditions in order to overcome attrition, thermal degradation and mechanical abrasion.

Thermally Suitable: The adsorbent must be thermally suitable at industrial adsorption/desorption temperatures.

Economical synthesis process: The synthesis process and raw materials required to produce the adsorbent should be simple, easy to scale up and inexpensive in order to compete with existing CO_2 capture technologies.

Finding an adsorbent that can satisfy all these characteristics is still a challenge for CO_2 capture. There are several proposed adsorbents that are being researched for CO_2 capture (Lee & Park, 2015; International Energy Agency, 2016; Berger & Bhown, 2011 and Bolland, 2014). These adsorbents are classified as either non-carbonaceous or carbonaceous and have different properties.

2.4.2.1. Non-Carbonaceous Adsorbents

Non-carbonaceous adsorbents are characterised by the fact that they do not contain the element carbon in their chemical structures. Examples of non-carbonaceous adsorbents are zeolites and silica materials.

Zeolites

Zeolites are three-dimensional porous crystalline aluminosilicates which are composed of alkali and alkaline earth elements, such as sodium, potassium, and calcium (Hardie et al., 2005). Different types of zeolites can be synthesized by alteration of Si/Al ratio during the synthesis process to give different zeolites that are suitable for different processes. Zeolites possess certain characteristics which have made them desirable for gas separation. Zeolites are commonly used in industry as selective catalysts, ion exchangers and adsorbents (Yang, 1997). Zeolites are currently being extensively studied for CO_2 capture due to their desirable properties as adsorbents. These characteristics include, uniform molecular pore size (generally about 3 to 8 Å), high adsorption capacity, reversible and selective gas adsorption (Hardie et al., 2005).

The crystalline lattice structure of zeolites makes them polar. This gives them a high affinity for other polar molecules such as H_2O (Hardie et al., 2005). CO_2 adsorption studies on zeolites have shown the primary mechanism of adsorption to be physisorption. Although chemisorption has been shown to occur which makes desorption difficult (Spigarelli, 2013). Spigarelli reports that the adsorption capacity of zeolites ranges from 4 - 216 g CO_2/ kg zeolite, with moderate operating conditions (temperatures ranging 0-100 ºC and pressure ranging from 0.1 - 1 bar) (Spigarelli, 2013). However, zeolites have a greater affinity for H_2O than for CO_2 because of their polar nature. It has been reported that the CO_2 adsorption capacity of zeolites drops significantly in the presence of moisture (Crittenden & Thomas, 1998). A summary of the advantages and disadvantages associated with zeolites is given in Table 2.2.

Table 2.2: Advantages and disadvantages of zeolites (Adapted from (Crittenden & Thomas, 1998), (Hardie et al. 2005) and (Spigarelli, 2013))

Advantages		Disadvantages	
i)	Favourable adsorption kinetics	i)	Presence of impurities (NOx, SOx, and H_2O) significantly impact performance
ii)	High adsorption capacity at mild operating conditions (0-100 ºC, 0.1-1 bar)	ii)	CO_2 has been shown to chemisorb to the zeolite surface
iii)	Suitable for post-combustion CO_2 capture	iii)	For complete regeneration, desorption must occur via the energy and time intensive TSA

Silica Materials

Silica materials are based on silica (SiO_2) and are a relatively new technology for CO_2 capture. Silica materials possess certain properties which have made them desirable for gas separation. These characteristics include high surface area, high internal pore volumes, desirable thermal stability, desirable mechanical strength, desirable chemical stability and pore size that can be manipulated. Most applications of silica materials for CO_2 capture make use of silica material that has been impregnated or grafted with amines.

Amine functionalised silica materials are adsorbents which consist of a solid silica support onto which an amine has been immobilized or impregnated or grafted. The impregnation or grafting of amines onto a solid support deals with the major issues with amine adsorption such as high regeneration costs (from the large volume of liquid associated with absorption), equipment corrosion and loss of amine solvents due to evaporation. The most commonly used amine has been poly(ethyeneimine) (PEI). This amine was chosen due to its high amine concentration, roughly 33 % NH_2 by weight.

Silica materials show chemisorption, indicating that desorption will require a larger energy input. Also the amines undergo irreversible reactions with SO_x and NO_x to produce unwanted products (Spigarelli, 2013). Studies examining amine loaded MCM-41 and SBA-15 silica supports showed a 4-9 % loss in the CO_2 adsorption capacity of the regenerated adsorbent (Spigarelli, 2013). Adsorption capacities for amine functionalised silica materials at moderate operating conditions (0.05-1 bar and 25-75 ºC) range from 0.089 – 0.22 g CO_2 / kg adsorbent (Spigarelli, 2013). Although their CO_2 adsorption capacity it low, it has also been found adsorption capacity is not greatly affected by CO_2 partial pressure (Spigarelli, 2013). This makes then extremely suitable for post-combustion CO_2 capture. A summary of the advantages and disadvantages associated with silica materials is given in Table 2.3.

Table 2.3: Advantages and disadvantages of silica materials (Adapted from (Spigarelli, 2013))

Advantages		Disadvantages	
i)	Adsorption capacity minimally impacted by CO_2 partial pressure	i)	Degrade at temperatures around 100 ºC
ii)	Humid environments improve adsorption efficiency	ii)	Irreversible reactions with NO_x and SO_x produce unwanted by products
iii)	Favourable adsorption kinetics	iii)	4-9 % loss in adsorption capacity after desorption

2.4.2.2. Carbonaceous Adsorbents

Carbonaceous adsorbents are materials that are carbon based. Carbon offers several advantages as an adsorbent. These include, light weight, good mechanical strength, desirable electrical and heat conductivities, high thermal stability. One of the most significant advantages that carbon adsorbents give is that they are not affected by the presence of moisture. Carbon is a moderately inexpensive raw material when compared with non-carbonaceous adsorbents and due to its ability to operate at moderate pressures and temperatures it will also consume less energy when compared to non-carbonaceous adsorbents. Examples of carbonaceous adsorbents are activated carbon, carbon molecular sieves (CMSs), carbonized polymers and resins, metal organic frameworks (MOFs), carbon nanotubes (CNTs), porous polymers and amine impregnated CNTs.

Activated Carbon

Activated carbons are carbonaceous materials that have been treated with oxygen to form pores. Pores increases the surface area and allows for more CO_2 adsorption to occur (JECFA, 1992). Activated carbon comes in the form of black powder or granules and can be formed from a variety of carbon containing materials. It is advantageous that there is such a variety of raw materials. Activated carbon made from different sources do have differences in surface geometry. This has led to a wide variation in the CO_2 adsorption performance of different activated carbon.

CO_2 adsorption with activated carbon occurs via physisorption and the CO_2 adsorption capacity decreases with an increase in temperature. Activated carbons adsorb most efficiently at room temperature. The adsorption capacity of activated carbon at mild operating conditions (0.1 – 1 bar and 25 – 75 ºC) has been shown to be in the range of 3 – 154 g CO_2/kg activated carbon. At much higher pressures of 35 bar activated carbon was shown to have an adsorption capacity as high as 1130 g CO_2/kg activated carbon (Spigarelli, 2013)). This suggests that activated carbon has a good potential for CO_2 capture from gas streams with high pressure, such as pre-combustion and can be used for PSA. A disadvantage to activated carbons is that the CO_2 adsorption capacity has been shown to be negatively affected by the presence of NO_x, SO_x and moisture despite its hydrophobic nature. A summary of the advantages and disadvantages associated with activated carbon is given in Table 2.4.

Table 2.4: Advantages and disadvantages of activated carbons (Adapted from (JECFA, 1992) and (Spigarelli, 2013))

Advantages	Disadvantages
i) High thermal stability	i) Low CO_2 capacity at mild conditions
ii) Favourable adsorption kinetics	ii) Negatively impacted by NO_x, SO_x, and H_2O
iii) Wide range of starting materials for production of activated carbons Leads to lower raw material costs	iii) Wide variety of starting materials means a wide variety of pore characteristics is often seen between adsorbents
iv) Large adsorption capacity at elevated pressures	
v) Desorption can easily be accomplished by PSA	

Carbon Molecular Sieves, Carbonized Polymers and Resins

It is possible to manipulate the structure of activated carbons to produce carbon molecular sieves. Activated carbon is manipulated by coating the pore mouths with a carbonized or coked thermosetting polymer. This creates an adsorbent that has desirable adsorption kinetics and selectivity, however the adsorption capacity is somewhat lower than for activated carbons (Crittenden & Thomas, 1998).

Carbonized polymers and resins are produced from resins such as phenol formaldehyde and sulphonated styrene amongst others (Crittenden & Thomas, 1998). These resins are pyrolysed to produce carbonaceous adsorbents that have either micro, meso or macro pores. Applications of these carbonaceous adsorbents for the removal of organic compounds from water have been reported (Crittenden & Thomas, 1998). These adsorbents are still under research for applications in CO_2 capture but tend to be more hydrophobic than activated carbons which could potentially make them more suitable for use as an adsorbent for CO_2 capture.

Metal Organic Frameworks (MOFs)

MOFs are defined as three-dimensional microporous crystalline structures that are composed of transition elements such as cobalt, nickel, copper, zinc and organic linkers (Saha et al., 2012). MOFs possess certain properties that have made them desirable for gas separation and are commonly used in industry for separation, nonlinear optics and gas storage (Spigarelli, 2013).

The properties that make MOFs desirable for gas separation also make them desirable as adsorbents for CO_2 capture. These properties stem from the fact that when synthesising MOFs it is possible to manipulate parameters such as pore size and topography. MOFs have been reported to show physisorption rather than chemisorption. This means that desorption will be less energy intensive (Saha et al., 2012). Studies have shown that MOFs exhibit poor adsorption characteristics at low CO_2 partial pressure (Arstad et al., 2008). Milward et al. performed CO_2 adsorption with MOF-177 at room temperature and 35 bar and reported a CO_2 adsorption capacity of 1470 g CO_2 / kg MOF (Millward & Yaghi, 2005). This suggests that MOFs have good potential for CO_2 capture from gas streams with high pressure, such as pre-combustion and can be used for PSA. Although MOFs have enormous potential as adsorbents for CO_2 capture, there are major challenges that inhibit their use. These challenges include a high raw material cost, relatively complicated synthesis process and have a greater affinity for H_2O than for CO_2. In addition, it has been found that the CO_2 adsorption capacity of MOFs drops significantly in the presence of moisture and other impurities (SO_x and NO_x) (Crittenden & Thomas, 1998). A summary of the advantages and disadvantages associated with MOFs is given in Table 2.5.

Table 2.5: Advantages and disadvantages of MOFs (Adapted from (Arstad et al., 2008, Crittenden & Thomas, 1998, Millward & Yaghi, 2005 and Spigarelli, 2013))

Advantages	Disadvantages
i) High porosity	i) Presence of impurities (NOx, SOx, and H_2O) significantly impact performance
ii) High adsorption capacity at elevated pressures	ii) Low CO_2 adsorption capacity at low CO_2 partial pressures
iii) Ease of manipulation of pore characteristics	iii) High cost associated with raw material
	iv) High cost associated with operating at elevated pressures

Carbon Nanotubes

CNTs are cylinders of carbon which have the appearance of rolled tubes of graphite. CNTs are characteristically a several microns in length and a nanometer wide. CNTs have the potential to be good adsorbents for CO_2 capture because they are highly porous (Ferrari, 2011) and the structure of the nanotube allows for the possibility of the occurrence of adsorption both on the inside and outside of the nanotube (Ferrari, 2011), thus allowing for the increased adsorption of CO_2. CNTs are also hydrophobic (due to carbon

nature) and highly thermally suitable. When correctly functionalized and impregnated or grafted CNTs can have a strong selectivity for CO_2. The use of CNTs in CO_2 capture is currently being researched and is also considered in this study.

There are two main types of CNTs that are considered for CO_2 capture. These are single-walled carbon nanotubes (SWCNTs) and multi-walled carbon nanotubes (MWCNTs). There is a physical difference between the CNTs. SWCNTs are made up of one single layer of graphene cylinders, whilst MWCNTs are made up of several layers of graphene cylinders nested inside one another. Ganesh reported that there are approximately 50 cylinders in MWCNTs (Ganesh, 2013). The structural difference between SWCNTs and MWCNTs is depicted in Figure 2.10.

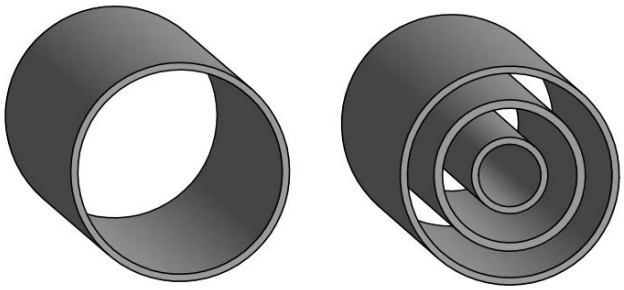

SWCNTs MWCNTs

Figure 2.10: Structural illustration of SWCNTs and MWCNTs (Adapted from (Dresselhaus et al., 2005))

The difference in structure gives SWCNTs and MWCNTs different characteristics that can either be advantageous or disadvantageous depending on the operation under consideration. For example, having more layers allows MWCNTs to have a larger surface area than SWCNTs but makes MWCNTs more complex than SWCNTs. This complexity leads to difficulty in understanding the properties of MWCNTs as compared with SWCNTs. In general, MWCNTs are considered to have many structural defects which gives rise to many regions of structural imperfections that could negatively affect the properties (Dresselhaus et al., 2001). These structural defects can cause a wide variation of adsorption performance between adsorbents. Osler et al. (2007) compared the characteristics and adsorption performance of SWCNTs and MWCNTs with respect to CO_2 capture. It was found that the SWCNTs showed approximately a 150% increase in CO_2 adsorption capacity when compared to MWCNTs. However, the higher cost of the SWCNTS is a mitigating factor when compared with MWCNTs (Osler et al., 2017).

A challenge facing the use of CNTs for use as an adsorbent for CO_2 capture is that CNTs have no affinity for CO_2 and will not selectively remove CO_2 from a mixed gas stream. The solution to this problem is to functionalize or impregnate CNTs with amines that have a higher affinity for CO_2 (Bullis, 2009). CNTs have characteristics that allow for the easy modification thus making functionalization and impregnation or grafting possible (Ferrari, 2011).

Porous Polymers

Porous polymers are porous solid materials that are synthesised from organic monomers. These polymers can be formed using inexpensive methods and there is vast potential to engineer porous polymers with a broad range of surface geometry. Porous polymers can be engineered to have a variety of chemical and biological agents present which can add different, interesting and useful functionalities. Porous polymers are biodegradable and non-toxic in nature because they are organic (Ngoy et al., 2014). Porous polymers could potentially have an application as adsorbents for CO_2 capture. Given that it is possible to synthesis infinite types of polymers and that these polymers can be engineered it is thus possible to conclude that it is possible to use porous polymers for CO_2 capture.

Amine Impregnated Carbon Nanotubes

Amine impregnation or grafting can be used to improve the surface chemistry of solid adsorbents. Builes and Vega (2013) define impregnation as a physical mixture of the amine and support and grafting as a process where a chemical bond is formed by the amine and the support. In order to improve the surface chemistry, the adsorbent is treated with chemicals in order to alter the properties such that the CO_2 adsorption will improve in terms of adsorption capacity, selectivity and moisture tolerance. Research has shown that the most promising adsorbent modification can be achieved by grafting or impregnating amines. The impregnation or grafting of amines onto a solid support deals with the major issues with amine adsorption such as high regeneration costs (from the large volume of liquid associated with absorption), equipment corrosion (due to the corrosive nature of amines) and loss of amine solvents due to evaporation. The most commonly used amine has been poly(ethyeneimine) (PEI). This amine was commonly chosen due to its high amine concentration, roughly 33 % NH_2 by weight.

Research has shown that grafting or impregnating amines onto the surface of a carbon nanotube (CNT) enhances the adsorption capacity of the CNT. Lee and Park (2015) reported that impregnating Polyethyleneimine (PEI) onto MWCNTs increased their CO_2 adsorption capacity by 200%. In the same vein, Ngoy et al. (2014) reported that grafting polyaspartamine onto MWCNTs increased their CO_2 adsorption capacity by nearly 500 %. In addition, Su and Chen (2011) demonstrated that a MWCNT/3-

aminopropyltriethoxysilane (APTS) composite adsorbent displayed good CO_2 adsorption performance, and displayed a low theoretical energy of desorption and superior cyclic stability.

Various polymers have been investigated for use in CO_2 capture. Amines impregnated or grafted on adsorbents are beneficial for CO_2 capture, but come with an environmental and health risk, that is already associated with CO_2 absorption. It is thus essential that the synthesized adsorbent materials be biodegradable and non-toxic. For example, PEI is the commonly utilized polymer because it has a large quantity of amine groups present which as previously shown is very beneficial for CO_2 capture. However, PEI is not biodegradable and is extremely toxic (Ngoy et al., 2014). Research has been conducted on developing biodegradable nontoxic polymers that can be used for CO_2 capture. This study proposes chitosan, a biodegradable non-toxic polymer that has the potential to be one such polymer due to the presence of amine groups.

2.5. Chitosan

Chitosan is a biodegradable non-toxic polymer most commonly derived from chitin. Chitin is naturally occurring and abundant in the exoskeletons of arthropods such as crustaceans, i.e. crabs, shrimps and lobsters (Kiruba et al., 2013). These exoskeletons would otherwise be considered as waste material and as such their use in CO_2 capture cannot only help mitigate climate change but help mitigate surface waste pollution. Chitin is the second most abundant polymer, after cellulose and its natural production is inexhaustible (Abdou et al., 2008). The arthropods that are composed of chitin make up 10^6 species of the 1.2×10^6 of the total species in the animal kingdom. Chitin is white in appearance, hard and inelastic in nature and is characterised as a nitrogenous polysaccharide polymer and consists of 2-acetamido 2-deoxy-β-D-glucose through a β (1→4) linkage (Abdou et al., 2008). Even though nitrogen is present in the chain, this polymer is regarded as cellulose in the hydroxyl C-2 replaced by an acetamido group.

The polymer derived from chitin and proposed for this study is chitosan. Chitosan is a linear aminopolysacchride of (1→4) linked N-acetyl glucosamine and glucosamine units. Like the chitin it is derived from, it is white in appearance, hard and inelastic in nature and is characterised as a nitrogenous polysaccharide (Divya et al., 2014).

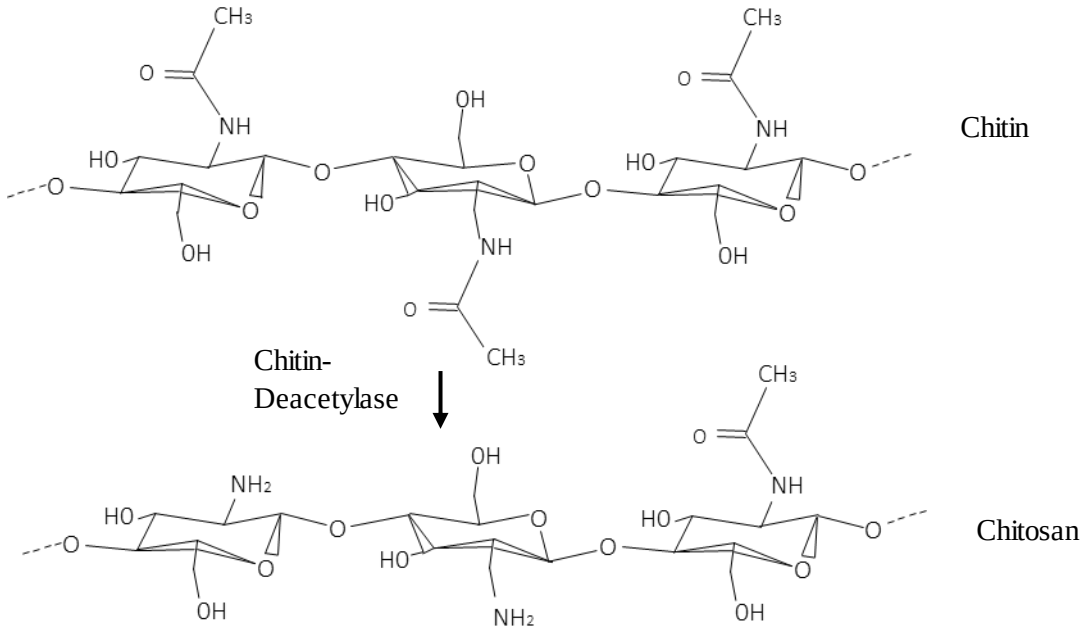

Figure 2.11: Schematic diagram of synthesis of chitosan from chitin (Adapted from (Younes & Rinaudo, 2015))

Figure 2.11 gives a schematic of the synthesis of chitosan from chitin. The synthesis process of chitosan from chitin involves four steps, namely, deproteinisation, demineralisation, decolourisation and deacetylation (DDA) (Kiruba et al., 2013 and Divya et al., 2014). The DDA is highly relevant when synthesizing chitosan for CO_2 capture because, as the acetyl group is removed, the number of NH_2 group's present increases and thus the available sites for CO_2 adsorption increase the relationship between DDA and CO_2 adsorption capacity of chitosan will be considered in this study.

Chitosan finds a variety of applications due to its high biodegradability, non-toxicity and antimicrobial properties. It is used in biomedical industries, agriculture, genetic engineering, food industry, environmental pollution control, water treatment, paper manufacture, photography and so on (Divya et al. 2014). While chitosan has not been extensively studied as an adsorbent for CO_2 capture it contains many glucosamine functional groups which will be able to chemisorb CO_2.

Sneddon et al. prepared CO_2 adsorbents by coating chitosan onto mesoporous silicas. The CO_2 adsorption capacity of these chitosan based adsorbents was found to be between 12.76 – 43.12 gCO_2/kg adsorbent using 100 % CO_2, a pressure of 1 atm and a temperature of 20 ºC (Sneddon et al., 2015). Fujiki and Yogo prepared chitosan-derived activated carbon adsorbents. The prepared adsorbent showed an extremely high

CO_2 adsorption capacity of 70.4 gCO_2/kg adsorbent, however the experiments were performed at 25 ºC and 15 kPa (Fujiki and Yogo, 2016). The adsorption pressure of 15 kPa is much higher than the pressure of flue gas which is usually close to atmospheric pressure. To avoid the high cost associated with operating at such high pressures it would be necessary to understand the CO_2 adsorption capacity of chitosan at pressures near atmospheric. However, the CO_2 adsorption capacity of pure chitosan at lower partial pressures has not been extensively reported in open literature. This research effort aims to determine if chitosan would be suitable to use as an adsorbent for CO_2 capture at moderate temperatures and pressures.

2.6. Understanding the Adsorption Mechanism of Chitosan and Chitosan Impregnated Carbon Nanotubes

Porous polymers and amine impregnated solid adsorbents have become a popular and promising potential adsorbent for CO_2 capture. This research study focuses on chitosan (porous polymer) and chitosan impregnated CNTs (amine impregnated solid adsorbents) for use in CO_2 capture. In order to better understand the potential of these adsorbents, it is necessary to understand the method by which they adsorb CO_2.

Chitosan should in theory undergo chemisorption due to the presence of amine groups, which act as the anchoring site that the CO_2 will attach to. CO_2 is slightly acidic and will react with the alkaline amines to form weak intermediate carbamates (-COO-) (Ngoy et al., 2014). Due to the formation of chemical bonds chitosan undergoes chemisorption. This results in a larger energy requirement for desorption. There are many reaction methods for the chemisorption of CO_2. This study considers the reaction between CO_2 and the amine group (NH_2) to form carbamate. This reaction is given by equation 2.7:

$$CO_2 + 2RNH_2 \leftrightarrow RNH_3^+ + NHCOO^- \quad (2.7)$$

Chitosan impregnated CNTs should in theory undergo both chemisorption and physisorption. Chemisorption will occur due to the formation of carbamate from the reaction between CO_2 and amines. Physisorption will occur on the surface of the CNTs where chitosan has not been impregnated. It is expected that the large surface area of the CNTs combined with the porous chitosan will produced a suitable adsorbent for CO_2 capture.

2.7. Statistical Modelling using RSM

Response surface methodology (RSM) is a collection of mathematical and statistical techniques for the development of empirical models to describe a system. The objective of RSM is to optimize the response of a system (output variable) that is influenced by several independent input variables. This is achieved by two steps; the first is the careful plan of experiments where the response is to be evaluated in order to obtain the data to develop the model. The second is the choice of an approximate empirical model that will describe

the experimentally observed behaviour. The empirical model is determined from experimental data. Thus the efficiency of the empirical model is dependent on the accuracy of the designed experiment.

An important aspect of RSM is the design of experiments (DoE) and the interpretation of the results. DoE is defined as the planned approach for determining cause and effect relationships. DoE is a sequence of steps taken to ensure that the obtained data will allow for the accurate development of an empirical model that is statistically significant. A measure of the efficiency of a DoE is if the design is simultaneously rotaTable and orthogonal (Minitab, 2015). A DoE is orthogonal if the effects of the independent variables balance out across the effects of the other independent variables. A DoE is rotaTable if the variance of the response at a point depends only on the distance from the design centre point (Minitab, 2015). Orthogonally blocked designs let model terms and block effects be estimated independently and minimize the variation in the regression coefficients. RotaTable designs provide the preferred property of constant prediction variance at all points that are equidistant from the design centre, thus improving the quality of the prediction (Minitab, 2015).

In DoE the independent variables that have the largest effect on the response are considered. The independent variables are then varied and the effect on the response of the system is determined and measured. In this way accurate data about the system is obtained. The possible settings of each independent variable in the N-dimension space are called levels. Some common methods of DoE include (but are not limited to): factorial design, central composite design, and Box-Behnken designs (Lazic, 2004).

Central composite designs (CCD) are first order 2^k designs which are augmented by centre and axial points. These additional points have an advantage over full factorial designs because they allow for the estimation of the turning parameters that are required for a second order polynomial model (Alvarez, 2000). Figure 2.12 illustrates a CCD for 3 independent variables that are varied at 2 levels. The lines of the cube, dots, triangles and square represent the upper and lower levels, experiment points and the axial points and central point, respectively.

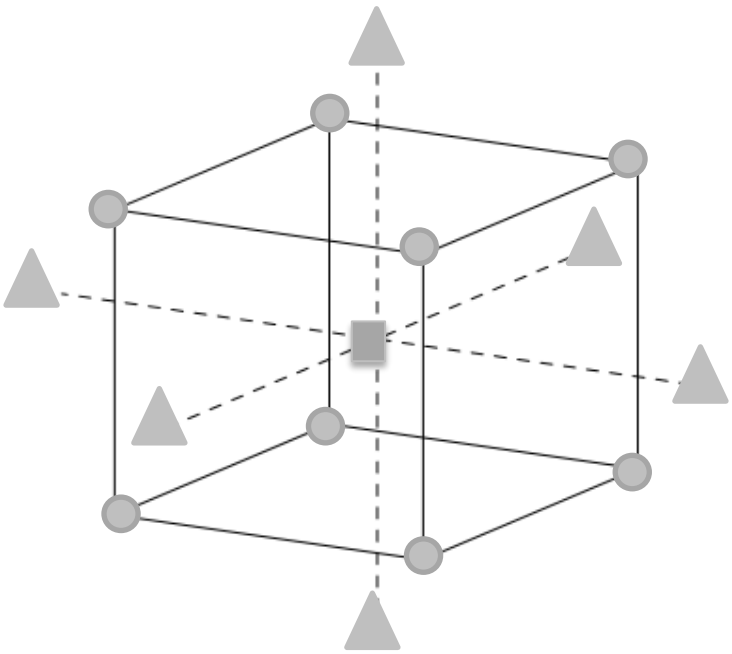

Figure 2.12: CCD for 3 independent variables at 2 levels

CCD is an advantageous DoE as it requires fewer experiments than a full factorial designs and is rotaTable and orthogonal whereas full factorial designs and Box-Behnken design are not (Minitab, 2015).

In CCD the axial points are determined using constant called alpha (α). Alpha, along with the number of centre points, determines whether a design can be orthogonally blocked and is rotaTable (NIST/SEMATECH, 2012). The distance of each axial point from the centre point is a multiple of α. The multiple that is used is the distance from the centre point to the factorial points. An α value that is less than one puts the axial points inside the cube and an α value greater than one puts the axial points outside the cube (Minitab, 2015). To maintain orthogonality and rotatability α depends on the number of independent experimental runs in the factorial portion (edges of the cube) of the CCD (NIST/SEMATECH, 2012). The equation to calculate alpha is given by equation 2.8.

$$\alpha = (Number\ of\ Factorial\ Runs)^{1/4} \quad (2.8)$$

2.8. Summary

Carbon dioxide capture is essential to reducing CO_2 emissions in an attempt to mitigate climate change and capturing CO_2 via adsorption is a promising technology to achieve this.

In adsorption the adsorbate molecules (CO_2) are adsorbed onto the surface of an adsorbent. Adsorption processes need to be cyclic in order to recover the adsorbent and release CO_2 for storage. Hence, it is necessary to desorb the CO_2 from the adsorbent. This is achieved via PSA, TSA, ESA and VSA.

Different types of solid adsorbents exist. These adsorbents are classified as either carbonaceous or non-carbonaceous. Carbonaceous adsorbents are based entirely on carbon whereas non-carbonaceous adsorbents are not. Examples on carbonaceous adsorbents are activated carbon, CMSs, carbonized polymers and resins, MOFs, CNTs, porous polymers and amine impregnated CNTs. Example of non-carbonaceous adsorbents are zeolites and silica materials.

CNTS are promising as adsorbents for CO_2 capture. A challenge facing their use for CO_2 adsorption is that they do not have an affinity for CO_2 and will not selectively remove CO_2 from a mixed gas stream.

It is possible to modify the surfaces of solid adsorbents by grafting or impregnating amines onto the surface of the adsorbents. This could enhance the adsorption of CO_2 because the amines act as CO_2 anchoring sites by forming carbamates with the CO_2. Commonly used amines such as PEI are not biodegradable and are extremely toxic (Ngoy et al., 2014). This study proposes that chitosan, a biodegradable and non-toxic polymer could be a suitable alternative because of the presence of the desired amine groups. Against this background, the current research investigated the synthesis and performance evaluation of a novel material for CO_2 capture.

Chapter 3 Materials and Experimental Procedure

This chapter contains the materials and equipment that was utilized. The methods and experimental procedures that were followed in the study are explained.

3.1. Introduction

In this study chitosan and chitosan/MWCNTs composite adsorbents were synthesized. Chitosan is a biodegradable and non-toxic polymer that has potential to be used as an adsorbent for CO_2 capture. Chitosan was impregnated onto MWCNTs in order to enhance the physical properties, CO_2 adsorption capacity and CO_2 affinity of the MWCNTs. The physicochemical properties of the synthesised materials were evaluated using FTIR, TGA, Raman spectroscopy, N_2 physisorption and SEM techniques. The CO_2 adsorption capacity of the synthesised material was evaluated using TGA and custom built CO_2 adsorption equipment.

3.2. Materials and Equipment

Commercially available chitin was obtained from Lagos Bar Beach in Lagos, Nigeria. Chemicals, such as hydrochloric acid (HCl), sodium hydroxide (NaOH), potassium permanganate, nitric acid and oxalic acid were obtained from Sigma Aldrich (Pty) South Africa. MWCNTs were obtained from Sigma Aldrich (Pty) SA. The MWCNTs have an outer diameter ranging between 110 - 170 nm with a length of 5 - 9 μm and ≥ 90% purity. The gaseous N_2, CO_2, Air and N_2/CO_2 mixture (15 % CO_2 and 85% N_2) of analytical grade was obtained from Afrox, South Africa. All distilled water, glassware, thermometers, timers, magnetic stirrers, vacuum pumps and reflux equipment were obtained from the school's laboratory.

The equipment used in this study includes N_2 Physisorption. Scanning Electron Microscope (SEM), Fourier Transform Infrared Spectroscopy (FTIR), Raman Spectroscopy, Thermogravimetric Analysis (TGA) and custom built CO_2 adsorption equipment.

3.3. Summary of Experimental Procedure

In this study, chitosan was synthesized from chitin. Fifteen unique chitosan samples were synthesized. The purpose of this being to evaluate the influence that the synthesis variable had on the DDA of the chitosan in order to develop an empirical model for the synthesis of chitosan. The properties of the synthesized chitosan was evaluated using N_2 physisorption, SEM, FTIR, TGA and custom built CO_2 adsorption equipment. MWCNTs were covalently functionalised and impregnated with chitosan to produce a chitosan/MWCNTs composite adsorbent. The properties of the chitosan/MWCNTs composite adsorbent were evaluated as an adsorbent for post combustion CO_2 capture using N_2 physisorption, SEM, FTIR, Raman Spectroscopy and TGA. The CO_2 adsorption capacity of the chitosan/MWCNTs was evaluated

using TGA and custom built CO_2 adsorption equipment. A summary of the experimental procedure in the form of a flow diagram is given in Figure 3.1.

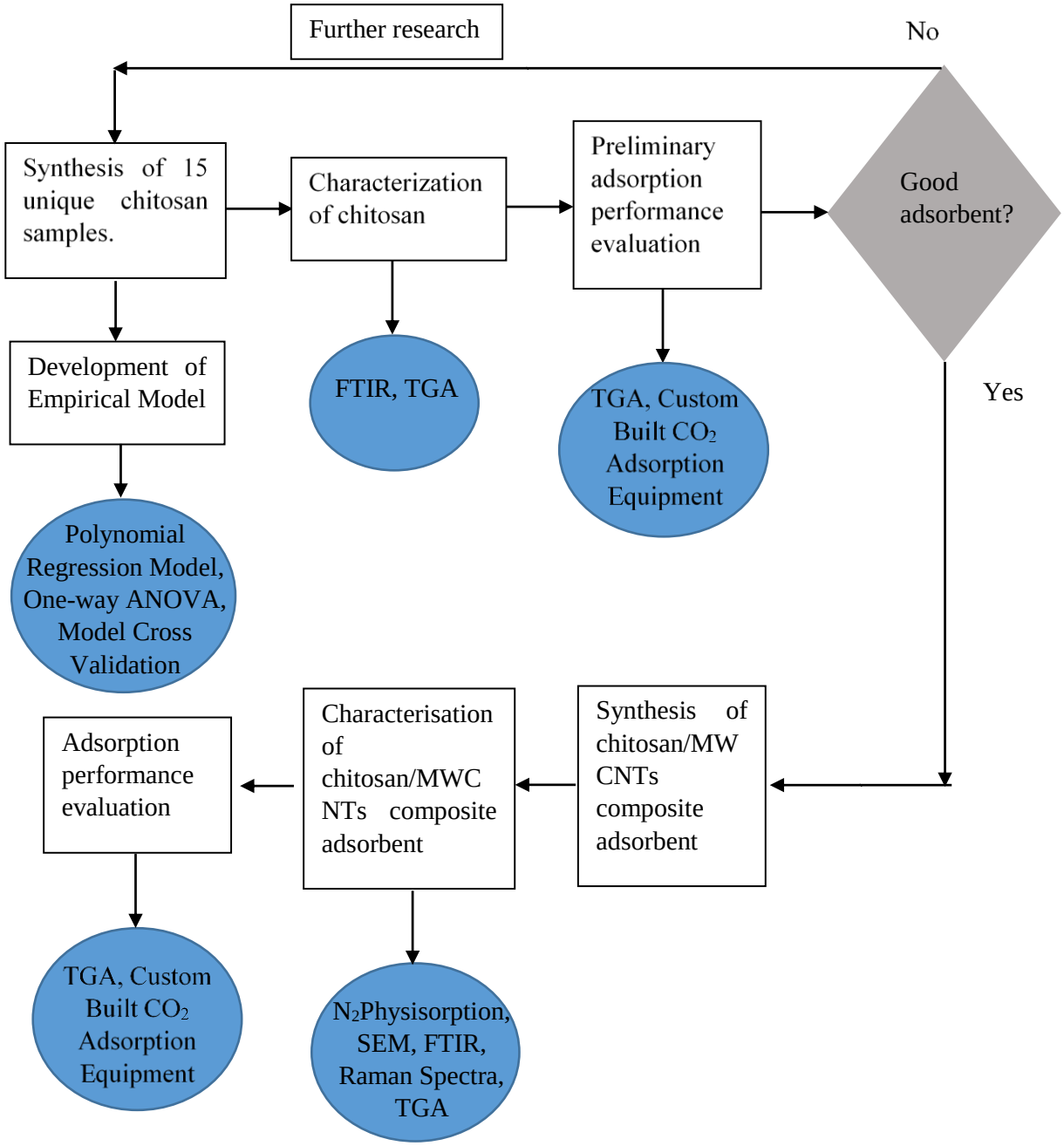

Figure 3.1: Flow diagram showing the summary of the experimental procedure

3.4. Synthesis of Chitosan and Chitosan/MWCNTs

Chitin was pulverised and sieved to less than 150 μm prior to the chitosan synthesis. Chitosan was synthesised from chitin by deproteinisation, demineralisation and deacetylation steps. For chitosan that is used for biological purposes, such as drug delivery, it is necessary to carry out a decolourisation step prior to deacetylation. However, for CO_2 capture this step is not necessary and was omitted. The procedure and operating conditions for the synthesis of chitosan are as follows:

Deproteinisation: was carried out with a 6 mass % NaOH solution at 60 ^{0}C for 2 h in a 2 L volumetric flask. The solution was continually stirred throughout using a magnetic stirrer. A chitin to solvent ratio of 1:20 was used. The alkaline solution was filtered (using a vacuum pump) from the chitin residue. The chitin residue was then washed with distilled water until the pH was neutral.

Demineralisation: was carried out with 6 mass % HCl solution at 60 ^{0}C for 2 h. in a 2 L volumetric flask. The solution was continually stirred throughout using a magnetic stirrer. A chitin to solvent ratio of 1:20 was used. The acid solution was filtered (using a vacuum pump) from the chitin residue. The chitin residue was then washed with distilled water until the pH was neutral.

Deacetylation: For the purpose of deacetylation an RSM approach via DOE (as explained in Chapter 2) was utilized. The chitin residue that had undergone deproteinisation and demineralisation underwent treatment with various NaOH concentrations, experimental time and temperature in this manner fifteen unique samples of chitosan were produced.

Previous research work on the synthesis of chitosan have revealed that the temperature, the NaOH concentration and the reaction time have the most significant effect on the DDA of the synthesised chitosan (Divya et al., 2014 and Kiruba et al., 2013) and were thus the independent variables considered. The degree of deacetylation (DDA) was the response variable. A Central Composite Design (CCD) of experiment was employed to design the experimental runs conducted. The CCD of experiments was selected because it is ideal for the statistically designed experiments where the objective is to determine the influence of independent variables on a response variable as well as to determine the optimum conditions. CCD was selected because the DoE is orthogonal, rotaTable, can be used to determine the turning parameters required to fit a second order polynomial model, and there is a significant reduction in the number of experiments to be carried out, such as 3^k full factorial designs which would require 27 experimental runs or a traditional approach which would require that s single variable be varied at a time. In addition, using this method makes it possible to measure the effects of two independent variables simultaneously in the response variable.

Table 3.1 shows the range and levels of the experimental variables used in the DoE. Table 3.2 shows the DoE plan. The three independent variables were varied simultaneously at two levels, making 8 factorial experiments ($2^3 = 1$), one centre experiment and six axial experiments, giving 15 experiments in total.

Table 3.1: Experimental range and levels

Variables	**Factor**	**Range and level**				
		-α	-1	0	1	+α
Temperature (ºC)	X_1	66.4	80	100	120	133.6
NaOH Concentration (% NaOH)	X_2	16.4	30	50	70	83.6
Time (min)	X_3	26.4	40	60	80	93.6

Table 3.2: Central composite design experimental plan.

Experimental Number	**Experimental Design**			**Experimental Plan**		
	Temp (ºC)	NaOH Conc (% NaOH)	Time (min)	X_1	X_2	X_3
1	-1	-1	-1	80	30	40
2	-1	-1	+1	80	30	80
3	-1	+1	-1	80	70	40
4	-1	+1	+1	80	70	80
5	+1	-1	-1	120	30	40
6	+1	-1	+1	120	30	80
7	+1	+1	-1	120	70	40
8	+1	+1	+1	120	70	80
9	0	0	0	100	50	60
10	-α	0	0	66.4	50	60
11	+ α	0	0	133.6	50	60
12	0	- α	0	100	16.4	60
13	0	+ α	0	100	83.6	60
14	0	0	- α	100	50	26.4
15	0	0	+ α	100	50	93.6

Note: $\alpha = (8)^{1/4}$ $\alpha = 1.682$

Each sample type was synthesized in duplicate to improve the accuracy of the results.

The chitosan/MWCNTs composite adsorbent was prepared from the chitosan sample that was found to be most suitable. The MWCNTs were oven dried at 110 ºC for 24 h to remove water and other impurities. The MWCNTs were then covalently functionalized by mixing 2 g of MWCNTs with 100 mL of nitric acid (30 %) at 110 ºC for 4 h in a 500 mL volumetric flask. The solution was constantly stirred using a magnetic stirrer and the experiment was carried out under reflux. The acidic solution was filtered and the residue was washed with distilled water and filtered using a vacuum pump until the pH was neutral. The residue was oven dried at 60 ºC overnight.

The functionalized MWCNTs were then impregnated by dissolving 0.4 g of chitosan in 20 mL of acetic acid (2 %) at 80 ºC for 1 h using a 500 mL volumetric flask. The solution was constantly stirred using a magnetic stirrer and the experiment was carried out under reflux. The MWCNTs were then added and the solution was once again stirred constantly with a magnetic stirrer under reflux at 80 ºC for 1 h. The residue was washed with distilled water and filtered using a vacuum pump until the pH was neutral. The chitosan/MWCNTs composite adsorbent was oven dried at 60 ºC for 24 h.

3.5. Characterisation of the Physicochemical Properties of Chitosan and Chitosan/MWCNTs

Chitosan was characterized using FTIR techniques and TGA techniques. Chitosan/MWCNTs was characterised using FTIR techniques, N_2 Physisorption techniques, Raman Spectroscopy techniques and SEM techniques.

3.5.1. N_2 Physisorption

N_2 Physisorption using BET theory was used to determine the surface geometry (surface area, pore size and pore volume) of the MWCNTs and chitosan/MWCNTs composite adsorbent. The surface geometry of the MWCNTs and chitosan/MWCNTs composite adsorbent were compared to determine the change in surface geometry caused by chitosan impregnation. N_2 physisorption was conducted using a Micromeritics Tristar-Surface area and Porosity analyser. Prior to analysis the instrument was calibrated using a material of known surface area, the calibration error bar was 5 %. For N_2 physisorption samples with an approximate mass of 0.2 g were degassed under the flow of N_2 gas at 150 $^{\circ}C$ for 4 h prior to analysis using a Micromeritics Flow Prep 060, sample degas system. 0.2 g of sample is sufficient to obtain accurate results with this type of analyser. N_2 physisorption analysis was performed in the School of Chemistry at the University of the Witwatersrand.

3.5.2. Scanning Electron Microscroscopy (SEM)

A Sigma Zeiss SEM was used to check the surface morphology of the chitosan, MWCNTs and chitosan/MWCNTs composite adsorbent. SEM analysis was performed in the School of Chemical and Metallurgical Engineering at the University of the Witwatersrand. The Sigma Zeiss SEM is serviced in June yearly.

3.5.3. Fourier Transform Infrared Spectroscopy (FTIR) Techniques

FTIR is an analytical technique that gives information of a solid, liquid or a gas through the infrared spectrum captured by absorption or emission. Every atom in a molecule vibrates at a specific wave numbers which makes atoms identifiable at that wave number. FTIR takes advantage of this, infrared radiation is shone on the sample which causes molecules to vibrate. The vibration causes the bonds between atoms being strained and stretched, in particular at the bands with infrared radiation being emitted. In this way it is possible to determine inter-atomic bonds in molecules which shows which functional groups are present.

FTIR was used to verify the functional groups present as well as determine the DDA of the chitosan samples. The intensities of bands at 1420 and 1320 cm^{-1} were used to determine the DDA. According to Brugnerottoa et. al. (2001) and Entsar et. al. (2008) the adsorption ratio A_{1320}/A_{1420} shows superior agreement between the absolute and estimated DDA values. The equation was used to calculate the DDA and is given in equation 3.1. This equation was adapted from (Brugnerottoa et al., 2001) and was also used by (Entar et al., 2008) to calculate the DDA of the chitosan.

$$DDA = 1 - 31.92 \times \left(\frac{A_{1320}}{A_{1420}}\right) - 12.20 \qquad r = 0.990 \tag{3.1}$$

Each sample type was synthesized in duplicate and the mean DDA was utilized.

FTIR was used to confirm that the functional groups present in chitosan were present for the chitosan/MWCNTs. This was used to verify that chitosan impregnation was successful.

A Bruker Tensor 27 FTIR spectrometer (in the frequency range 520 – 4000 cm^{-1}, each spectrum was an average of 64 scans with a resolution of 2 cm^{-1}) was used to obtain FTIR of the chitosan. The FTIR was performed in the School of Chemistry at the University of the Witwatersrand. The FTIR of the MWCNTs and chitosan impregnated MWCNTs was performed in the School of Chemistry at the University of South Africa (UNISA). A Perkin Elmer Frontier FTIR spectrometer was used in the frequency range 650 – 4000 cm^{-1}, each spectrum was an average of 8 scans with a resolution of 2 cm^{-1}. Prior to FTIR analysis the instrument was calibrated using a polystyrene standard, the calibration error is approximately 1 cm^{-1}.

3.5.4. Raman Spectroscopy Techniques

Raman Spectroscopy is an analytical technique which provides information on the surface properties of a sample. Raman spectroscopy is widely used in the characterisation of CNTs due to the good spatial resolution and sensitivity as well as the need for minimal sample preparation. Raman Spectroscopy was used to check the quality of the MWCNTs.

Raman spectra were acquired with the 514.5 nm line of an argon ion laser and a Horiba Jobin-Yvon LabRAM HR Raman spectrometer equipped with an Olympus BX41 microscope attachment. Prior to analysis the instrument was calibrated using single crystal silicon as the reference material. This calibrates the spectral readout of the instrument as well as the throughput on confocality. The incident beam was focused onto the sample with a 100x objective and the power at the sample was kept low (~ 0.6mW) to prevent localized heating by the laser. The backscattered light was dispersed via a 600 lines/mm grating onto a liquid nitrogen cooled CCD detector and the data was collected with LabSpec v5 software. The Raman Spectroscopy was performed in the School of Physics at the University of the Witwatersrand.

3.5.5. Thermogravimetric Analysis (TGA) Techniques

Thermogravimetric analysis is an analytical technique which provides information on how the mass of a sample varies with a change in temperature, gas flowrate and gas composition. TGA was used to determine the thermal stability of the synthesised chitosan. For the thermal stability experiments the samples of approximately 8 mg were heated to 700 ºC in air and the temperature was increased in a step-wise ramp fashion from 25 ºC to 700 ºC with a ramp rate of 5 ºC/min. The TGA was performed using a TA SDT Q600 TGA in the School of Chemical and Metallurgical Engineering at the University of the Witwatersrand. The TA SDT Q600 provides a simultaneous measurement of the weight change of the sample and a true differential heat flow from ambient temperature to 1 500 ºC. The TA SDT Q600 can measure samples up to 200 mg. The mass of the samples used in this study were in this range. The thermocouple of the TA SDT Q600 was replaced and the machine serviced and calibrated by TA Instrument Representatives the month before TGA experiments commenced. To calibrate the temperature of the TGA a high-purity magnetic standard must be analysed to determine its curie temperature. The observed and correct temperature is entered into the temperature calibration Table. The observed and the corrected temperatures correspond to the experimental and theoretical temperature of the calibrant. One to five temperature calibration points can be entered into the calibration Table. The more temperature calibration points used, the more accurate the calibration. The weight calibration is done automatically by the TA SDT Q600. The instrument control weight calibration functions guide the step-by-step calibration process.

3.6. Development of the Empirical Model

A model was developed using the experimental data. Various models were considered. The regression coefficients, mean error and variance for each of the proposed models were determined using Statistica Software. Statistica Software was then used to determine the equation coefficients and constants. A second order polynomial was adopted to fit the experimental data. The polynomial is given by Equation 3.2.

$$Y_{estimate} = b_0 + b_1X_1 + b_2X_2 + b_3X_3 + b_4X_1^2 + b_5X_2^2 + b_6X_3^2 + b_7X_1X_2 + b_8X_1X_3 + b_9X_2X_3 \quad (3.2)$$

Where, $Y_{estimate}$ is the response, $X_1, X_2\ and\ X_3$ are the coded variables, b_0 is the offset term, b_{1-3} are the first order effects, b_{4-6} are the quadratic effects, b_{7-9} and are the interaction effects

The response surfaces and their corresponding contours were plotted using Statistica. Furthermore, a one-way Analysis of Variance (ANOVA) test was conducted using Statistica to evaluate the statistical significance of the proposed model.

3.7. Evaluation of the CO_2 Adsorption Performance of Chitosan and Chitosan/MWCNTs

The CO_2 adsorption performance of the chitosan and chitosan/MWCNTs was evaluated first using TGA as a preliminary study. The CO_2 adsorption performance was then evaluated using custom built CO_2 adsorption equipment. The purpose of this equipment is to mimic flue gas conditions and to determine the effect of impurities on the CO_2 adsorption performance of the adsorbents.

3.7.1. Thermogravimetric Analysis (TGA) Techniques

Thermogravimetric analysis is an analytical technique which provides information on how the mass of a sample varies with a change in temperature, gas flowrate and gas composition. TGA was used to determine the CO_2 adsorption capacity of the chitosan and chitosan/MWCNTs.

For the CO_2 adsorption capacity experiments the samples of approximately 50 mg was swept with N_2 (flowrate = 60 mL/min) at atmospheric pressure and a temperature of 110 ºC for 30 minutes to desorb water and other gas impurities present on the surface of the adsorbent. After degassing, the samples were cooled (25, 35 and 45 ºC) an exposed to pure CO_2 (100 % CO_2) (flowrate 45, 60, and75 mL/min) under a pressure of 1.1 bar for 120 minutes, after which the process was stopped. The change in mass of the sample was measured and used to calculate the amount of CO_2 adsorbed, by equation 3.3 below.

$$CO_2\ adsorption\ capacity\ \left(\frac{mg}{g}, \frac{g}{kg}, \frac{kg\ of\ CO_2\ adsorbed}{ton\ of\ adsorbent}\right) = \frac{maximum\ wt\ \% - minimum\ wt\ \%}{minimum\ wt\ \%} \times 1000 \quad (3.3)$$

As a preliminary study the CO_2 adsorption capacity of all the synthesised chitosan samples was evaluated. From this study, the chitosan sample that gave the highest CO_2 adsorption capacity was determined. Further CO_2 adsorption experiments in which the effect of temperature and CO_2 flowrate on the CO_2 adsorption capacity were conducted using this sample. The CO_2 adsorption capacity of the chitosan/MWCNTs was also evaluated using the TGA.

The TGA was performed using a TA SDT Q600 TGA in the School of Chemical and Metallurgical Engineering at the University of the Witwatersrand. Please refer to section 3.5.5 for more information about this equipment.

3.7.2. Custom Built CO_2 Adsorption Equipment

Custom built CO_2 adsorption equipment (built by Chemvak) was used to mimic flue gas conditions to test the CO_2 adsorption capacity of the synthesised adsorbents at conditions that mimic industry operation. The adsorption equipment is located in the School of Chemical and Metallurgical Engineering at the University of the Witwatersrand. Figure 3.2 gives the process flow diagram of this equipment.

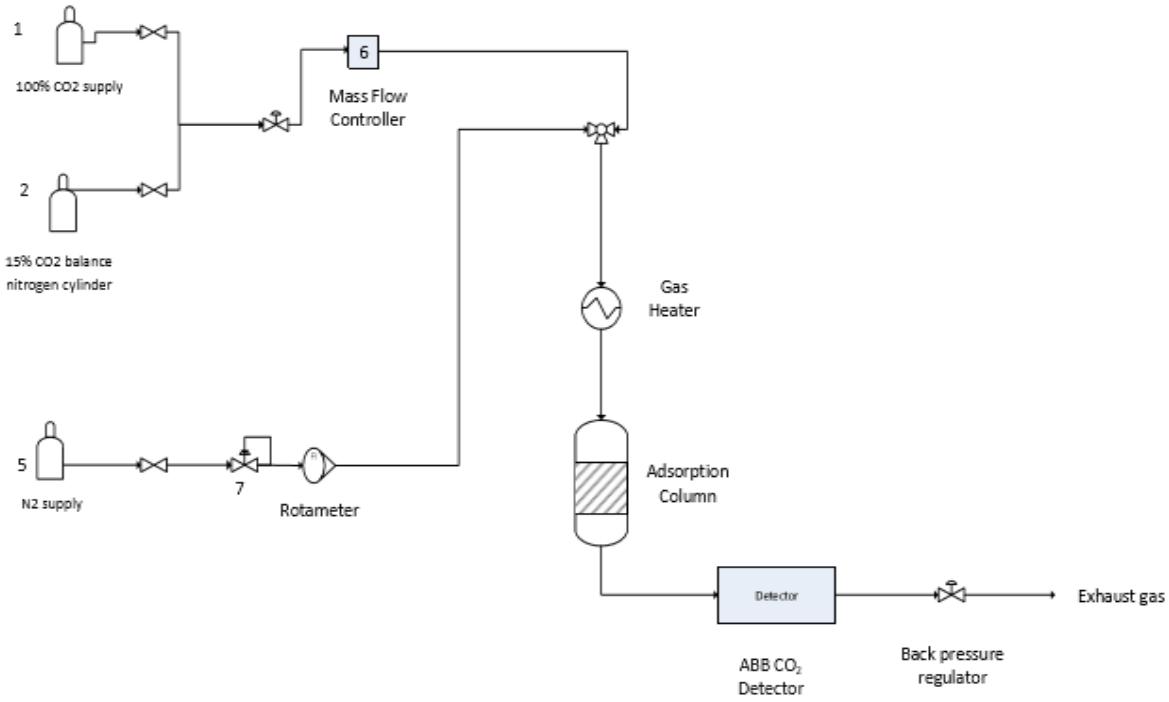

Figure 3.2: Process flow diagram of equipment used to mimic industry capture conditions

The adsorption equipment consists of a packed bed reactor, heater, mass flow controller and gas analyser, supplies gas at a concentration of either 100 vol % CO_2, 100 vol % N_2 or 15 vol % CO_2 and 85 vol % N_2. 15 vol % CO_2 is used to mimic the flue gas conditions in industry, such as would be found in a typical South African Coal Fired Power Station. The packed bed reactor was packed with a 0.01 g of adsorbent sample (packing height approximately 15 mm). N_2 was then passed over the sample at 110 ºC to desorb water and other gas impurities present on the surface of the adsorbent. The reactor temperature was decreased to 25 ºC and gas at 15 % CO_2 (50 mL/min) was then bypassed to the CO_2 analyser to read 15 % as an initial starting point. Flow is then diverted through the reactor where adsorption takes place and then through the CO_2 analyser. The CO_2 concentration reading given by the analyser decreases as CO_2 is adsorbed. The adsorption process is complete once the analysed reads 15 % CO_2 again. The inlet flowrate and CO_2 concentration from the gas analyser was used to calculate the CO_2 adsorbed by equation 3.4.

$$CO_2\ adsorbed\ \left({}^{g\ CO_2}/_{g\ adsorbent}\right) = \frac{PM_r t}{WRT}\left(\gamma_{CO_{2,out}} Q_{in} - \frac{\gamma_{CO_{2,out}}\left(1-\gamma_{CO_{2,in}}\right)Q_{in}}{1-\gamma_{CO_{2,out}}}\right) \quad (3.4)$$

Where, P is the pressure (bar). M_r is the molar mass of CO_2, t is the time (s), W is the mass of adsorbent (g), R is the universal gas constant $\left(\frac{ml\ bar}{K\ mol}\right)$, T is the temperature of the reactor (K), γ_{CO_2} is the volume % CO_2, Q is the flowrate (mL/min).

The equation assumes no N_2 is adsorbed and no CO_2 or N_2 is retained in the column.

The custom built CO_2 adsorption equipment was used to determine the CO_2 adsorption capacity of the chitosan, MWCNTs and chitosan/MWCNTs in the presence of impurities.

Chapter 4 Synthesis of Chitosan and Effect of the Synthesis Variables on the Degree of Deacetylation of Chitosan

This chapter contains the results pertaining to the synthesis and characterisation of the synthesised chitosan samples. The influence of the synthesis variables on the degree of deacetylation of the synthesised chitosan is considered.

4.1. Introduction

Organic materials can be synthesized to have different properties. The different properties of organic materials are caused by a difference in chemical structure. This difference in chemical structure can be caused by the difference in chemical species, functional groups, intra-molecular bonding and intermolecular bonding. The differences in the properties can be manipulated to synthesize materials with ideal properties for specific functionality. After the synthesis process, the biological, chemical, mechanical and physical properties of the material should be determined. This provides information on the success of the synthesis process and on where and how the material should be applied.

In this study several techniques were used to check the properties of the synthesized chitosan. The characterisation techniques used in this study were quantification (to determine the efficiency of the synthesis process), TGA (to determine the thermal stability of the synthesised chitosan) and FTIR (to determine the DDA and verify the functional groups present in the synthesized chitosan. The DDA of chitosan will affect the CO_2 adsorption capacity of the synthesised chitosan. The greater the DDA, the more the amine groups present, indicating more sites for CO_2 adsorption to occur. Research studies conducted on the synthesis of chitosan have found that temperature, NaOH concentration and reaction time have the most significant effect on the DDA of the chitosan (Divya et al., 2014). The main and interactive influence of these variables on the DDA of the synthesised chitosan was evaluated using an RSM approach as explained in Chapter 3.

4.2. Synthesis of Chitosan

Fifteen unique samples of chitosan were synthesized from chitin through demineralization, deproteinisation and deacetylation. The same method for demineralization and deproteinisation were used for all 15 samples. The chitosan samples differ in the method of deacetylation. The synthesized chitosan samples have different DDA because of the different deacetylation conditions used. Each sample type was synthesized in duplicate and the mean DDA was used to improve accuracy of the results. An RSM approach via DoE (as explained in Chapter 2) was utilized to evaluate the effect of the synthesis variables and a second order polynomial was adopted to fit the experimental data.

4.3. Characterization

The amount of chitosan was quantified and the physicochemical properties to confirm whether the target material was actually synthesized. Furthermore, the information obtained was used to evaluate the influence of the synthesis variables on the DDA of chitosan.

4.3.1. Yield

The yield was calculated to determine the efficiency of the synthesis process in terms of the quantity of chitosan obtained. Two batches of each sample were synthesized and the yield was calculated. The yield was calculated using equation 4.1. The yield and standard deviation are shown in Table 4.1. Appendix A1 contains the yield percentage calculations for all synthesized chitosan samples.

$$\%\, Yield = \frac{total\ mass\ of\ product}{total\ mass\ of\ reactant} \times 100 \qquad (4.1)$$

Table 4.1: Chitosan synthesis yields

Sample	Yield (%)	Standard Deviation
1	20.28	7.10
2	13.22	5.76
3	5.65	5.37
4	6.36	1.36
5	16.51	6.36
6	6.39	4.72
7	4.21	0.89
8	6.80	0.36
9	17.88	1.45
10	10.16	3.08
11	8.83	4.40
12	22.25	6.23
13	6.70	2.05
14	5.16	1.92
15	7.29	3.13

The percentage yield of the synthesised chitosan was low for all samples. The high mass loss could be attributed to the nature of the synthesis process. The chitin samples underwent demineralization and deproteinisation steps in which the minerals and proteins were removed, thus it is expected for the yield to be low. Kucukgulmez et al. (2011) reported a yield of 17.5 % with deacetylation carried out at 50 % NaOH at 120 ºC and Hongpattarakere and Riyaphan (2008) reported a yield of 14.6 % with deacetylation carried out at 50 % NaOH at 100 ºC for 60 min. The deacetylation conditions used by Kucukgulmez et al. (2011) are similar to the deacetylation conditions used to synthesize samples 5 and 11 in this study. Sample 5 and sample 11 display yields of 16.51 and 8.83 % respectively. The yields of sample 5 and the yield reported by Kucukgulmez et. al. (2011) are comparable. The yield of sample 11 is not as comparable, but this was attributed to the slightly higher temperature used to synthesis sample 11 (133.6 ºC) which would lead to a decrease in yield. The deacetylation conditions used by Hongpattarakere and Riyaphan (2008) are the same as the deacetylations conditions used to synthesize sample 9. The yield of sample 9 was 17.88 %. This is comparable to the yield of chitosan reported by Hongpattarakere and Riyaphan (2008).

4.3.2. TGA Analysis

TGA analysis was used to measure the thermal stability of the synthesised chitosan. Thermal stability determination is important to reveal the maximum temperature in which the synthesized material can operate. Appendix A2 contains the raw data for the thermal stability analysis.

Figure 4.1 shows the thermal stability of the synthesized chitosan. The sudden decrease in the weight % from 0 - 100 ºC is attributed to the evaporation of impurities such as water and other gases present on the surface of the chitosan. The presence of these impurities confirms that it is necessary to sweep the chitosan samples with N_2 gas at 110 ºC to remove these impurities prior to adsorption. The weight % remains fairly suitable until approximately 280 ºC where the chitosan undergoes oxidative decomposition of the chitosan backbone and a rapid decrease in weight % is seen in Figure 4.1. When the chitosan undergoes oxidative decomposition amine groups are destructed to form crosslinked fragments. Between 350 ºC and 450 ºC this new crosslinked material undergoes destruction (Eldin et al., 2015). At approximately 600 ºC there is no sample remaining.

From the thermal stability analysis, it is possible to conclude that chitosan is safely thermally suitable up to a temperature of 280 ºC, which is well above 100 ºC - the common temperature for TSA. The chitosan will be able to operate at industrial adsorption desorption temperatures. Diab et al. (2012) reported chitosan with a thermal stability of 295 ºC. The comparability of the thermal stability to literature implies that chitosan was successfully synthesized.

Figure 4.2 compares the thermal stability of sample 1 before and after adsorption. Before adsorption has occurred the sudden decrease in weight % (0 – 100 ºC) is seen, however this sudden decrease is not seen for the sample after adsorption has occurred. This is because impurities such as water and other gases were removed when the sample was swept with N_2 and because the chitosan sample was not removed from the TGA furnace between the adsorption and thermal stability experiment it was not expected that there would be any impurities on the chitosan.

From 100 ºC the thermal stability of the chitosan sample before and after adsorption remains almost identical – there is approximately a 2 ºC difference which is not significant. From the thermal stability analysis, it is possible to conclude that chitosan is safely suitable up to a temperature of 280 ºC both before and after adsorption has occurred. The adsorption process does not affect the thermal stability of chitosan which will be beneficial to the adsorption and desorption cycles. The slight 2 ºC difference can be attributed to the formation of carbamate which could prevent the crosslinking of amines and increase the thermal stability of the sample.

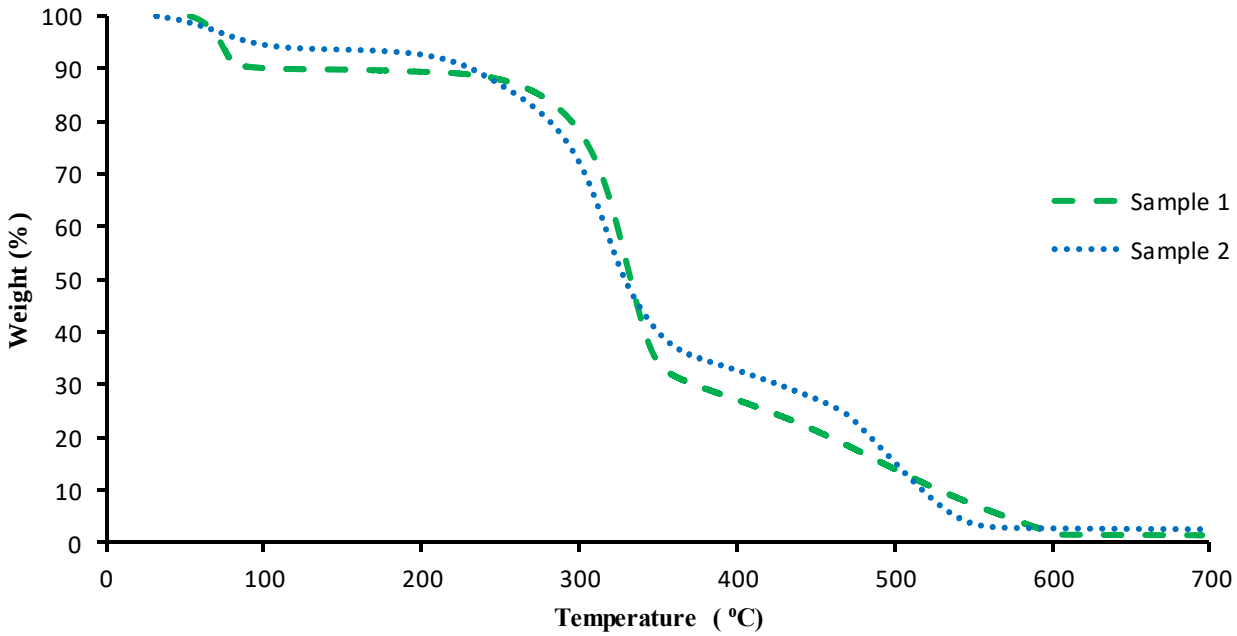

Figure 4.1: Thermal stability analysis of the synthesized chitosan samples 1 and sample 2

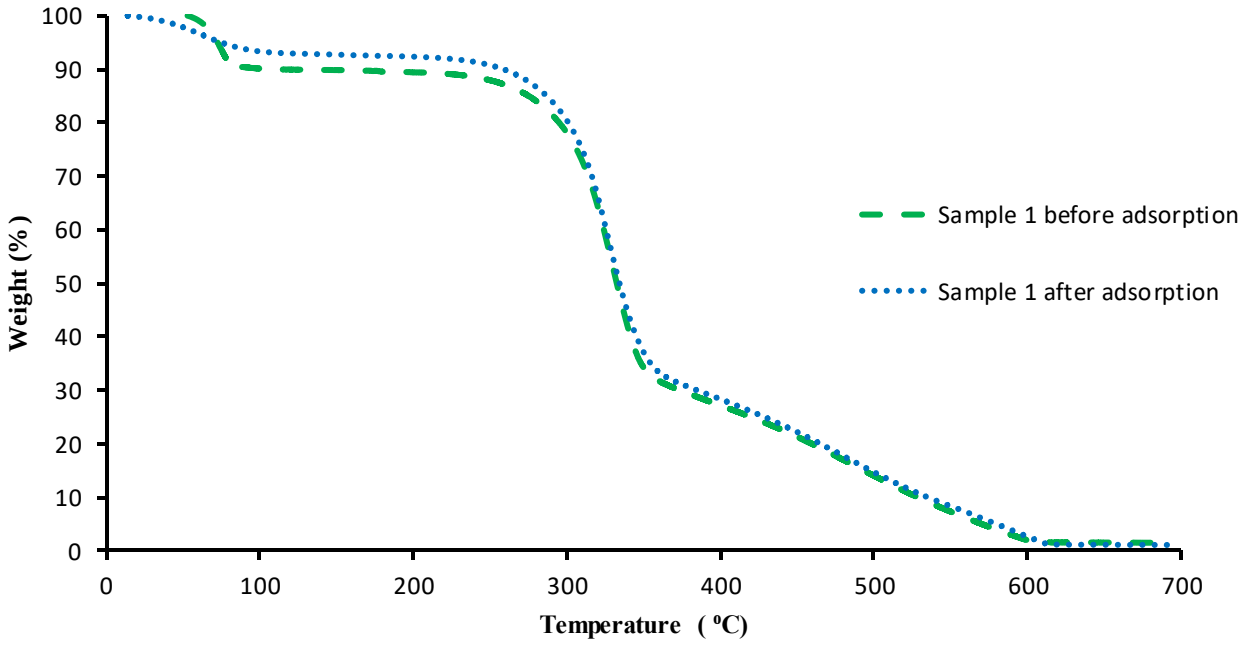

Figure 4.2: Thermal stability analysis of the synthesized chitosan sample 1 a) before adsorption b) after adsorption

4.3.3. FTIR Analysis

FTIR was used to verify the functional groups present in the synthesized chitosan. FTIR is commonly used to analyse the chemical bonds and functional groups that are present. FTIR can be used to study the surface chemistry and provide for a means to understand the interactions occurring at the surface during CO_2 adsorption. The FTIR spectra for all 30 samples were obtained and used to determine the DDA of the synthesized chitosan as explained in Chapter 3. Appendix A3 contains the FTIR for all 30 synthesized chitosan samples. Only a few have been included in the bulk of the report and are shown in Figure 4.3. Sample A and B for each sample type have been included. By comparing the A and B it is possible to see that the samples yield similar FTIR spectra, especially with respect to sample 6 and 14. The similarity between the FTIR spectra of the duplicate samples confirms that the synthesis process is repeaTable.

The FTIR spectra of the chitosan samples shows distinct peaks for the amine (N-H) (3300 - 3500 and 1370 cm^{-1}), alcohol (OH and COH) (3550 - 3200 and 1200 - 1020 cm^{-1}) and ether (COC) (1250 - 1050 cm^{-1}), CN (1430 and 1530 cm^{-1}) and CH (2950 and 2850) groups corresponding with the functional groups of chitosan. This confirms that chitosan was successfully synthesised. The FTIR spectra of the synthesized chitosan closely resembles what was obtained in literature (Brugnerottoa et al., 2001; Divya et al., 2014 and Entar

et al., 2008) again confirming the successful synthesis of chitosan. There are certain peaks that compete over the same wavenumbers, thereby causing reductions in the appearance and sharpness of the peaks.

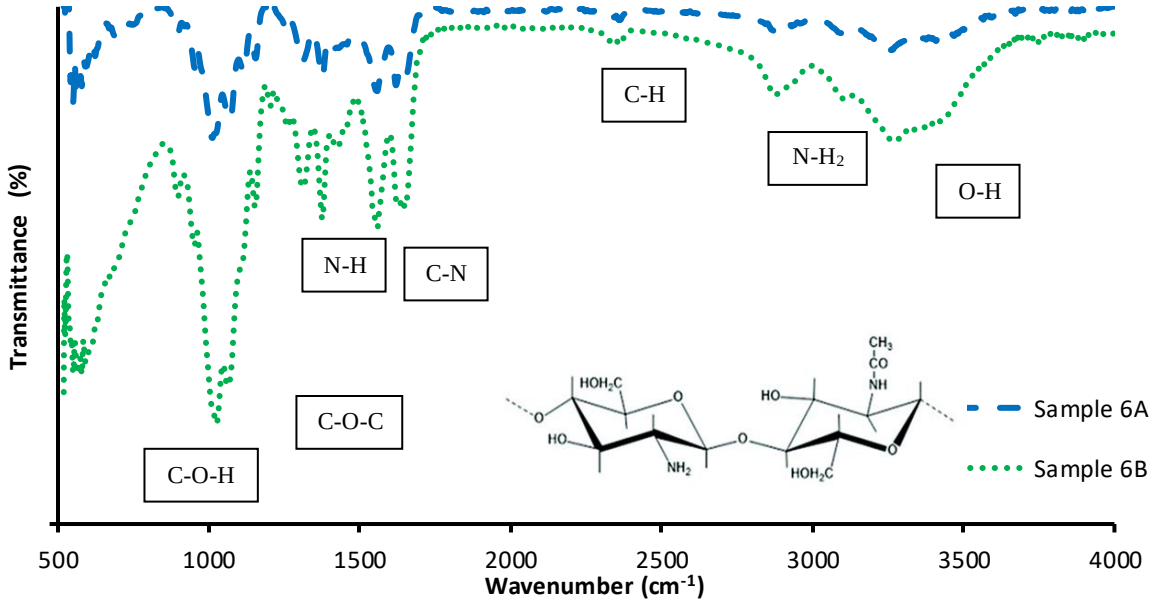

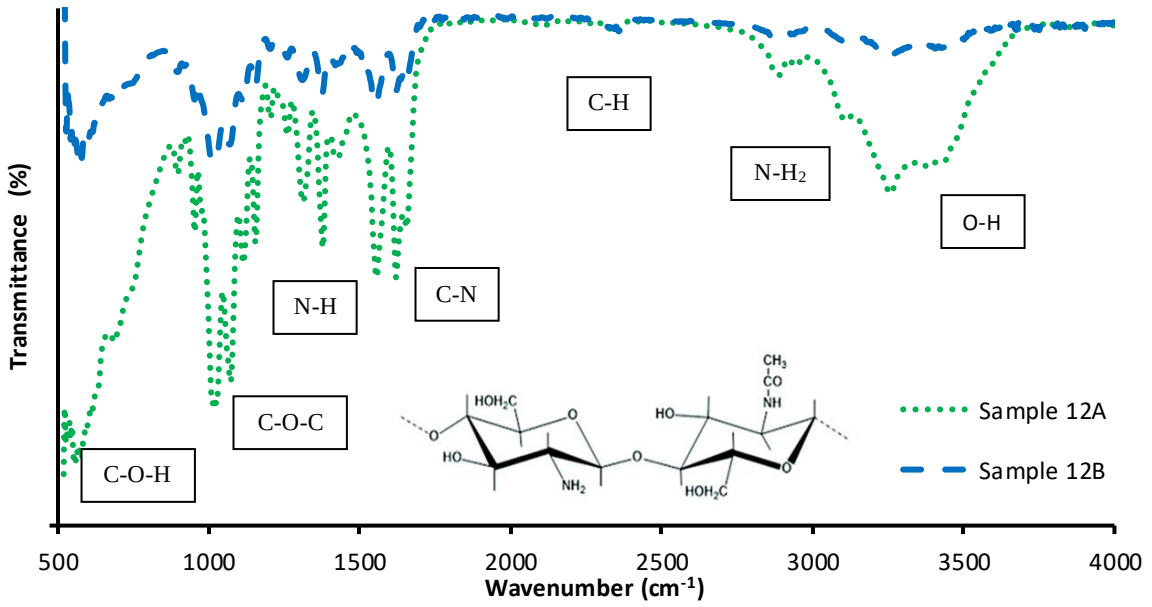

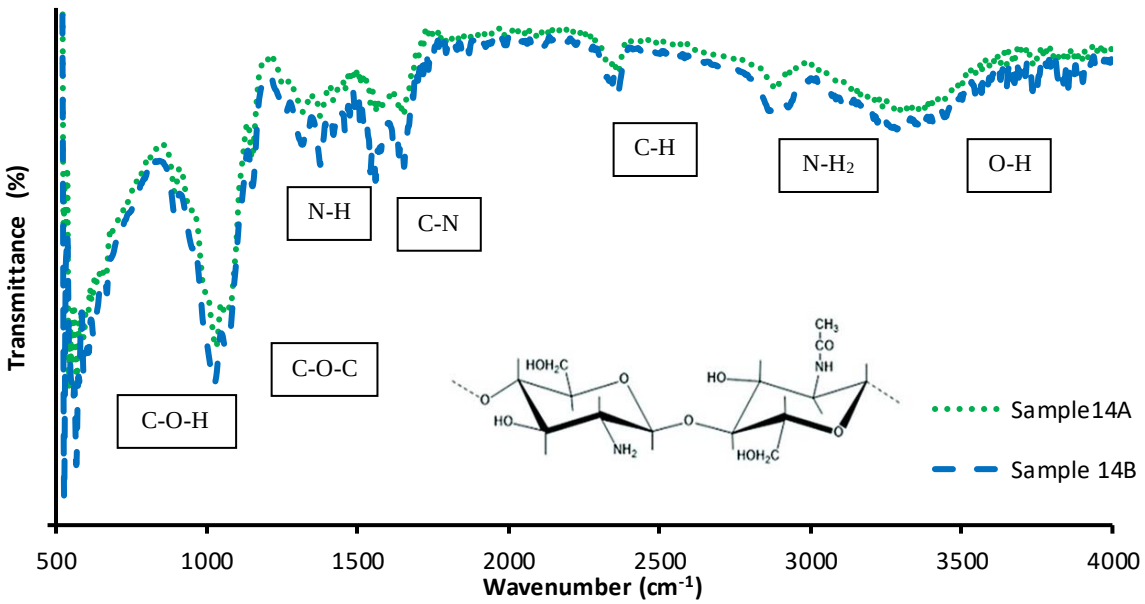

Figure 4.3: FTIR Spectra of a) Sample 6A and 6B; b) Sample 12A and 12B; c) Sample 14A and 14B

The presence of NH and NH_2 confirms the presence of a primary amine which is desirable for CO_2 capture because the primary amine will act as the anchoring site that the CO_2 will attach to. CO_2 is slightly acidic and will react with the alkaline amines to form weak intermediate carbamates (-COO-) (Ngoy et al., 2014). As shown in equation 2.7 from Chapter 2.

$$CO_2 + 2RNH_2 \leftrightarrow RNH_3^+ + NHCOO^- \quad (2.7)$$

The C-O, N-H and the C-N functional groups will form a bio-fission bond at which the molecule will break (Ngoy et al., 2014). This confirms that the synthesised chitosan is biodegradable. The biodegradability and the presence of the primary amine is the reason that chitosan was selected for this study and the FTIR spectra confirm that chitosan could potentially be an adsorbent for CO_2 capture depending on its performance during CO_2 adsorption experiments.

4.4. Influence of the Synthesis Variables on the Degree of Deacetylation of Chitosan

The DDA of chitosan will affect the adsorption capacity because the greater the DDA more the amine groups are present. Thus there are more sites for CO_2 adsorption to occur. Research studies conducted on the synthesis of chitosan have found that the temperature, the NaOH concentration and the reaction time have the most significant effect on the DDA of the synthesised chitosan (Divya et al., 2014). Against this

background, this chapter evaluated the influence of these variables on the DDA of the synthesised chitosan using an RSM approach. RSM is a statistical technique for designing experiments, building models and evaluating the relative significance of several independent variables at once and determining the optimum conditions for the desirable responses. The evaluation involved the use of RSM to find an applicable approximating function that is able to predict and determine the DDA based on the NaOH concentration, time and temperature used. The approximating function made it possible to determine the synthesis variables that yielded the optimum DDA. This will be further discussed under Model formulation and parameter estimation, one-way ANOVA test, effects of synthesis variables on the DDA of chitosan and model validation.

4.4.1. Model Formulation

Response surfaces were used to identify the main and interactive effects of the synthesis variables (NaOH concentration, time and temperature) on the DDA of the chitosan. There are three important stages when performing an RSM study and these are to design the experiments to obtain valuable data, to conduct statistically designed experiments from the experimental plan, to develop a mathematical model that adequately describes the behavior based on the experimental data. The experiment was designed and conducted and the DDA of the synthesized chitosan was calculated as explained Chapter 3.

Five candidate polynomial regression models were considered, making use of the responses obtained from the experimental data. The results obtained from the polynomial regression models were evaluated for their ability to predict the DDA based on the synthesis variables and the model. The mean error, mean variance, mean square error and R^2 closest to 1 was considered when selecting the best model. The mean error, mean variance, mean square error and R^2 of the selected polynomial regression model is given in Table 4.2.

Table 4.2: R^2 and mean square error of the polynomial regression model

Mean Error	0.64
Mean Variance	0.867
R^2	0.95
Mean Square Error	1.74

The polynomial regression model that was found to be the best is given by equation 4.2.

$$Y_{estimate} = b_0 + b_1X_1 + b_2X_2 + b_3X_3 + b_4X_1^2 + b_5X_2^2 + b_6X_3^2 + b_7X_1X_2 + b_8X_1X_3 + b_9X_2X_3 \quad (4.2)$$

Where, $Y_{estimate}$ is the response, $X_1, X_2\ and\ X_3$ are the coded variables (Temperature, NaOH concentration and time respectively), b_{1-9} are the regression coefficients, b_0 is the offset term, b_{1-3} are the first order effects, b_{4-6} are the quadratic effects, b_{7-9} and are the interaction effects.

Equation 4.1 considers all the synthesis variables investigated in this study. The polynomial has three components, a linear part, a quadratic part and a second quadratic part that considers the effects of the interactions of the synthesis variables considered.

The regression coefficients are substituted into equation 4.3

$$\%\,DDA = -5.2384 + 1.1988X_1 + 0.3345X_2 + 0.3118X_3 - 0.00564X_1^2 - 0.0039X_2^2 - 0.0007X_3^2 + 0.0019X_1X_2 - 0.002X_1X_3 - 0.003X_2X_3 \quad (4.3)$$

The DDA predicted by the polynomial regression model, the experimental DDA obtained and the error is given in Table 4.3. The error between the DDA predicted by the polynomial regression model and the experimental DDA is low, showing that the selected polynomial regression model is suitable to predict the DDA based on the synthesis variables used.

Table 4.3: Experimental vs predicted values

Sample	Experimental Conditions			Experimental	Predicted	Absolute Error
	Temperature (ºC)	NaOH Concentration	Time (minutes)			
1	80	30	40	69.8	70.01	-0.215
2	80	30	80	70.7	72.07	-1.37
3	80	70	40	73.1	73.63	-0.53
4	80	70	80	75.7	75.80	0.42
5	120	30	40	70.9	71.77	-0.87
6	120	30	80	70.5	70.42	0.08
7	120	70	40	79.4	78.48	0.92
8	120	70	80	76.5	76.73	-0.23
9	100	50	60	76.6	77.64	-1.04
10	66.4	50	60	70.1	69.76	0.344
11	133.6	50	60	76.8	75.55	1.25
12	100	16.4	60	70.1	68.92	1.18
13	100	83.	60	76.8	77.36	-0.56
14	100	50	26.4	76.9	76.71	0.19
15	100	50	93.6	77.4	76.97	0.43

A correlation graph was plotted to show how the predicted DDA compared to the experimentally obtained DDA for the model and is shown in Figure 4.4. The correlation graph confirms that the selected polynomial regression model is suitable to predict the DDA based on the synthesis variables used.

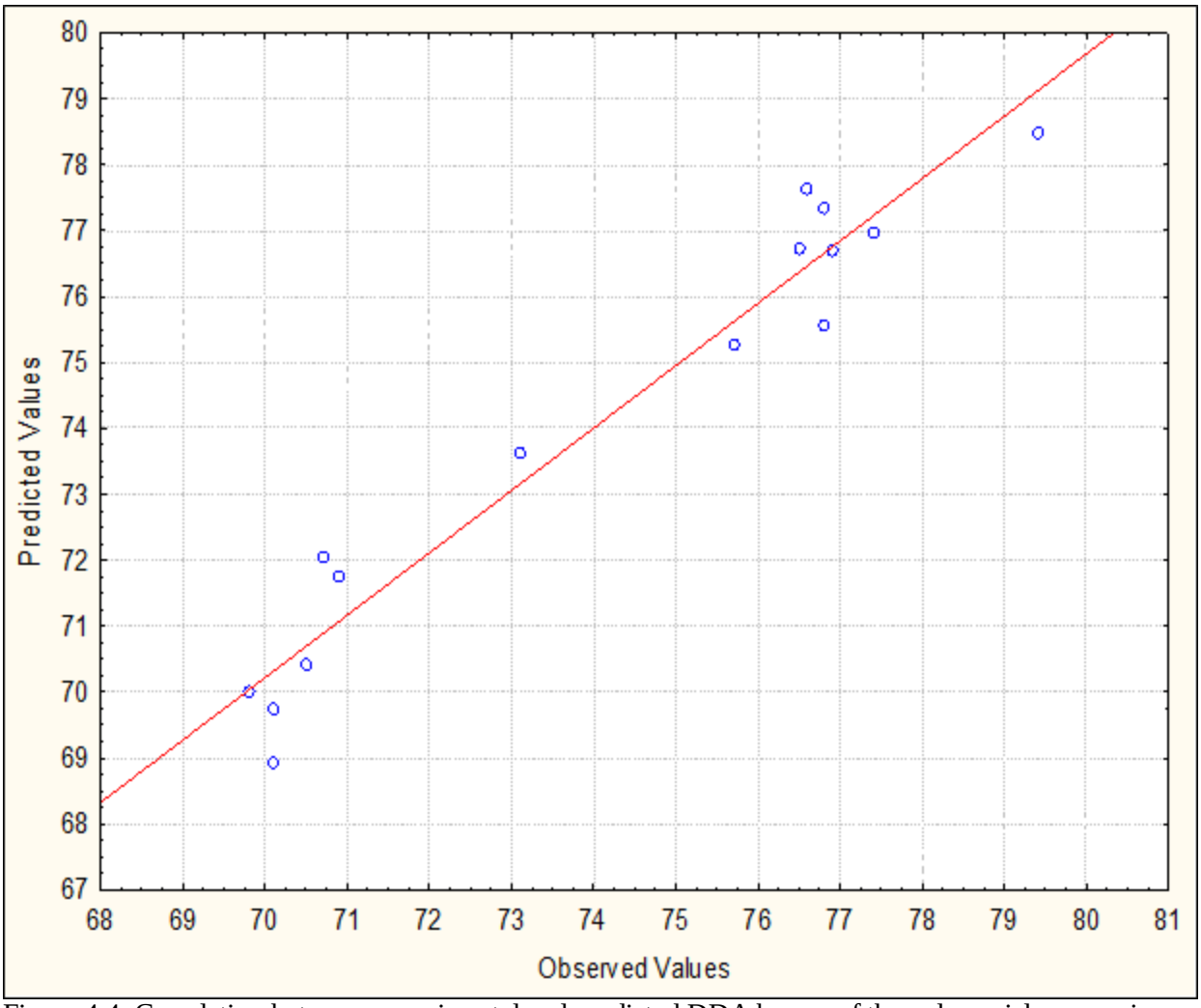

Figure 4.4: Correlation between experimental and predicted DDA by use of the polynomial regression model

4.4.2. One-Way Analysis of Variance (ANOVA) Test

A One-Way ANOVA test was performed by the use of Statistica. The results are shown in Table 4.4. The linear and quadratic effects for each factor, the interaction effects for each factor, degrees of freedom, sum of squares, mean squares, f-value and p-value for this analysis are all reported and considered. The statistical significance of the quadratic polynomial equation revealed that the regression is highly statistically significant for the linear effects of temperature and NaOH concentration and for the quadratic effects of temperature and very significant for the quadratic effects of NaOH concentration. ($P \sim 0.0001$). The regression is moderately significant for the linear and quadratic effects of time, temperature by NaOH

concentration and NaOH concentration by time. The effects of these synthesis variables will be considered in more detail in the next section.

Table 4.4: ANOVA of the model

	ANOVA Source of Variation	SS	df	MS	F value	p Value
Factor	Linear/Quadratic/Interaction					
Temperature	Linear	43.17	1	43.17	24.80	0.004
	Quadratic	29.07	1	29.06	16.70	0.001
NaOH Concentration	Linear	42.22	1	42.22	24.25	0.004
	Quadratic	19.81	1	19.81	11.38	0.019
Time	Linear	2.420	1	2.420	1.390	0.291
	Quadratic	0.625	1	0.625	0.359	0.575
Temperature and NaOH Concentration	Interaction of temperature by NaOH concentration	4.805	1	4.805	2.760	0.158
Temperature and Time	Interaction of temperature by time	5.780	1	5.780	3.320	0.128
NaOH Concentration and Time	Interaction of NaOH concentration by time	0.080	1	0.080	0.046	0.839
	Error	8,704	5	1.74179		
		162,21	1			
	Total SS	73	4			

SS: sum of squares, MS: mean squares, DF: degrees of freedom,

4.4.3. Effects of Synthesis Variables on the DDA of the Synthesized Chitosan

To understand the effect of each synthesis variable (temperature, NaOH concentration and time three dimensional (3D) plots were made for the estimated DDA. This allowed for the analysis and investigation of the interactive effect of the three factors on the DDA.

Figure 4.5Figure *4.5* shows the effect of the NaOH concentration and temperature (in ºC) on the DDA of the synthesized chitosan. Figure 4.5 also show the interactions of the NaOH concentration and temperature. The observed trend was that there is a quadratic relationship between NaOH concentration and temperature with a maximum turning point at 50 % NaOH and 96.67 ºC. As NaOH concentration is increased, the DDA

increased but only up to an NaOH concentration of 50 %. A NaOH increase above 50 % NaOH showed a decrease in DDA of the chitosan. This is because the higher NaOH promotes the degradation of the acetyl group. As this occurs, more amine groups are formed, thus increasing the DDA of the sample. But a NaOH of greater than 50 % promotes the degradation of the sample as a whole. A similar trend is observed for the temperature, as the temperature increases in isolation, the DDA increases. The increase in DDA with an increase in temperature is an exponential trend and the increase in DDA from an increase in temperature slows down. This is because the higher temperature increases the kinetic energy allowing for more reactions to occur thus promoting the degradation of the acetyl group. As this occurs, more amine groups are formed, thus increasing the DDA of the sample. A temperature increase to greater than 96.67 ºC decreases the DDA, it can be assumed that the reaction reaches equilibrium at 100 ºC. However, for each of the two factors, the DDA decreases with a decrease in one of the two factors regardless of the one increasing. This shows that for these two factors, the factor decreasing in value has more influence than the factor increasing, for both NaOH concentration and temperature. At a temperature of 100 ºC and NaOH concentration of 60 % the DDA is 79 %, if the temperature is decreased by half to 50 ºC the DDA decreases to 61 %. Similarly, if the NaOH concentration is decreased by half to 30 % the DDA decreases to 74 %. Thus there is a decrease in the DDA if either of the factors is varied however, the decrease in temperature had a more significant effect on the decrease of DDA than that observed by the decrease in NaOH concentration. Thus temperature is more significant than NaOH concentration. A DDA of 61 % is achieved with a temperature of 130 ºC and NaOH concentration of 10 % and with a temperature of 50 ºC and NaOH concentration of 60 %. This reinforces the observation that a decrease in the DDA occurs regardless of which factor is decreased and shows that temperature has a more significant effect on the DDA than NaOH concentration. These results support the observations described.

Figure 4.5 shows the contours obtained from the 3D surface. Figure 4.5 confirms that the DDA increases for both an increase in NaOH concentration and temperature. The interaction of NaOH concentration and temperature is such that the greatest DDA is approximately 50 % which coincides with the temperature of approximately 100 ºC. The contour diagram also confirms that of the two variables studied, whichever variable is decreasing has more influence than the increasing variable.

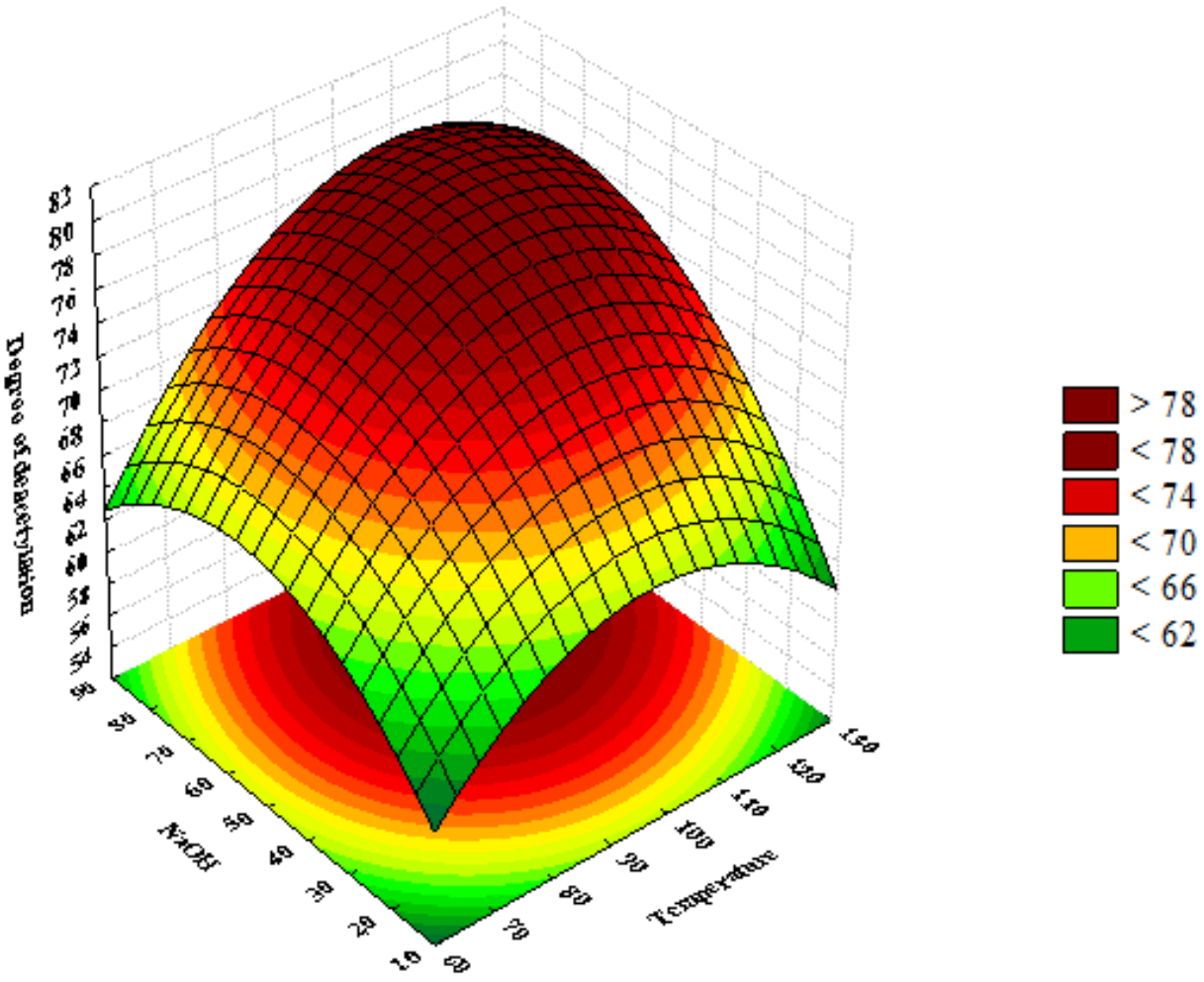

Figure 4.5: 3D surface response of DDA with respect to NaOH concentration and temperature at a time of 60 minutes

Figure 4.6 shows the effect of the NaOH concentration in (% NaOH) and time (in minutes) on the DDA of the synthesized chitosan. Figure 4.6 also shows the interactions of the NaOH concentration and time. The general observed trend was there is a quadratic relationship between NaOH concentration and time, with a maximum turning point at 50 % NaOH and 60 minutes. As the NaOH concentration was increased in isolation, the DDA increased up to an NaOH concentration of 50 %. An increase after 50 % showed a decrease in the DDA of the chitosan. This is because the higher NaOH promotes the degradation of the acetyl group. As this occurs, more amine groups are formed, thus increasing the DDA of the sample. But a NaOH of greater than 50 % promotes the degradation of the sample as a whole. A similar trend is seen with an increase in time, although the increase in DDA is not as significant. This is because as the reactants are kept in contact for longer the reaction is allowed to proceed further. It was found that after a reaction time of 60 minutes the DDA began to decrease. The reaction reaches completion at 60 minutes the DDA then decreases. At a NaOH concentration of 50 % and time of 100 minutes the DDA of the synthesised chitosan is 77 %, at a NaOH concentration of 100 % and a time of 50 minutes the DDA of the synthesised chitosan is 74 %, and if the time is increased to 60 minutes the DDA of the synthesised chitosan is still 74 %. The increase in time does not affect the DDA. At a NaOH concentration of 10 % and time of 50 minutes the DDA of the synthesised chitosan will be 66.7, if the time is doubled to 100 minutes the DDA of the synthesised chitosan increases slightly to 67.1 %. If the NaOH concentration is doubled to 20 % the DDA of the synthesised chitosan increases more significantly to 71 %. Thus, the effect of time on the DDA of the synthesized chitosan is not as significant and the effect of NaOH concentration. These results support the observations described.

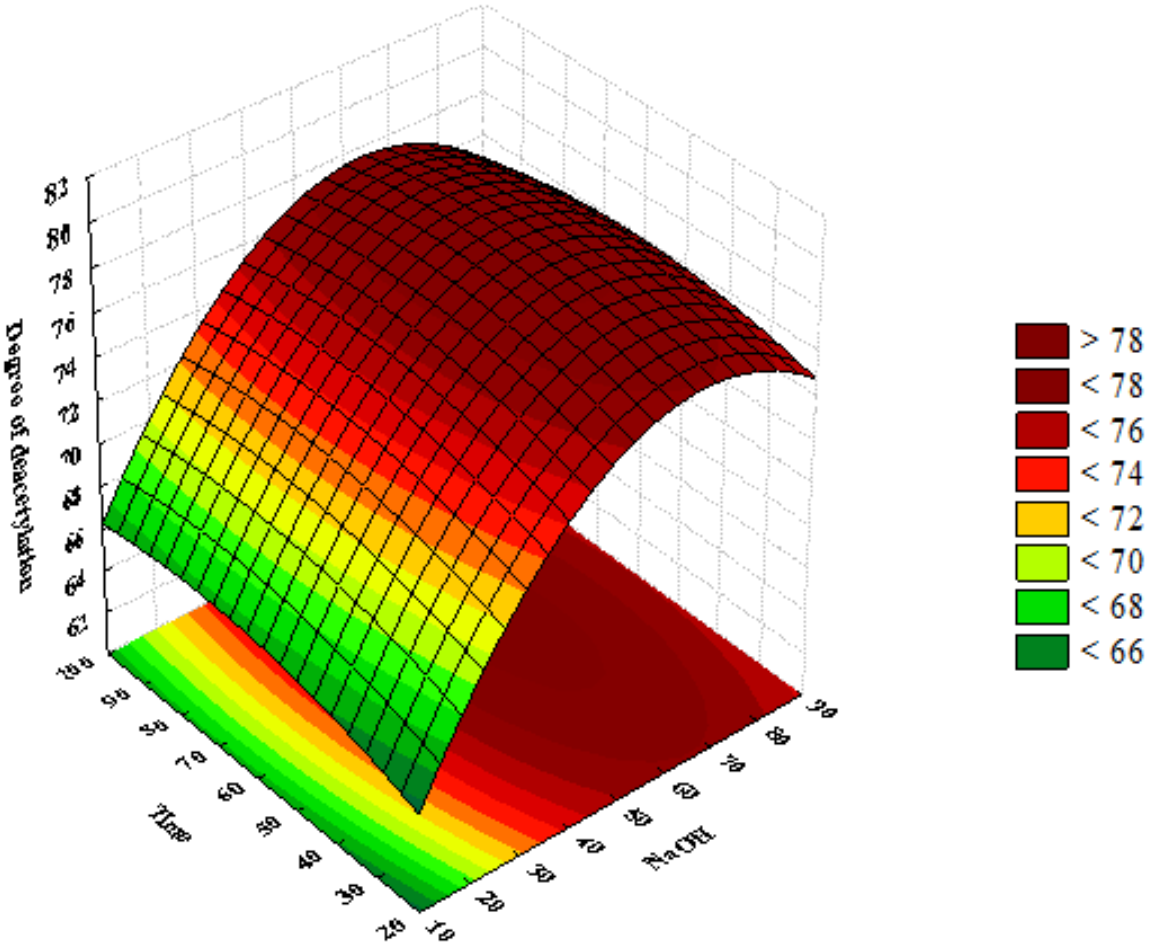

Figure 4.6: 3D surface response of DDA with respect to NaOH concentration and time at a temperature of 100 ºC

Figure 4.7 shows the effect of the temperature in ºC and time in minutes on the DDA of the synthesized chitosan. Figure 4.7 also show the interactions of the temperature and time. The general observed trend is that there is an exponential relationship between temperature and time. There is no observable turning point, hence the relationship is not quadratic. As the temperature increased in isolation, the DDA of the chitosan increased. The increase in DDA with an increase in temperature is an exponential trend and the increase in DDA from an increase in temperature slows down. This is because the higher temperature increases the kinetic energy allowing for more reactions to occur thus promoting the degradation of the acetyl group. As this occurs, more amine groups are formed, thus increasing the DDA of the sample. A temperature increase to greater than 100 ºC decreases the DDA, it can be assumed that the reaction reaches completion at 96.67 ºC and the DDA decreases. A similar trend is seen with an increase in time, although the increase in DDA is not as significant. This is because as the reactants are kept in contact for longer the reaction is allowed to proceed further. It was found that after a reaction time of 60 minutes the DDA began to decrease. The reaction reaches completion at 60 minutes the DDA then decreases. If a temperature of 100 ºC and a time of 20 minutes is used the DDA of the synthesised chitosan sample is 76 %. If the temperature is decreased to 80 ºC and the time is increased to 60 minutes the DDA of the synthesised chitosan sample is 75 %. The decrease in the temperature effected the DDA more significantly than the increase in time. The interactions between time and temperature are not as significant as the interactions between temperature and NaOH concentration. Thus, the effect of time on the DDA of the synthesized chitosan is not as significant and the effect of temperature. These results support the observations described. Figure 4.7 shows the contours obtained from the 3D surface. The contour plot confirms that NaOH concentration has a more significant effect on the DDA than the time.

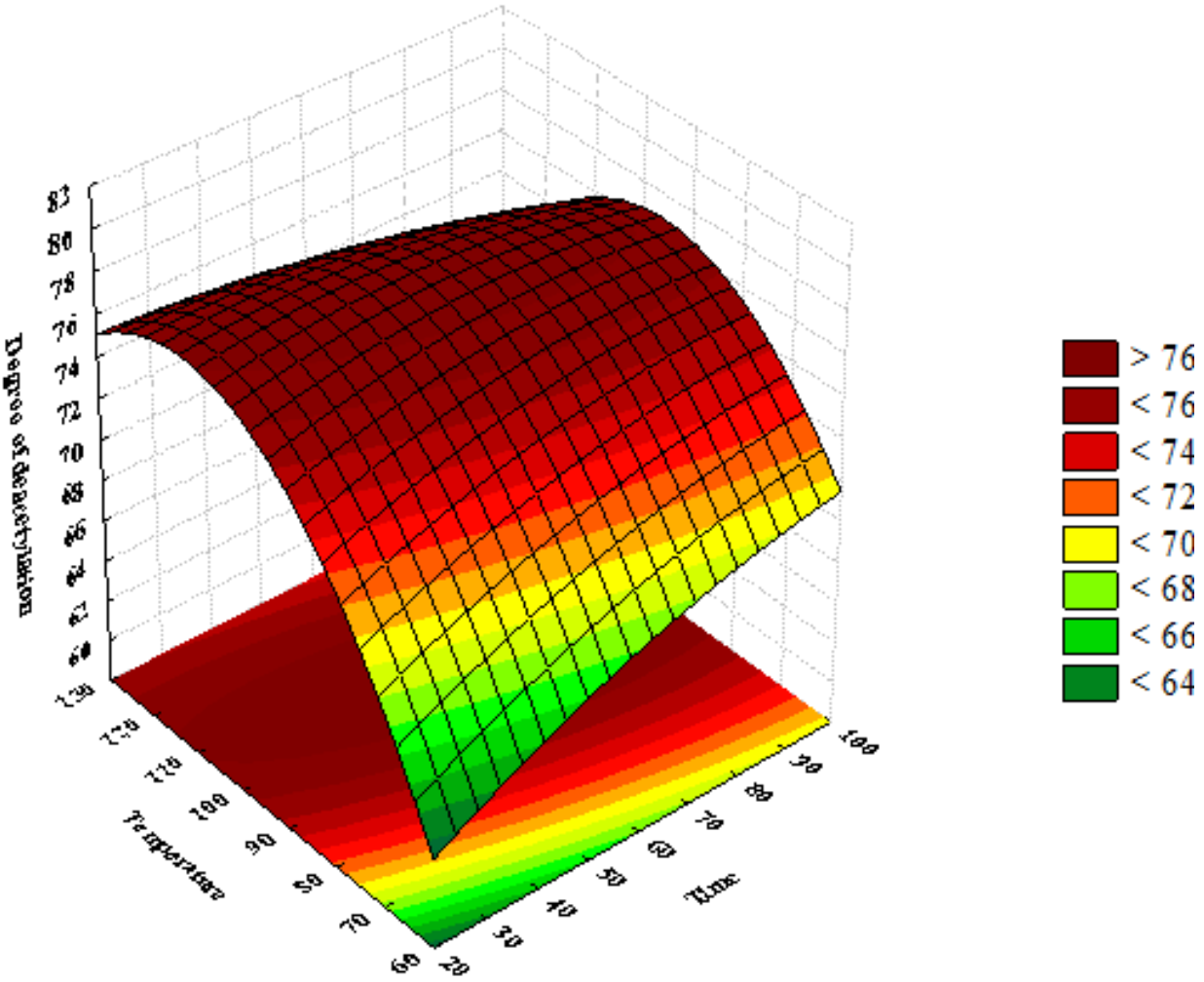

Figure 4.7: 3D surface response of DDA with respect to temperature and time at a NaOH concentration of 50 %

The conclusions from the study of the effects of the synthesis variables on the DDA of the synthesized chitosan concur and confirm the conclusions from the one-way ANOVA test which is that NaOH concentration and temperature have a more significant effect of the DDA of the synthesised chitosan. Furthermore, it was found that the interactions between NaOH concentration and temperature are more significant than the interactions between time and NaOH concentration or time and temperature.

The polynomial regression model found that the highest DDA (79.4 %) was achieved using a temperature of 96.67 ºC, NaOH concentration of 50 % and time of 60 minutes. This is in correlation with the turning

points of the parabolas as it was found that the DDA decreases as temperature is increased beyond 96.67, as NaOH concentration is increased beyond 50 % and time is increased beyond 60 minutes.

4.4.4. Model Validation

The validity of the model was evaluated by using the model equation to predicting the DDA of chitosan samples and to compare the predicted DDA with the experimentally determined DDA. Studies from literature where chitosan was synthesised were used. The synthesis variables used in this study were obtained and the model was used to obtain a predicted DDA, this DDA was compared to the DDA experimentally determined and reported in literature. Table 4.5 shows the literature study, temperature, NaOH concentration and time used for the synthesis. It compares the reported and predicted DDA by giving the percentage error. Table 4.5 shows that the model gives fairly accurate results, with the largest error being 9 %. In section 4.4.3 it was found that if temperature was increased above 60 minutes there was a decrease in the DDA of the chitosan sample. This relationship was confirmed with the results presented by Hongpattarakere & Riyaphan (2008).

Table 4.5: Model validation using results from studies

Literature Study	(Hongpattarakere & Riyaphan, 2008)	(Hongpattarakere & Riyaphan, 2008)	(Yen et al. 2009)
Temperature (ºC)	100	100	105
NaOH Concentration	50	50	40
Time	60	120	60
Experimental DDA	74.80	74.19	83.3
Model Predicted DDA	78.0	76.3	76.4
% Error	4.1	2.8	9.0

The proposed polynomial regression model is fairly accurate.

4.5. Summary

The DDA of the chitosan gives an indication of the amount of amine groups present. The more amine groups present, the more sites for adsorption to occur. The DDA of chitosan will affect the adsorption capacity. Research studies conducted on the synthesis of chitosan have found that the temperature, the NaOH concentration and the reaction time have the most significant effect on the DDA of the synthesised chitosan (Divya et al., 2014). Fifteen (15) samples of chitosan were synthesised. Each sample was

synthesised with different synthesis conditions to give samples with different DDAs. The synthesised chitosan was characterised. The characterisation methods used in this study were synthesis yield (to determine the efficiency of the synthesis process), TGA (to determine the thermal stability of the synthesised chitosan) and FTIR (to determine the DDA and verify the functional groups present in the synthesized chitosan).

The percentage yield of the synthesised chitosan is low for all samples. The high mass loss can be attributed to the nature of the synthesis process. The chitin samples underwent demineralization and deproteinisation steps in which the minerals and proteins were removed, thus it is expected for the yield to be low. The low yields are comparable with literature (Hongpattarakere & Riyaphan, 2008 and Kucukgulmez et al., 2011).

The synthesized chitosan is thermally suitable up to a temperature of 280 ºC. This is comparable to literature (Diab et al. 2012). The thermal stability of the chitosan was evaluated before and after adsorption. These tests showed that the thermal stability of the synthesised chitosan is not affected by the adsorption process.

The FTIR spectra confirm the presence of the functional groups corresponding with chitosan. This confirms that chitosan was successfully synthesised. The FTIR spectra of the synthesized chitosan closely resembles what was obtained in literature (Brugnerottoa et al., 2001; Divya et al., 2014 and Entar et al. 2008) again confirming the successful synthesis of chitosan.

RSM was used to identify the main and interactive effects of the synthesis variables (NaOH concentration, time and temperature) on the DDA of the chitosan. The DDA of the synthesized chitosan was determined using DDA. A polynomial regression model fitted to the data and is given in Equation 14. The regression coefficient for the polynomial regression model is 0.95.

A one-way ANOVA test was performed by the use of Statistica. The statistical significance of the quadratic polynomial equation revealed that the regression is highly statistically significant for the linear effects of temperature and NaOH concentration and for the quadratic effects of temperature and very significant for the quadratic effects of NaOH concentration. ($P \sim 0.0001$). The regression is moderately significant for the linear and quadratic effects of time, temperature by NaOH concentration and NaOH concentration by time.

To understand the effect of each synthesis variable (temperature, NaOH concentration and time three dimensional (3D) plots were made for the estimated DDA. This allowed for the analysis and investigation of the interactive effect of the three factors on the DDA. The conclusions from the study of the effects of the synthesis variables on the DDA of the synthesized chitosan confirm the conclusions from the ANOVA test which is that NaOH concentration and temperature have more significant effects on the DDA of the synthesised chitosan. Furthermore, it was found that the interactions between NaOH concentration and

temperature are more significant than the interactions between time and NaOH concentration or time and temperature.

The model was validated by using the model to predict the DDA of chitosan samples reported in literature and comparing the predicted DDA with the DDA determined experimentally and reported. There were errors of 2.8 - 9 % when compared to literature. The proposed polynomial regression model is fairly accurate.

Chapter 5 Evaluation of the CO_2 Adsorption Capacity of the Synthesised Chitosan

This chapter contains the results obtained from the evaluation of the CO_2 adsorption capacity of the synthesised chitosan.

5.1. Introduction

An adsorbent is the solid material that is used to target and remove adsorbate molecules from the bulk fluid in an adsorption process. It is important that the adsorbate be effectively removed from the bulk fluid as this is the target of any separation process. The efficiency and economic viability of the adsorption process is dependent on the adsorbent used. Chitosan was proposed as a potential adsorbent for CO_2 capture. The CO_2 adsorption capacity of chitosan was evaluated to determine if chitosan could be a suitable adsorbent for CO_2 capture. This was done using TGA and custom built CO_2 adsorption equipment. As a preliminary study, the CO_2 adsorption capacity of all the synthesised chitosan samples was evaluated. From this preliminary study it was found that sample 12 was the most suitable adsorbent of the synthesised chitosan samples. Subsequent adsorption evaluation experiments were performed on sample 12. The effect of temperature and flowrate on the CO_2 adsorption capacity was evaluated using TGA. Lastly, the custom built adsorption equipment was used to evaluate the CO_2 adsorption capacity of the synthesised chitosan using a mixed gas stream to mimic flue gas conditions.

5.2. Preliminary Evaluation of the CO_2 Adsorption Capacity of the Synthesised Chitosan

TGA was used to perform the preliminary evaluation of the CO_2 adsorption capacity of the synthesised chitosan. The purpose of this was to determine the effect of DDA on the CO_2 adsorption capacity. The most suitable of the synthesised chitosan samples was determined for further experiments. For the CO_2 adsorption capacity experiments, the samples of approximately 50 mg was swept with N_2 (flowrate = 60 mL/min) at atmospheric pressure and a temperature of 110 ºC for 30 minutes to desorb water and other gas impurities present on the surface of the adsorbent. After degassing, the samples were exposed to pure CO_2 (100 % CO_2) (flowrate 60 mL/min) under a pressure of 1.1 bar for 120 minutes, after which the process was stopped. With all CO_2 adsorption experiments, it was found that when the temperature started to decrease to the adsorption temperature, the mass of the sample began to increase. This indicates that adsorption was already occurring. This was caused by the CO_2 that was desorbed from the sample remaining inside the TGA reaction chamber. When the temperature became favourable for CO_2 adsorption to occur the CO_2 remaining inside the TGA reaction chamber was adsorbed by the sample. A vacuum pump could be used to remove the desorbed CO_2 prior to decreasing the temperature inside the TGA reaction chamber. The observed CO_2 adsorption capacity of the sample would be lower if calculated from when the adsorption

temperature was reached. To overcome this, the CO_2 adsorption capacity of the sample was calculated from the time that the sample mass started to increase.

Gaseous impurities and different CO_2 flowrates were added at a later stage with the most suitable of the synthesised chitosan samples. The change in mass of the sample was measured and used to calculate the amount of CO_2 adsorbed, by equation 3.3.

One adsorption run was performed per sample with the average CO_2 adsorption capacity calculated thereafter. The raw data for each adsorption experiment can be found in Appendix B1. Table 5.1 shows the average CO_2 adsorption capacity in g CO_2/kg chitosan. The CO_2 adsorption capacities are low. The highest CO_2 adsorption capacity was achieved by sample 12. Sample 12 will be used for subsequent experiments. There are no studies in open literature on the CO_2 adsorption capacity of chitosan. The adsorption capacity of the chitosan is compared to other adsorbents used for CO_2 capture in Table 5.2. The Methyl Amine/Polysuccinide/ Ethylenediamine Hybrid and Mono-EthanolAmine//Polysuccinide/ Ethylenediamine Hybrid adsorbents reported by Chitsiga (2016) have CO_2 adsorption capacities that are comparable to the highest CO_2 adsorption capacities achieved by the synthesised chitosan. The CO_2 adsorption capacities of the other adsorbents considered from literature are significantly higher than the synthesised chitosan. While the CO_2 adsorption capacity of the synthesised chitosan lower than the literature, it is important to consider that the polymer is derived from a waste material and as such it is possible to cost effectively utilize a large amount.

Table 5.1: CO_2 adsorption capacity of the synthesised chitosan

Sample	Experimental Conditions			% DDA	Average CO_2 Adsorption Capacity (gCO_2 /kg Chitosan)	Standard Deviation
	Temperature (^oC)	NaOH Concentration	Time (minutes)			
1	80	30	40	70.01	9.40	0.52
2	80	30	80	72.07	6.76	0.25
3	80	70	40	73.63	4.35	0.12
4	80	70	80	75.28	0.38	0.06
5	120	30	40	71.77	4.56	0.32
6	120	30	80	70.42	2.68	1.02
7	120	70	40	78.48	1.09	0.41
8	120	70	80	76.73	1.64	0.62
9	100	50	60	77.64	0.00	0.00
10	66.4	50	60	69.76	3.02	0.86
11	133.6	50	60	75.55	2.06	0.11
12	100	16.4	60	68.92	10.38	0.15
13	100	83.6	60	77.36	3.19	0.72
14	100	50	26.4	76.71	2.32	1.16
15	100	50	93.6	76.97	1.11	0.70

Table 5.2: CO_2 adsorption capacity of adsorbents

Adsorbent	Operating Conditions (Temperature (^{0}C), Pressure (bar)	Average CO_2 adsorbed (g CO_2/ kg adsorbent)	Reference
Polysuccinide	25, 1.1	25	(Ngoy et al., 2014)
Polyaspartamide	25,1.1	47.1	(Ngoy et al., 2014)
Methyl Amine	40, 1.1	44.5	(Chitsiga, 2016)
Methyl Amine/Polysuccinide/ Ethylenediamine Hybrid	40, 1.1	9.8	(Chitsiga, 2016)
Mono-Ethanol Amine	40, 1.1	43.6	(Chitsiga, 2016)
Mono-EthanolAmine//Polysuccinide/ Ethylenediamine Hybrid	40, 1.1	9.59	(Chitsiga, 2016)
Chitosan Sample 12 (DDA: 68.92 %)	45, 1.1	10.38	(This study)

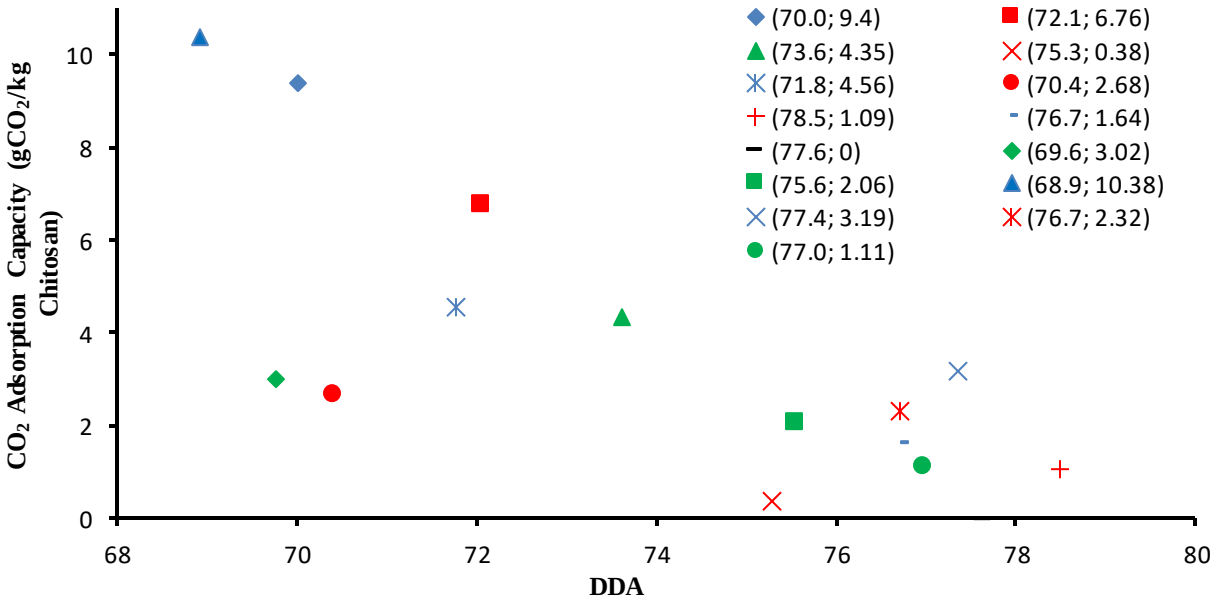

Figure 5.1 shows the effect of DDA on the CO_2 adsorption capacity of the synthesised chitosan. In Chapter

4 it was hypothesised that the DDA of chitosan will affect the CO_2 adsorption capacity of the synthesised chitosan. The greater the DDA more the amine groups are present. Thus there are more sites for adsorption to occur.

Figure 5.1

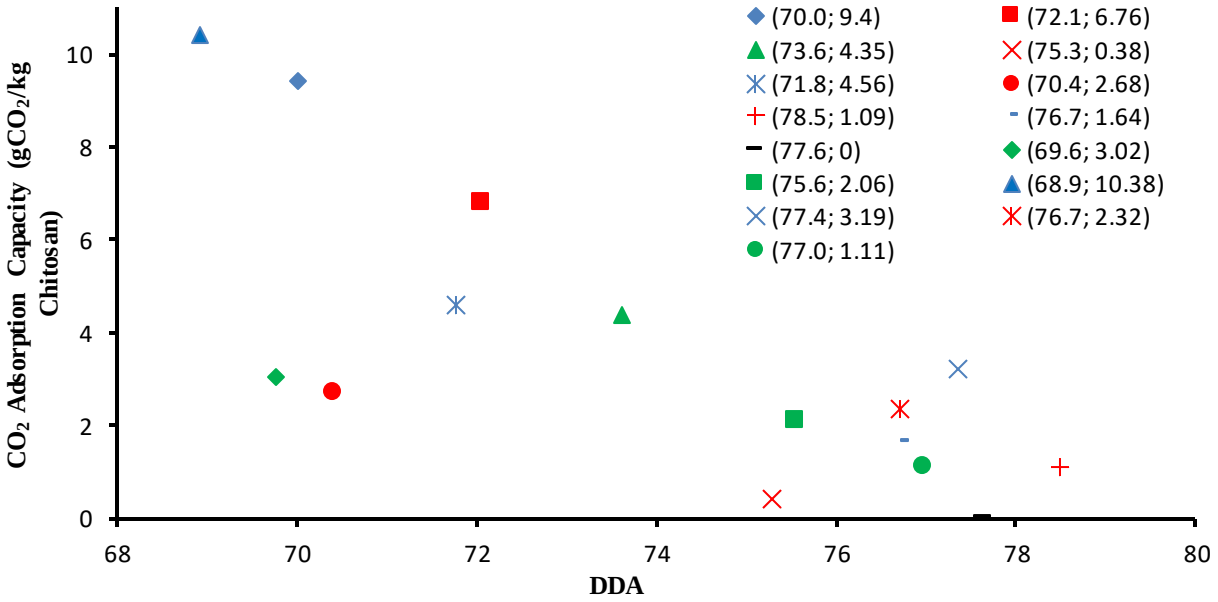

Figure 5.1 shows that the CO_2 adsorption capacity of the synthesised chitosan is highest with a DDA of approximately 70 %. There after there is a linear decrease in the CO_2 adsorption capacity with an increase in the DDA. This is not what was expected. This could potentially be attributed to the cross-linking of amines. Cross-linking occurs when polymers are chained together due to the presence of covalent or ionic bonds (Ngoy et al., 2014). In this particular polymer, the amines could have cross-linked during the deacetylation process resulting in the loss of adsorption sites. The cross-linking could have occurred as the NaOH concentration increased. A greater NaOH concentration promotes the degradation of the acetyl group and more amine groups are formed, the increase in the amine groups leads to a cross-linkage.

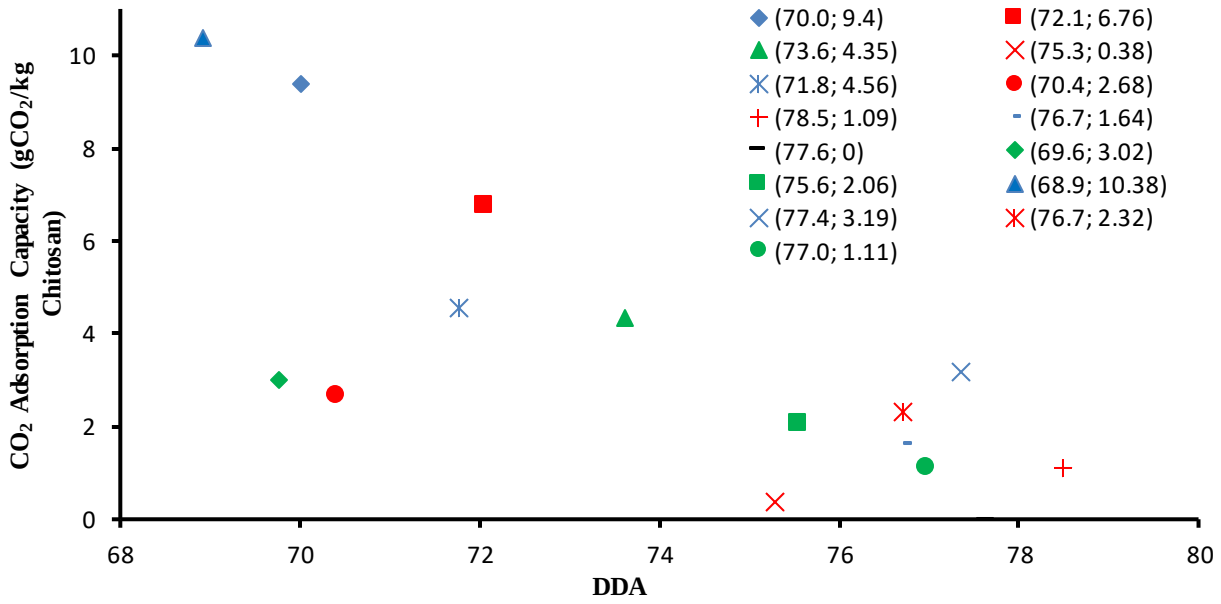

Figure 5.1: Effect of DDA on the CO_2 adsorption capacity of the synthesised chitosan

5.3. Evaluation of the CO_2 Adsorption Capacity of the Sample 12

Preliminary CO_2 adsorption evaluation experiments determined that sample 12 was the most suitable of the synthesised adsorbents. The DDA of sample 12 was 68.92 %. The CO_2 adsorption performance of sample 12 was evaluated using TGA to vary the temperature and flowrate. Subsequent to the TGA the CO_2 adsorption performance of sample 12 was evaluated using the custom built CO_2 adsorption equipment. The purpose of the custom built CO_2 adsorption equipment is to mimic flue gas conditions.

5.3.1. Thermogravimetric Analysis

More extensive TGA experiments performed on sample 12. For the CO_2 adsorption capacity experiments the samples of approximately 50 mg was swept with N_2 (flowrate = 60 mL/min) at atmospheric pressure and a temperature of 110 ºC for 30 minutes to desorb water and other gas impurities present on the surface of the adsorbent. After degassing, the samples were cooled to 25, 35 and 45 ºC an exposed to pure CO_2 (100 % CO_2) (flowrate 45, 60 and 75 mL/min) under a pressure of 1.1 bar for 120 minutes, after which the process was stopped. With all CO_2 adsorption experiments, it was found that when the temperature started to decrease to the adsorption temperature, the mass of the sample began to increase. This indicates that adsorption was already occurring. This was caused by the CO_2 that was desorbed from the sample remaining inside the TGA reaction chamber. When the temperature became favourable for CO_2 adsorption to occur the CO_2 remaining inside the TGA reaction chamber was adsorbed by the sample. A vacuum pump could

be used to remove the desorbed CO_2 prior to decreasing the temperature inside the TGA reaction chamber. The observed CO_2 adsorption capacity of the sample would be lower if calculated from when the adsorption temperature was reached. To overcome this, the CO_2 adsorption capacity of the sample was calculated from the time that the sample mass started to increase. The change in mass of the sample was measured and used to calculate the amount of CO_2 adsorbed, by the equation 3.3.

One adsorption run was performed per sample with the average CO_2 adsorption capacity calculated thereafter. The raw data for each adsorption experiment can be found in Appendix B2.

5.3.1.1. Evaluation of the Effect of Temperature on CO_2 Adsorption Capacity

The effect of temperature on CO_2 adsorption capacity is an important factor for post-combustion CO_2 capture processes. It is expected that the temperature will influence the nature of the adsorption that occurs, i.e., physisorption or chemisorption. The effect of temperature on CO_2 adsorption was evaluated using TGA. The temperature was varied and the CO_2 flowrate was kept constant at 60 mL/min. Table 5.3 shows the effect of temperature on CO_2 adsorption capacity. The highest adsorption capacity was obtained at 25 ^oC. Figure 5.2 shows the decrease in CO_2 adsorbed with an increase in temperature. The observed trend is that the CO_2 adsorption decreased with increase in temperature. This observation is consistent with literature because adsorption of gases decreases with an increase in temperature. At a constant pressure, the kinetic energy of gases increases with temperature, resulting in lesser surface coverage of CO_2 gas. The observed trend can be attributed to the exothermic nature of the adsorption process. Le Chatlier's principle explains this, when it is applied to predict the extent of an exothermic process states that increasing the temperature will decrease the magnitude of an exothermic reaction.

It was expected that the nature of the adsorption would be chemisorption. Fogler is in agreement and states that with chemisorption the magnitude of the adsorption will initially increase to a maximum with an increase in temperature and will decrease thereafter (Fogler, 2010). Fogler suggests that this is because with chemisorption the activation energy has to be achieved first, thereafter the reaction occurs and the subsequent decrease is attributed to exothermic nature of the reaction (Fogler, 2010). This was not the observed trend with the chitosan. Ngoy reported that while this chemisorption trend is possible, it is not always the case (Ngoy, 2016).

The adsorption mechanism for chitosan can either be both physisorption and chemisorption or can be purely chemisorption. It is recommended that experiments considering the heat of adsorption of chitosan be conducted in an attempt to fully quantify and understand the CO_2 adsorption mechanism of chitosan.

Table 5.3: Effect of temperature on CO_2 adsorption capacity. Constant CO_2 flowrate of 60 mL/min

Temperature	CO_2 Adsorption Capacity (g CO_2/kg Chitosan)
25 ºC	11.86
35 ºC	10.38
45 ºC	8.07

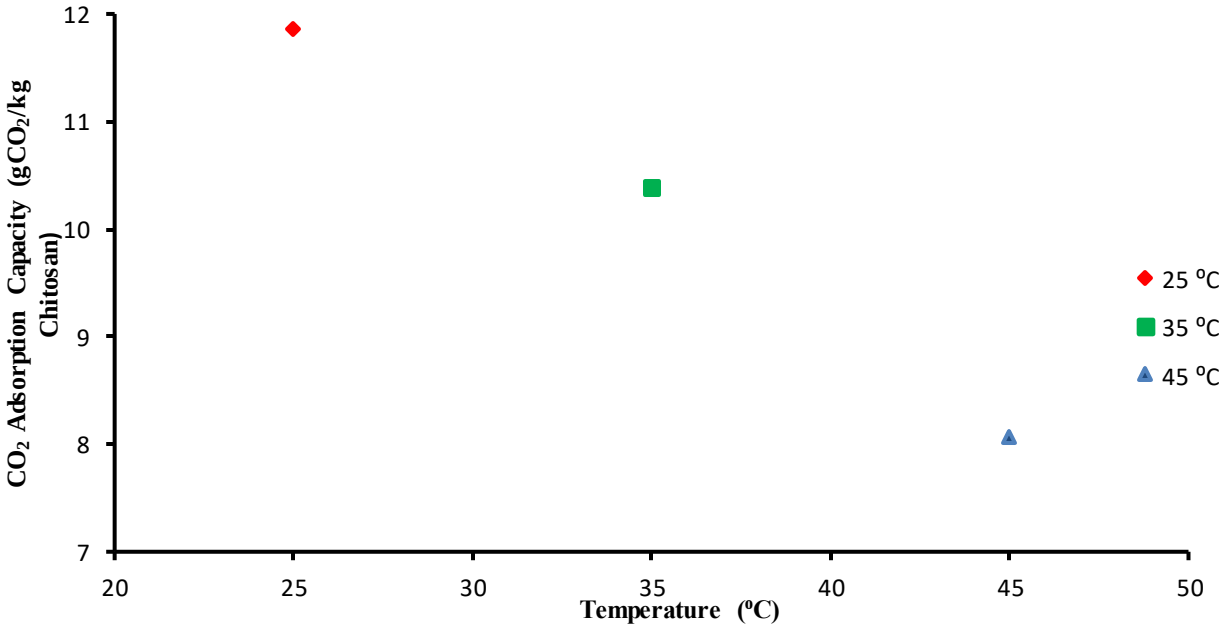

Figure 5.2: Effect of temperature on CO_2 adsorption capacity. Constant CO_2 flowrate of 60 mL/min

5.3.1.2. Evaluation of the Effect of Flowrate on CO_2 Adsorption Capacity

The effect of flowrate on CO_2 adsorption capacity is an important factor for post-combustion CO_2 capture processes. It is expected that the flowrate will influence the amount of CO_2 adsorbed. The effect of flowrate on CO_2 adsorption was evaluated using TGA. The flowrate was varied while the temperature was kept constant at 35 ºC. Table 5.4 shows the effect of flowrate on CO_2 adsorption capacity. The highest CO_2 adsorbed was achieved using a flowrate of 60 mL/min. The CO_2 adsorbed with a flowrate of 45 and 75 mL/min are both lower than that achieved with a flowrate of 60 mL/min. Figure 5.3 shows this trend graphically. It can be seen that the trend appears to be quadratic, with a maximum CO_2 adsorption capacity at 60 mL/min. It is hypothesised that higher flowrate increases the force and pushes the CO_2 gas onto he chitosan surface and there is an increase in CO_2 adsorbed. This happens up to a point, where the maximum

CO_2 adsorbed. A further increase in flowrate decreases the contact time between the CO_2 gas and the adsorbent and thus decreases the CO_2 adsorbed. Osler et al. showed the same trend when using MWCNTs as an adsorbent for CO_2 capture (Osler et al., 2017). It is necessary to conduct further experiments at a wider range of flowrates to confirm this hypothesis.

Table 5.4: Effect of flowrate on CO_2 adsorption capacity. Constant temperature of 35 ºC

Flowrate	CO_2 Adsorption Capacity (g CO_2/kg Chitosan)
45 mL/min	9.10
60 mL/min	10.38
75 mL/min	8.67

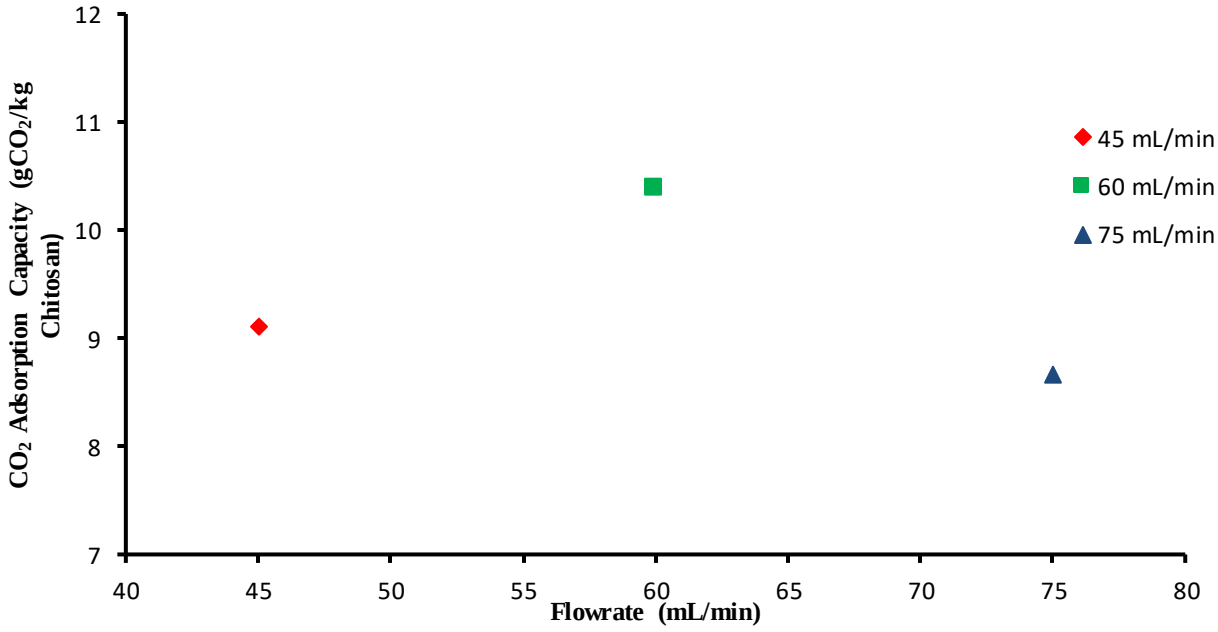

Figure 5.3: Effect of flowrate on CO_2 adsorption capacity. Constant temperature of 35 ºC

5.3.1.3. Evaluation of the Rate of CO_2 Adsorption with Time

The CO_2 adsorbed as a function of time and is shown in Figure 5.4. The observed trend is that when the chitosan sample is fresh and there are many available adsorption sites the rate of adsorption is high. As the absorption sites fill with CO_2 and there are fewer free adsorption sites and the rate of adsorption decreases, the amount of CO_2 adsorbed per minute decreases. At 95 minutes the adsorption process reached

equilibrium. No more CO_2 was adsorbed after this point. The trend observed is comparable to literature (Ngoy, 2016; Chitsiga, 2016).

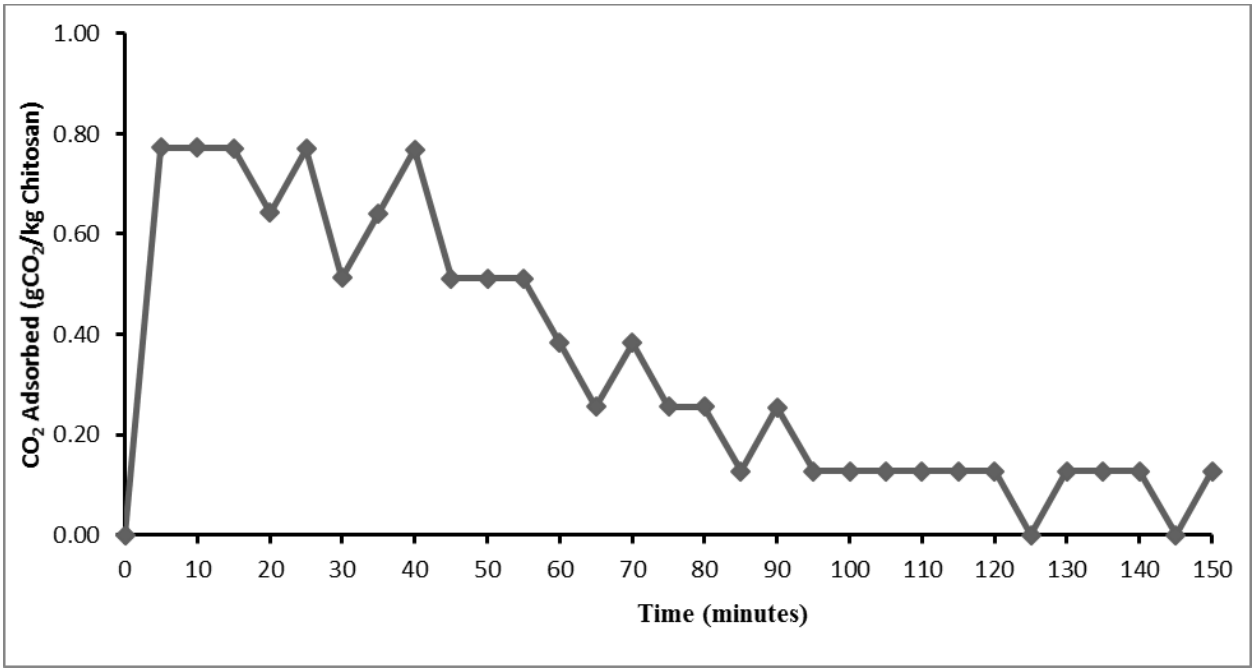

Figure 5.4: CO_2 adsorbed per minute

5.3.2. Custom Built CO_2 Adsorption Equipment

Custom built CO_2 adsorption equipment (built by Chemvak) was used to mimic flue gas conditions to test the CO_2 adsorption capacity of the synthesised chitosan at conditions that mimic industry operation. The adsorption equipment consists of a packed bed reactor, heater, mass flow controller and gas analyser, supplies gas at a concentration of either 100 % CO_2, 100 % N_2 or 15 % CO_2 and 85 % N_2. 15 % CO_2 is used to mimic the flue gas conditions in industry, such as would be found in a typical South African Coal Fired Power Station. The packed bed reactor was packed with a 0.01 g of adsorbent sample (packing height approximately 15 mm). N_2 was then passed over the sample at 110 ºC to desorb water and other gas impurities present on the surface of the adsorbent. The reactor temperature was decreased to 25 ºC and gas at 15 % CO_2 (50 mL/min) was then bypassed to the CO_2 analyser to read 15 % as an initial starting point. Flow is then diverted through the reactor where adsorption takes place and then through the CO_2 analyser. The CO_2 concentration reading given by the analyser decreases as CO_2 is adsorbed. The adsorption process is complete once the analysed reads 15 % CO_2 again. The inlet flowrate and CO_2 concentration from the gas analyser was used to calculate the CO_2 adsorbed by the equation 3.4.

Under these conditions the synthesised chitosan had a CO_2 adsorption capacity of 279 g CO_2/kg chitosan. This is significantly higher than the CO_2 adsorption capacity achieved using the TGA. This is attributed to the packed column allowing for direct contact between the gas and the adsorbent. The direct contact increases the CO_2 adsorbed because it allows for all the adsorption sites to be filled.

The high CO_2 adsorption capacity achieved by the chitosan in the presence of impurities confirms that chitosan is able to selectively remove CO_2 from a mixed gas stream, such as flue gas. However, these results are debateable as there were problems with the custom-built CO_2 adsorption equipment. The results given by this equipment are not comparable to literature as they not a true reflection on the CO_2 adsorption ability of the chitosan. Chitosan could potentially be a suitable adsorbent for CO_2 capture. It is recommended that the experiments with the custom-built CO_2 adsorption equipment be conducted using more accurate equipment.

5.4. Summary

Chitosan was proposed as a potential adsorbent for CO_2 capture. The CO_2 adsorption capacity of chitosan was evaluated to determine if chitosan is a suitable adsorbent for CO_2 capture. As a preliminary investigation, the CO_2 adsorption capacity of all the synthesised chitosan samples was determined. It was found that the CO_2 adsorption capacities of the synthesised chitosan was lower than some adsorbents used in literature. But was also comparable to adsorbents reported by Chitsiga (2016). However, it is important to note that the polymer is derived from a waste material. It is possible to cost effectively utilize a large amount of chitosan.

The CO_2 adsorption capacity of the synthesised chitosan was considered with respect to the sample's DDA. In Chapter 4 it was hypothesised that the DDA of chitosan will affect the CO_2 adsorption capacity of the synthesised chitosan. The greater the DDA more the amine groups are present. Thus there are more sites for adsorption to occur. In contradiction to this, it was found that the highest CO_2 adsorption capacity was given from sample 12 which had a DDA of 68.92 %. This could potentially be attributed to the cross-linking of amines. Subsequent CO_2 adsorption experiments were conducted using only sample 12.

The effect of temperature on CO_2 adsorption was evaluated using TGA. The temperature was varied and the CO_2 flowrate was kept constant at 60 mL/min. The observed trend is that the CO_2 adsorption decreased with increase in temperature. This observation is consistent with literature. The observed trend can be attributed to the exothermic nature of the adsorption process.

The effect of flowrate on CO_2 adsorption was evaluated using TGA. The flowrate was varied while the temperature was kept constant at 35 ºC. The observed trend appears to be parabolic with a maximum CO_2

adsorption capacity at 60 mL/min. It is hypothesised that higher flowrate increases the force and pushes the CO_2 gas onto the chitosan surface and there is an increase in CO_2 adsorbed. This happens up to a point, where the maximum CO_2 adsorbed. A further increase in flowrate decreases the contact time between the CO_2 gas and the adsorbent and thus decreases the CO_2 adsorbed.

Custom built CO_2 adsorption equipment (built by Chemvak) was used to mimic flue gas conditions to test the CO_2 adsorption capacity of the synthesised chitosan at conditions that mimic industry operation. The synthesised chitosan had a CO_2 adsorption capacity of 279 g CO_2/kg chitosan. The high CO_2 adsorption capacity achieved by the chitosan in the presence of impurities confirms that chitosan is able to selectively remove CO_2 from a mixed gas stream, such as flue gas. However, as explained in chapter 3 these results are not accurate as there were problems with the custom-built CO_2 adsorption equipment.

Chapter 6 Synthesis, Characterisation and Evaluation of the CO_2 Adsorption Capacity of the Chitosan/MWCNTs.

This chapter contains the results pertaining to the synthesis, characterisation and evaluation of the CO_2 adsorption capacity of the synthesised chitosan/MWCNTs.

6.1. Introduction

Reports from literature have shown that grafting or impregnating a surfactant onto the surface of a CNT enhances the CO_2 adsorption capacity of that CNT (Lee & Park, 2015; Ngoy et al., 2014 and Su & Chen, 2011). However, many of the amine-based polymers used in these studies are not biodegradable and are toxic. In order to develop an alternative biodegradable and non-toxic polymer, chitosan was impregnated onto the surface of MWCNTs. A chitosan/MWCNTs composite adsorbent was synthesised. The chitosan/MWCNTs were characterized to study the effects of impregnation on the surface properties of the MWCNTs. Characterisation methods utilized were Raman spectroscopy, N_2 physisorption, SEM and FTIR.

Subsequent to the characterisation of the chitosan/MWCNTs, the CO_2 adsorption capacity of the novel adsorbent was evaluated. This was done using TGA and custom built CO_2 adsorption equipment. The main emphasis of this evaluation was placed on the degree to which chitosan impregnation improved the CO_2 adsorption capacity of the MWCNTs.

6.2. Synthesis

Synthesised chitosan (sample 12) was impregnated onto the MWCNTs. MWCNTs were purchased from Sigma Aldrich (Pty) South Africa. The MWCNTs were covalently functionalised prior to impregnation. Chitosan impregnation was performed by dissolving chitosan in acetic acid and stirring the solution at 80 ºC under reflux for 1 h. MWCNTs were then added and the mixture was again stirred at 80 ºC under reflux for 1 h. The chitosan/MWCNTs were washed with distilled water and filtered using a vacuum pump until the pH was around 7. The chitosan/MWCNTs were oven dried at 60 ºC for 24 h.

6.3. Characterisation

Characterization was performed to determine the quality of the MWCNTs and synthesised chitosan/MWCNTs. Characterisation was also used to confirm that the target material was actually synthesized.

6.3.1. Raman Spectroscopy

Raman spectroscopy is widely used in the characterisation of CNTs due to the good spatial resolution and sensitivity. Raman Spectroscopy was used to check the quality of the MWCNTs Figure 6.1 shows the

Raman spectra results of the MWCNTs. A band between 1000 and 1200 cm^{-1} can be seen. This band was caused by the over light used and is not caused by the sample.

Radial breathing modes (RBM) peaks are specific to the Raman spectra of single-walled CNTs. RBM peaks are caused by the radial expansion and contraction of a single graphene cylinder, similar to if the tube was 'breathing' (Sethi & Barron, 2009). With multi-walled CNTs having many graphene cylinders the expansions and contractions are drowned out and not RBM peak is seen. For single-walled CNTs the RBM peak is found between 75 cm^{-1} and 300 cm^{-1} (Sethi & Barron, 2009). The RBM peak is an obvious method to distinguish between multi-walled and single-walled CNTs. There is no RBM peak in Figure 6.1. This indicates that the CNTs are multi-walled.

D-bands are longitudinal optical phonon modes and are located between 1330 cm^{-1} and 1360 cm^{-1}. The D-peak originates from the presence of impurities (such as catalyst remains and amorphous carbon) (Sethi & Barron, 2009). A larger D-peak compared to the G-peak indicates more impurities and structural defects present in the MWCNTs (Dresselhaus et al., 2005). The D-peak in Figure 6.1 is small in comparison to the G-peak. This indicates that there are few impurities or structural defects.

G-bands, also known as the tangential mode, correspond to the planar vibrations of carbon atoms. The G-peak is located at approximately 1600 cm^{-1}. The ratio of the D-peak to the G-peak is used to determine the quality of the CNTs (Costa et al., 2008). For the MWCNTs, this ratio (D-peak: G-peak) is small. This indicates that for the MWCNTs there is very little presence of amorphous carbon and they are of excellent structural quality.

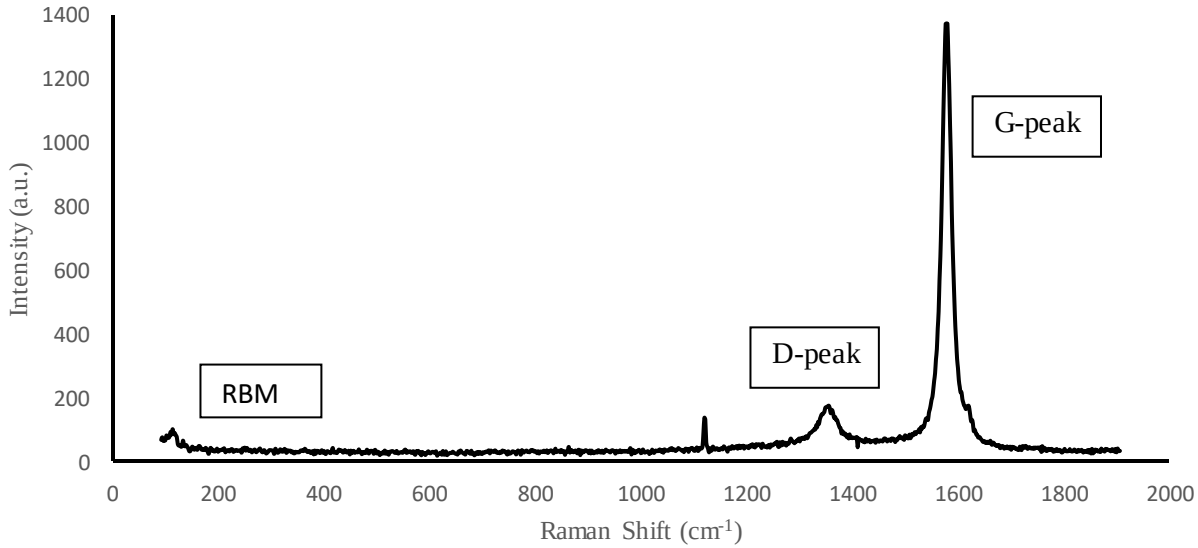

Figure 6.1: Raman spectra of the MWCNTs

6.3.2. N_2 Physisorption

N_2 physisorption was conducted using a Brunauer-Emmett-Teller theory as discussed in chapter 2. N_2 physisorption was used to determine the surface geometry (surface area, pore size and pore volume) of the MWCNTs and chitosan impregnated MWCNTs. Table 6.1 shows the results of the surface area, pore size and pore volume. These results are compared to literature.

Large surface area is a desired characteristic of any adsorbents because a larger surface area implies a larger amount of surface on which CO_2 adsorption can occur. The surface area of the MWCNTs used in this study is low. This indicates that the MWCNTs are not suitable as adsorbents for CO_2 capture. However, the surface area of the MWCNTs increase by 590 % after impregnation with chitosan. Chitosan impregnation improved the surface area of the MWCNTs.

Porosity is the collective term that is given to these pores and their distribution in the structure of a solid. Pores are the minute openings in solids that are accessible to gases. Pore size refers to the diameter of the pores (Mosher, 2011). Pore size is an important characteristic for adsorption for two reasons, the first being that different gases display different particle sizes based on the intramolecular forces and bond strengths experienced. For adsorption to take place it is necessary for the gas particles to be able to enter into the pores of the adsorbent. If the gas particle is too large for the pores, then adsorption is less likely to occur.

The second reason that pore size is important for the determination of a good adsorbent is that different pore sizes have been shown to behave differently during adsorption. For example, micropores (width not exceeding 2 nm) will primarily experience physisorption at a pore-filing stage only. This differs to mesopores (width between 2 nm and 50 nm) and macropores (width exceeding 50 nm) which show multilayer adsorption. Mesopores have been shown to be the best for CO_2 gas adsorption (Mosher, 2011). The MWCNTs used in this study are mesoporous, indicating that multilayer adsorption will occur. After chitosan impregnation, the pore size remains mesoporous.

Pore volume is the ratio of air volume to the total volume of a porous material and is an indication of the free space available inside the porous material. A high pore volume is a desirable property of an adsorbent because it implies that there is more space available for adsorption to occur.

A greater the pore volume will allow for a greater amount of CO_2 to be adsorbed within the pores of the walls of the CNTs. The pore volume of the MWCNTs used in this study is much smaller than MWCNTs used in literature. The pore volume of the MWCNTs was substantially increased after impregnation. Chitosan impregnation improved the pore volume of the MWCNTs.

Ngoy et al. separately impregnated polyaspartamine and polysuccininde onto MWCNTs to generate two different composite adsorbents. Ngoy et al. reported that the surface geometry of the MWCNTs was decreased after impregnation in both instance (Ngoy et al., 2014). It is expected that as you impregnate amines there will be a decrease in the surface geometry because the amine occupies space on the surface. In this study, it was found that impregnating the MWCNTs with chitosan significantly improved the surface geometry of the MWCNTs. Paktool et al. impregnated activated carbon with chitosan. Table 6.1 shows the surface geometry of the activated carbon before and after impregnation. Paktool et al. reported that after chitosan impregnation the surface geometry of the activated carbon improved (Patkool et al., 2014). This is in agreement with the findings of this study. Chitosan is unique when compared to other amines based polymers because it has been reported to be able to improve the surface geometry of the solid after impregnation. Chitosan is more suitable for solid impregnation than other amines. The improvement in the surface geometry of the MWCNTs after chitosan impregnation is attributed to the small size (and thus larger surface area and pore volume) of chitosan in comparison to the size of the MWCNTs. The hypothesis that the size of chitosan is small in comparison to the MWCNTs will be confirmed using SEM.

Table 6.1: N_2 Physisorption of MWCNTs, Chitosan/MWCNTs and adsorbents from literature

Absorbent	**Surface Area (m^2/g)**	**Pore Volume (cm^3/g)**	**Pore Size (nm)**	**Reference**
MWCNTs	11.88	0.045	14.71	This study
Chitosan/MWCNTs	82.18	0.47	22.40	This study
Activated Carbon	301.9	0.16	Not reported	(Patkool et al., 2014)
Chitosan/Activated Carbon	531.3	0.29	Not reported	(Patkool et al., 2014)
MWCNTs	452.69	0.74	6.56	(Ngoy, 2016)
Polyaspartamine/ MWCNTs	60.44	0.404	13.76	(Ngoy, 2016)
Polysuccinide/ MWCNTs	305.76	0.67	8.44	(Ngoy, 2016)

6.3.3. Scanning Electron Microscopy

SEM was used to obtain visual images of the MWCNTs and chitosan/MWCNTs. This gave the surface morphology of these adsorbents. Figure 6.2 are the SEM images for the MWCNTs. The SEM images show that the MWCNTs are multi-walled and have few impurities. The SEM images of the MWCNTs confirm the findings from Raman spectra. Figure 6.3 are the SEM images for the chitosan/MWCNTs. The SEM images illustrate that the chitosan has been successfully impregnated onto the surface of the MWCNTs. Figure 6.3 shows MWCNTs and chitosan in the same images. It can be seen that chitosan is much smaller than the MWCNTs. This confirms the hypothesis from N_2 physisorption.

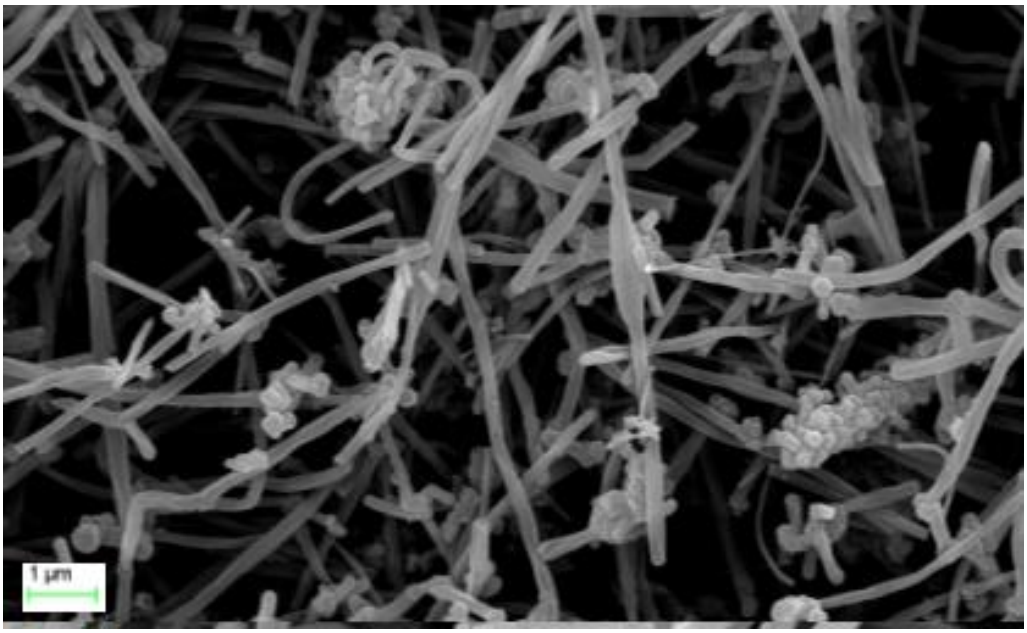

Figure 6.2: SEM images for MWCNTs

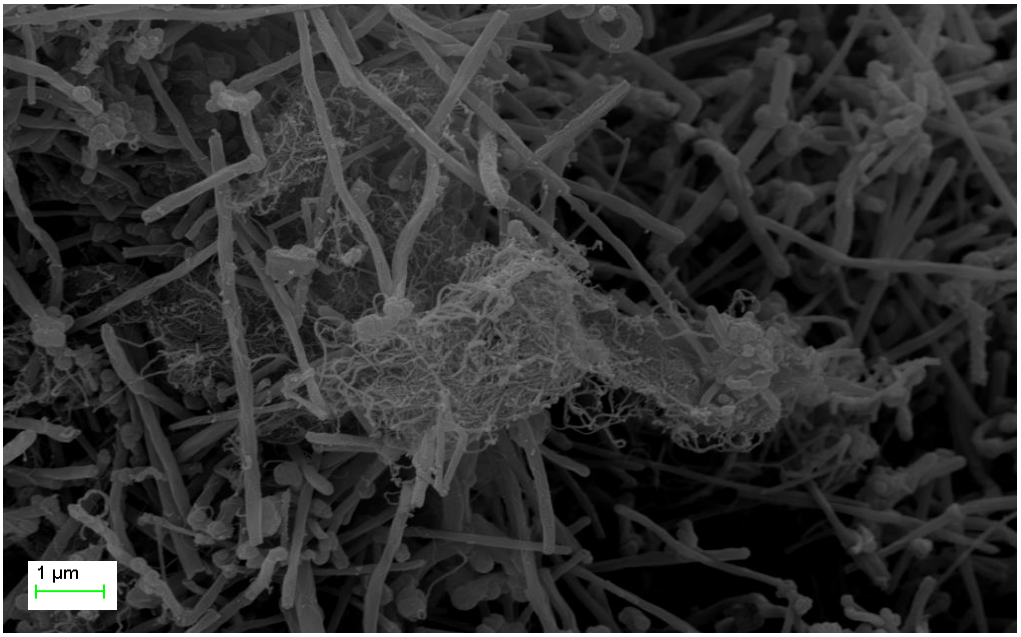

Figure 6.3: SEM Images for Chitosan/MWCNTs

6.3.4. FTIR Analysis

FTIR is commonly used to analyse the chemical bonds and functional groups that are present and was used to confirm that chitosan impregnation was successful. FTIR was used to verify the functional groups present in the chitosan/MWCNTs and to confirm that the functional groups associated with chitosan were present for the chitosan/MWCNTs. Figure 6.4 shows the FTIR spectra of the MWCNTs, chitosan and chitosan/MWCNTs respectively. The FTIR spectra for the MWCNTs and the chitosan/MWCNTs gave noise and the curves needed to be smoothened. The presence of noise is attributed to the MWCNTs being comprised of carbon. The C-C found at approximately 1000 cm^{-1} is a characteristic of the MWCNTs (Gupta & Saleh, 2011). The FTIR spectra of the chitosan/MWCNTs show the expected functional groups of chitosan as discussed in Chapter 4. Chitosan impregnation was successful. Chitosan/MWCNTs was successfully synthesised.

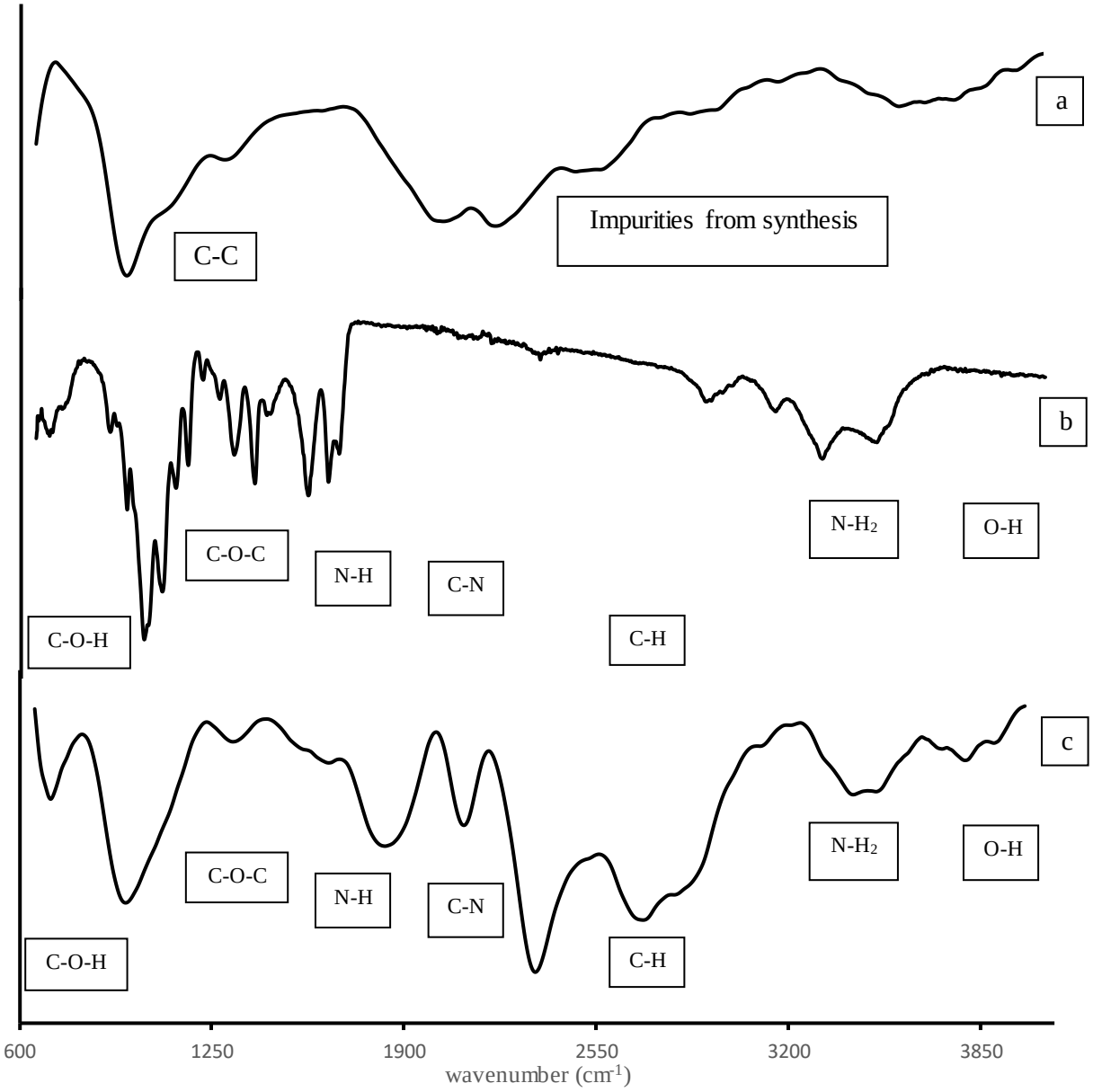

Figure 6.4: FTIR Spectra of a) MWCNTs, b) Chitosan, c) Chitosan/MWCNTs

6.4. Preliminary Evaluation of the CO_2 Adsorption Capacity of the Chitosan/MWCNTs

TGA was used to perform a preliminary evaluation the CO_2 adsorption capacity of the synthesised chitosan/MWCNTs. The purpose of this was to quantify the extent by which the CO_2 adsorption capacity of the MWCNTs was improved by chitosan impregnation. For the CO_2 adsorption capacity experiments the samples (chitosan, MWCNTs and chitosan/MWCNTs) of approximately 50 mg was swept with N_2 (flowrate = 60 mL/min) at atmospheric pressure and a temperature of 110 ºC for 30 minutes to desorb water and other gas impurities present on the surface of the adsorbent. After degassing, the samples were cooled to 45 ºC an exposed to pure CO_2 (100 % CO_2) (flowrate 60 mL/min) under a pressure of 1.1 bar for 120 minutes, after which the process was stopped. With all CO_2 adsorption experiments it was found that when the temperature started to decrease to the adsorption temperature the mass of the sample began to increase. This is attributed to the desorbed CO_2 remaining inside the TGA. When the conditions become favourable for adsorption to occur this CO_2 adsorbed onto the chitosan/MWCNTs. To overcome this, the CO_2 adsorbed was calculated from the time that the sample mass started to increase. A vacuum pump would be necessary to overcome this. The MWCNTs and the chitosan/MWCNTs began to adsorb the CO_2 at approximately 50 ºC and 90 ºC. Chitosan/MWCNTs adsorb CO_2 at a higher temperature than the MWCNTs. This is because the MWCNTs show physisorption only and the chitosan/MWCNTs show both physisorption and chemisorption. Chemisorption can occur at higher temperatures than physisorption. This confirms that chitosan impregnation was successful.

The change in mass of the sample was measured and used to calculate the amount of CO_2 adsorbed, by equation 3.3.

The TGA raw data can be found in Appendix C1. Table 6.2 shows that CO_2 adsorption capacity of chitosan, MWCNTs, chitosan/MWCNTs. The CO_2 adsorption capacity of the MWCNTs is compared to the CO_2 adsorption capacity of MWCNTs reported in literature. The MWCNTs used in this study showed an extremely low CO_2 adsorption capacity, 0.4 gCO_2/kg MWCNT. This CO_2 adsorption capacity is much lower than what has previously been reported in literature, which range from 12.03 – 21.5 g CO_2/kg adsorbent. The CO_2 adsorption capacity of the MWCNTs used in this study are not comparable with literature. The MWCNTs used in this study are not suitable for use as an adsorbent for CO_2 capture because of the low CO_2 adsorption capacity exhibited. This agrees with the conclusions from the characterisation of the MWCNTs. For the chitosan, the CO_2 adsorption capacity was found to be 9.10 g CO_2/kg chitosan at the same conditions. The CO_2 adsorption capacity of the chitosan/MWCNTs was found to be 3 g CO_2/kg adsorbent. Chitosan impregnation increased the CO_2 adsorption capacity of the MWCNTs by 650 %. This is a very substantial increase. Lee et al. reported that impregnating polyethyleneimine onto MWCNTs

increase their CO_2 adsorption capacity by 200 % (Lee & Park, 2015). Ngoy et al. reported that grafting polyaspartamine onto MWCNTs increased their adsorption capacity by nearly 500 % (Ngoy et al., 2014). The CO_2 adsorption capacity of the chitosan/MWCNTs is low however, the percentage increase of the CO_2 adsorption capacity of the MWCNTs is far greater than what has been reported in literature. The low CO_2 adsorption capacity of the chitosan/MWCNTs is attributed to the low CO_2 adsorption capacity and undesired adsorbent characteristics of the MWCNTs used. It is hypothesised that if chitosan were to be impregnated onto the surface of a more suitable CNT then the chitosan would improve the CO_2 adsorption capacity of the CNT by 650 %.

Table 6.2: CO_2 adsorption capacity of chitosan, MWCNTs, chitosan/MWCNTs and MWCNTs from literature

Adsorbent	**Operating Conditions (Temperature (ºC), Pressure (bar)**	**Average CO_2 adsorbed (mg CO_2/ g adsorbent)**	**Reference**
Chitosan	45, 1.1	9.10	This study
MWCNTs	45,1.1	0.4	This study
Chitosan/MWCNTs	45,11	2.94	This study
MWCNTs	25, 1.1	12.03	(Ngoy et al., 2014)
MWCNTs	50,1.01	21.50	(Su & Chen, 2011)
MWCNTs	25, 1.1	21.02	(Lee & Park, 2015)

6.5. Evaluation of the CO_2 Adsorption Capacity of the Chitosan/MWCNTs

Custom built CO_2 adsorption equipment (built by Chemvak) was used to mimic flue gas conditions to test the CO_2 adsorption capacity of the synthesised chitosan at conditions that mimic industry operation. The adsorption equipment consists of a packed bed reactor, heater, mass flow controller and gas analyser, supplies gas at a concentration of either 100 % CO_2, 100 % N_2 or 15 % CO_2 and 85 % N_2. 15 % CO_2 is used to mimic the flue gas conditions in industry, such as would be found in a typical South African Coal Fired Power Station. The packed bed reactor was packed with a 0.01 g of adsorbent sample (packing height approximately 15 mm). N_2 was then passed over the sample at 110 ºC to desorb water and other gas impurities present on the surface of the adsorbent. The reactor temperature was decreased to 25 ºC and gas at 15 % CO_2 (50 mL/min) was then bypassed to the CO_2 analyser to read 15 % as an initial starting point. Flow is then diverted through the reactor where adsorption takes place and then through the CO_2 analyser. The CO_2 concentration reading given by the analyser decreases as CO_2 is adsorbed. The adsorption process

is complete once the analysed reads 15 % CO_2 again. The inlet flowrate and CO_2 concentration from the gas analyser was used to calculate the CO_2 adsorbed by equation 3.4.

The effect of impregnation on the rate CO_2 adsorbed as well as the effect of temperature and of the chitosan/MWCNTs was considered. The effect of chitosan impregnation on the rate of CO_2 adsorbed was measured using the custom-built CO_2 adsorption equipment. Due to the debateable results from the custom-built CO_2 equipment the rate of CO_2 adsorbed is considered and not the exact amount of CO_2 adsorbed as this value is not a true reflection of the actual CO_2 adsorbed. The raw data for this is contained in Appendix C2. The gas analyser initially reads 15 % CO_2 before any CO_2 adsorption has occurred. The CO_2 concentration reading from the gas analyser then begins to decrease in small increments. In reality, the actual CO_2 concentration of the stream would decrease very quickly but the gas analyser can't decrease the reading at the same pace, there is an unavoidable time delay from the CO_2 gas analyser. Figure 6.5 shows the reading fraction CO_2 concentration given by the gas analyser per unit time. It can be seen that the CO_2 reading decreases reaches a minimum and then increases.

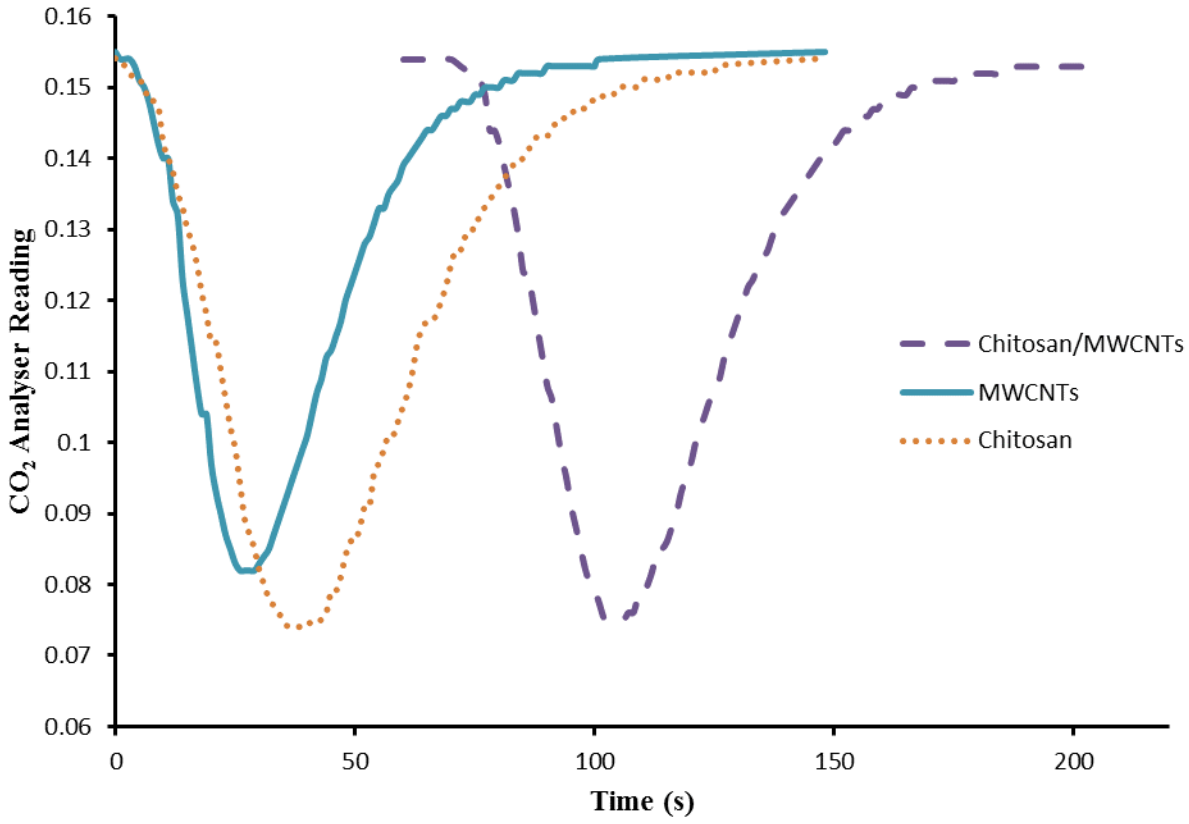

Figure 6.5: CO_2 concentration given by the gas analyser per second

The amount of CO_2 adsorbed per unit time is initially slow and then begins to increase. It reaches a maximum and then decreases again as the CO_2 adsorption sites are filled. This is contrary to literature. In literature the amount of CO_2 adsorbed per unit time is initially high and then starts to decrease as the CO_2 adsorption sites are filled (Chitsiga, 2016) (Lee & Park, 2015) (Ngoy et al., 2014) (Su & Chen, 2011) (Patkool et al., 2014). It is never initially low. This is attributed to the nature of the equipment. The reason that the CO_2 adsorption is low initially is that CO_2 gas analyser is not able to change the reading immediately and does so in small increments, as explained above. There is no way to quantify the actual CO_2 concentration with the equipment available. The way to overcome this problem would be to have a flowmeter and N_2 gas analyser at the exit of the reactor. Once the CO_2 adsorption was complete N_2 would be used to desorb the CO_2 adsorbed by the adsorbent. This would make it possible to quantify the CO_2 that was adsorbed.

The results from the custom-built CO_2 adsorption equipment were also contradictory to the results from the TGA. The TGA results showed that the CO_2 adsorption capacity of the chitosan was the highest, then followed by the chitosan/MWCNTs and the MWCNTs gave the lowest CO_2 adsorption capacity. From the results of the custom-built CO_2 adsorption equipment the chitosan/MWCNTs gave then highest CO_2 adsorption capacity, then followed by the MWCNTs and lastly the chitosan. This is again attributed to the nature of the equipment. The flowmeter controlling the flow of CO_2 into the reactor was not able to give a constant flowrate. This flowmeter was bypassed and a bubble flowmeter was used. When the flowrate was checked again using the bubble flowmeter without any adjustments having been made to the flowrate it was found that there was a change in flowrate (sometimes there was an increase in flow and at other times there was a decrease in flow), this could either be due to an inefficient valve or human error such as a leak to the bubble flowmeter. It is concluded that the flowrate during these experiments was not constant. The results of the TGA are assumed to be accurate while the results of the custom-built CO_2 adsorption equipment are inaccurate. The basis for the assumption that the TGA results were accurate was that the results were reproducible when experiments were repeated and comparable with literature. The basis for the assumption that the custom-built CO_2 adsorption equipment were inaccurate was that the results were not reproducible when experiments were repeated.

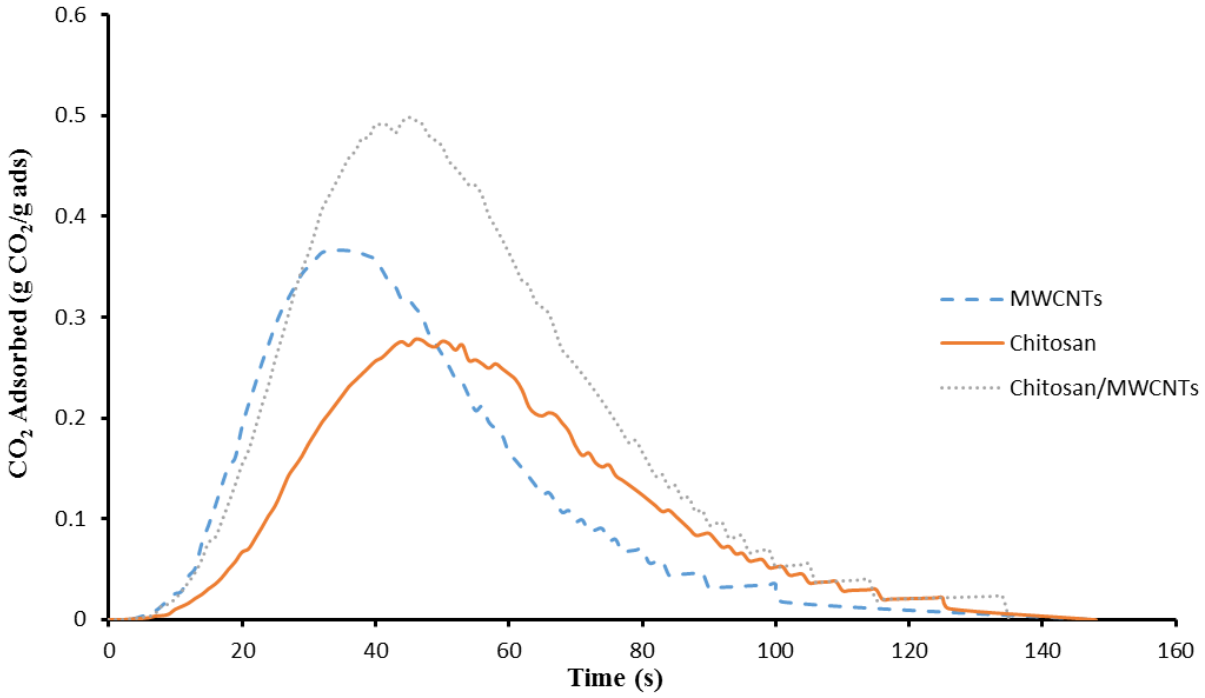

Figure 6.6: Effect of chitosan impregnation on rate of CO_2 adsorbed

6.6. Summary

Chitosan was successfully impregnated onto the surface of MWCNTs to produce a composite adsorbent. The composite adsorbent was called chitosan/MWCNTs. The chitosan/MWCNTs was characterized to confirm if impregnation was successful and to study the effects of impregnation on the surface properties of the MWCNTs. Characterisation methods used were Raman spectroscopy, N_2 physisorption, SEM and FTIR.

Raman spectroscopy was used to check the quality of the MWCNTs. The MWCNTs were found to be of excellent quality with few structural defects or impurities.

N_2 physisorption was used to check the surface geometry of the MWCNTs before and after impregnation. The surface geometry of the MWCNTs improved after impregnation. This is beneficial as surface geometry usually decreases after impregnation with other amine polymers. The change in surface geometry confirmed that chitosan impregnation was successful.

SEM images gave the surface morphology of the MWCNTs before and after impregnation. SEM images showed that chitosan was present on the surface of the MWCNTs after impregnation. This confirms that impregnation was successful.

FTIR was used to verify that the functional groups present associated with chitosan were present on the chitosan/MWCNTs. This confirmed that chitosan impregnation was successful. Chitosan/MWCNTs was successfully synthesised.

The CO_2 adsorption capacity of the novel adsorbent was evaluated. This was done using TGA and custom built CO_2 adsorption equipment. The main emphasis of this evaluation was placed on the degree to which chitosan impregnation improved the CO_2 adsorption capacity of the MWCNTs.

TGA results showed that the CO_2 adsorption capacity of the MWCNTs was low. The MWCNTs used in this study were not suitable for use as an adsorbent for CO_2 capture. The CO_2 adsorption capacity of the MWCNTs was improved by 650 % after impregnation. Reports from literature where an amine has been impregnated onto a CNT showed a CO_2 adsorption capacity increase of 500 % and 200 % (Ngoy et al., 2014) (Lee & Park, 2015) respectively. It is hypothesized that if chitosan were impregnated onto a more suitable CNT for CO_2 adsorption then it would improve the CO_2 adsorption capacity of that CNT by 650 % and would produce a superior novel CO_2 solid adsorbent.

The CO_2 adsorption capacity was also evaluated using custom built CO_2 adsorption equipment. This results from this equipment were found to be inconclusive due to the nature of the equipment.

Chapter 7 General Conclusions and Recommendations

7.1. Conclusions

Climate change is a significant problem that the world is currently facing. There is an increase in the global demand and dependence on energy. This energy is commonly supplied by the combustion of fossil fuels. The combustion of fossil fuels produces CO_2, a GHGs and a major contributor to climate change. Several options exist to reduce CO_2 emissions. The Paris agreement made at COP 21 has a plan set out. This plan incorporates CCS. CCS is a promising technology to South Africa because the CO_2 capture plant can be retrofitted to the already existing coal fired power plants.

The most mature technology that is applied to the capture of CO_2 is absorption via amine based solvents. This method has its drawbacks, amines are toxic when emitted to the air, there is a huge cost and efficiency penalty and the regeneration of the spent amine solvent is energy intensive. For this reason, this study was aimed at developing an alternative CO_2 capture technology, adsorption. This work proposed an alternative non-toxic biodegradable polymer that could be suitable as an adsorbent for CO_2 capture – chitosan. In the commencement of this study, the main aims of this study were to successfully synthesis chitosan from chitin and to impregnate chitosan onto carbon nanotubes (CNTs) to produce a composite adsorbent (chitosan/MWCNTs). Then characterize and evaluate the CO_2 adsorption performance of these materials (both chitosan and chitosan/MWCNTs) for use as adsorbents for post combustion CO_2 capture. To achieve the aforementioned aims, the questions below were expected to be answered in the course of the study.

i. Can chitosan, with desirable properties for CO_2 capture, be synthesised from chitin?
ii. What is the effect of independent variables during the synthesis stage on the degree of deacetylation of chitosan derived from chitin?
iii. Can chitosan be impregnated onto CNTs to produce a composite adsorbent with desirable properties for CO_2 capture?
iv. What is the CO_2 adsorption performance of this composite adsorbent material in the presence of impurities?

The main objective of this study was to develop a chitosan based adsorbent for post combustion CO_2 capture. Other objectives are:

i. To synthesize chitosan, with desirable properties for CO_2 capture from chitin.
ii. To study the effect of synthesis variables on degree of deacetylation of chitosan synthesised from chitin by using a statistical approach.

iii. To impregnate chitosan onto CNTs to produce a composite adsorbent with desirable properties for CO_2 capture.
iv. To evaluate the CO_2 adsorption performance of chitosan and chitosan/MWCNTS.

The following outcomes resulted from this research effort:

i. Synthesized chitosan with desirable properties for CO_2 capture.
ii. Information on the effect of synthesis variables on the synthesis of chitosan from chitin and the optimum synthesis conditions possible for the material.
iii. A synthesized chitosan/MWCNTs composite adsorbent with more desirable properties for CO_2 capture relative to the base material (MWCNTs).
iv. Peer reviewed paper publications and conference presentations
v. A well-documented report in the form of a dissertation and an award.

Chitosan was successfully synthesised from chitin. This was confirmed by FTIR techniques. The synthesised chitosan had desirable properties for CO_2 capture. This was confirmed using TGA and custom built CO_2 adsorption equipment. The synthesised chitosan samples were inexpensive, had amine groups and were thermally suitable at industrial CO_2 capture operational temperatures. The CO_2 adsorption capacity of the synthesised chitosan was generally low when compared with literature. However, it is important to consider that the polymer is derived from a waste material and as such it is possible to cost effectively utilize a large amount.

The effect of synthesis variables on the synthesis of chitosan from chitin was studied using RSM. A polynomial model was developed that can predict the DDA of the synthesised chitosan based on the synthesis variables used was developed. This polynomial model was found to be statistically significant. The polynomial model showed the optimum synthesis conditions to yield the highest DDA.

Chitosan was successfully impregnated onto MWCNTs. This was confirmed by FTIR techniques. The synthesised chitosan/MWCNT adsorbent was not suitable for CO_2 capture. This was confirmed using Raman spectroscopy, N_2 physisorption, SEM TGA and custom built CO_2 adsorption equipment. The CO_2 adsorption capacity of the synthesised chitosan/MWCNTs was low. However, chitosan/MWCNTs did have more suitable characteristics for CO_2 adsorption and showed an increase in CO_2 adsorption capacity when compared to the base material (MWCNTs).

The aims and expected outcomes that were set out at the commencement of this study have all been met.

7.2. Recommendations

Chitosan was synthesised and it was found that it possess properties that make the polymer suitable for use as an adsorbent for CO_2 capture. It should be noted that this study serves as an initial study on the use of chitosan as a novel adsorbent for CO_2 capture. Several research ideas may be generated with this study as the background work. It is recommended that research be conducted into the kinetics and kinetic modelling of the CO_2 adsorption of chitosan. Kinetics for the adsorption process are an important aspect for industrial CO_2 capture processes. Adsorption is merely the first stage of the CO_2 capture process. The second stage involves desorption. Desorption recovers the captured CO_2 and regenerates the adsorbent material. It is recommended that studies on desorption be performed. The empirical model developed to predict the DDA of chitosan based on the synthesis conditions was found to be statistically significant. However, during model validation an error of 2.9 - 9 % between the DDA predicted by the model and the experimentally determined DDA was found. The error is not insignificant, there is need to perform further investigations into the regression analysis as well as propose higher order polynomials to model the synthesis of chitosan more accurately. Further investigations can include considering the chitin source, the DDA of chitin synthesis prior to chitosan synthesis and other synthesis variables such as solvent ratio and stirrer speed.

Chitosan was impregnated onto MWCNTs with a high ratio of MWCNTs to chitosan. It is recommended that studies with a higher ratio of chitosan to MWCNTs be conducted. Chitosan is significantly cheaper than CNTs. More chitosan and less CNT could produce a more cost effective adsorbent.

This research mostly considered pure CO_2. It was not possible to properly understand the effect of impurities due to the equipment available. This study attempted to consider the effects of impurities however there were several issues with the custom built CO_2 adsorption equipment set up. These are explained below.

- The mass flowmeter for the CO_2 was not accurate. The flowmeter did not give an accurate flow rate. When the flow was set to zero the flowrate that was shown on the digital display was not zero, also when trying to set the flowrate to a particular value it would not stabilise but rather show a very significant fluctuation – more than 20 mL/min either way. The extent of the inaccuracy is unknown. To overcome this problem a bubble flowmeter was used instead. However, with any bubble flowmeter there is a degree of human error. Furthermore, when the flowrate was checked again with the bubble flowmeter without any adjustments having been made to the flowrate it was found that there was a change in flowrate (sometimes there was an increase in flow and at other times there was a decrease in flow), this could either be due to an inefficient valve or human error such as a leak to the bubble flowmeter.

- There is no mass flow controller at the exit of the adsorption column. For a more accurate mass balance it would be beneficial to have a mass flowmeter at the exit of the adsorption column.
- Equation 3.4 assumes that no N_2 is adsorbed and no CO_2 or N_2 is retained in the column. This assumption is necessary for the mass balance to be performed. However, there is no vacuum pump that ensure that no gases remain inside the adsorption column, so there will be gases inside the adsorption column. This means that when the gas is changed from N_2 to CO_2 there is N_2 that is still inside the adsorption column which gets pushed out of the adsorption column and through the gas analyser and decreases the reading of the CO_2 concentration. There will also be competitive adsorption between this extra N_2 and the CO_2/N_2 gas mixture. This has resulted in an over estimation of the CO_2 adsorbed. There is no means of quantifying the amount of N_2 or how it mixes with the CO_2 with the equipment that is available. Had the gas analyser also been able to measure N_2 then it would be possible to wait for the analyser to indicate 0 % N_2 before the adsorption experiments were initiated. In addition, the experimental data could have been correct using a correction factor if it was possible to verify the amount of N_2 trapped in the adsorption column before the commencement of the adsorption segment of the experiment.

These issues with the custom-built CO_2 adsorption equipment resulted in data that is not accurate because it is not a fair representation of the adsorption capacity of the adsorbents and thus the results cannot be reported in literature (i.e. a journal article). However, for the purpose of this dissertation the results obtained from the custom-built CO_2 adsorption equipment have been included to show depth of research. The author of this paper would like to state that they do not condone the publication of the results obtained using the custom-built CO_2 adsorption equipment. It is recommended that the custom-built CO_2 adsorption equipment be redesigned. The custom-built CO_2 adsorption equipment should be calibrated with an adsorbent of known adsorption capacity before experiments are conducted. Once the custom-built adsorption equipment has been proved to give accurate results further investigations with impurities, and a combination of adsorption and desorption should be carried out. Optimizations studies should be carried out to determine the exact conditions where adsorption and desorption will be maximized. Finally, an economic evaluation would be necessary alongside these further performance tests to determine the feasibility of utilizing chitosan as an adsorbent at a fairly large scale.

References

Abdou, E. S., Nagy, K. S., & Elsabee, M. Z. (2008). Extraction and characterisation of chitin and chitosan from local sources. *Bioresource Technology 99(5)*, 1359 - 1367. DOI: 10:1016/j.biortech.2007.01.051

Alvarez, L. F. (2000). Design Optimization Based on Genetic Programming. Bradford: University of Bradford.

Arstad, J., Fjellvåg, H., Kongshaug, K. O., Swang, O., & Blom, R. (2008). Amine functionalised metal organic frameworks (MOFs) as adsorbents for carbon dioxide. *Adsorption, 14*(6), 755-762.

Berger, A. H., & Bhown, A. S. (2011). Comparing Physisorption and Chemisorption Solid Sorbents for use. *Energy Procedia, 4*(1), 562–567.

Bolland, O. (2014). *CO_2 Capture in Power Plants*.[Lecture Notes]. Lecture Notes for a Carbon Capture Workshop at the University of the Witwatersrand.

Brugnerottoa, J., Lizardi, J., Goycoolea, F. M., ArguÈelles-Monal, W., DesbrieÁres, J., & Rinaudo, M. (2001). An infrared investigation in relation with chitin and chitosan. *Polymer, 42*(1), 3569-3580.

Builes, S., & Vega, L. F. (2013). Effect of Immobilized Amines on the Sorption Properties of Solid Materials: Impregnation versus Grafting. *Langmuir, 29*(1), 199-206.

Bullis, K. (2009). *MIT Technology Review*. Retrieved April 2014, from www.technologyreview.com/news/416457/carbon-capture-with-nanotubes/

Chitsiga, T. L. (2016). Optimization of the Synthesis and Performance of Polyaspartamide (PAA) Material for Carbon Dioxide Capture in South African Coal-fired Power Plants. (Masters Dissertation). Johannesburg: University of the Witwatersrand. Retrieved from http://mobile.wiredspace.wits.ac.za/bitstream/handle/10539/21104/Master%20Of%20Science%20Final%20Submission-Tafara%20Leonard%20Chitsiga-514286.pdf?sequence=2&isAllowed=y

Costa, S., Borowiak-Palen, E., Kruszyñska, M., Bachmatiuk, A., & Kalenczuk, R. J. (2008). *Characterization of Carbon Nanotubes by Raman Spectroscopy*. Centre of Knowledge Based Nanomaterials and Technologies, Institute of Chemical and Environment Engineering, Szczecin University of Technology.

Costa, S., Borowiak-Palen, E., Kruszyñska, M., Bachmatiuk, A., & Kalenczuk, R. J. (n.d.). *Characterization of Carbon Nanotubes by Raman Spectroscopy*. Centre of Knowledge Based

Nanomaterials and Technologies, Institute of Chemical and Environment Engineering, Szczecin University of Technology.

Crittenden, B., & Thomas, W. J. (1998). *Adsorption Technology and Design*. Elsevier Science & Technology Books. Retrieved from http://s1.downloadmienphi.net/file/downloadfile2/200/1402405.pdf

Czaun, M., Goeppert, A., May, R. B., Peltier, D., Zhang, H., Surya Prakash, G. K., & Olah, G. A. (2013). Organoamines-grafted on nano-sized silica for carbon dioxide captureJ. *Journal of CO2 Utilization, 1*, 1-7.

Diab, M. A., El-Sonbati, A. Z., Al-Halawany, M. M., & Bader, D. M. (2012). Thermal Stability and Degradation of Chitosan Modified. *Open Journal of Polymer Chemistry, 2*(1), 14-20.

Diffen. (2014, March 24). *Adsorption vs Adsorption*. Retrieved March 5, 2017, from Diffen.com: www.diffen.com/difference/Absorption_vs_Adsorption

Divya, K., Rebello, S., & Jisha, M. S. (2014). A Simple and Effective Method for Extraction of High Purity Chitosan from Shrimp Shell Waste. *A Simple and Effective Method for Extraction of High Purity Chitosan from Shrimp Shell Waste. 4th*, pp. 141 - 145. Kuala Lumpur: Institute of Research Engineers and Doctors.

Dresselhaus, M., Dresselhaus, D., & Avouris, P. (2001). *Carbon Nanotubes: Synthesis, Structure, Properties and Applications*. Berlin: Springer.

Dresselhaus, M., Dresselhaus, G., Saito, R., & Jorio, A. (2005). Raman Spectroscopy of Carbon Nanotubes. *Physics Reports, 409*(2), 47-99.

Eldin, M. S. M. Hashem, A. I. Omer, A. M. Tamer, T. M. (2015), Preparation, characterization and antimicrobial evaluation of novel cinnamyl chitosan Schiff base. International Journal of Advanced Research. 3, (3), 741-755

Entar, A. S., Nagy, K. S., & Maher, E. Z. (2008). Extraction and Characterisation of Chitin and Chitosan from Local Sources. *Bioresources Technology, 99*(1), 1359-1367.

EPA - Office of Air and Radiation. (2000). *Carbon Dioxide as a Fire Suppressant:*. Washington, DC 20460: U.S. Environmental Protection Agency.

EPA. (2013). Underground Injection Control (UIC). EPA.Retrieved March 5, 2017 from https://www.epa.gov/uic

EPA. (2015). Greenhouse Gas Emissions. Retrieved March 5, 2017, from http://www.epa.gov/climatechange/ghgemissions/

Eskom. (2015). Eskom. Retrieved March 5, 2017, from http://www.eskom.co.za/AboutElectricity/ElectricityTechnologies/Pages/Coal_Power.aspx

Ferrari, M.-C. (2011). Nanotubes for Carbon Capture. *EPSRC Pioneering Research and Skills*. Retrived from http://www.geos.ed.ac.uk/ccs/Meetings/cornwall-april2011/CFerrari.pdf

Fletcher, A. (2008). Porosity and Sorption Behaviour. Retrieved March 5, 2017, from http://personal.strath.ac.uk/ashleigh.fletcher/adsorption.htm#top

Florini, K., Mansell, A., & Mardiney, A. (2014). The World's Carbon Market: A Case Study Guide to Emissions Trading. Washington: Environmental Defense Fund; International Emissions Tradign Association.

Fogler, H. S. (2010). Elements of Chemical Reaction Engineering (4 ed.). Upper Saddle River NJ: Prentice Hall PTR/Pearson Education Internat.

Fujiki J. and Yogo K., (2016). The Increased CO_2 Adsorption Performance of Chitosan-Derived Activated Carbons with Nitrogen Doping. *Chemical Communications*, 186-189. DOI: 10.1039/C5CC06934C

Ganesh, E. (2013). Single Walled and Multi Walled Carbon Nanotube Structure, Synthesis and Applications. *International Journal of Innovative Technology and Exploring Engineering (IJITEE), 2*(4), 2278-3075.

Global CCS institute. (2014). *How CCS works - capture*. Retrieved March 5, 2017, from Global CCS Institute: http://www.globalccsinstitute.com/content/how-ccs-works-capture

Gray, M., Champagne,, K., Fauth, D., Baltrus , J., & Pennline, H. (2008). Performance of immobilized tertiary amine solid sorbents for the capture of carbon dioxide. *International Journal of Greenhouse Gas Control*, 3 - 8.

Gupta, V., & Saleh, T. A. (2011). Syntheses of Carbon Nanotube-Metal Oxides Composites; Adsorption and Photo-degradation, Carbon Nanotubes - *From Research to Applications*. doi:10.5772/18009

Hardie, S., Garnett, M., Fallick, A., Rowland, A., & Ostle, N. (2005). Carbon Dioxide Capture Using a Zeolite Molecular Sieve Sampling System for Isotopic Studies (13C and 14C) of Respiration. *RADIOCARBON, 47*(3), 441–451.

Herzog, H., Meldon, J., & Hatton, A. (2009). *Advanced Post-Combustion CO2 Capture.* Doris Duke Foundation.

Herzog, H., Meldon, J., & Hatton, A. (2009, April). Advanced Post-Combustion CO_2 Capture. *Advanced Post-Combustion CO2 Capture*. Clean Air Task Force.

Hongpattarakere, T., & Riyaphan, O. (2008). Effect of deacetylation conditions on antimicrobial activity of chitosans prepared from carapace of black tiger shrimp (Penaeus monodon). *Songklanakarin Journal of Science and Technology, 30*(1), 1-9.

Intergovernmental Panel on Climate Change. (2005). *Carbon Dioxide Capture and Storage.* New York: Cambridge University Press.

International Energy Agency. (2015). *IEA Statistics: Carbon dioxide emissions from fuel combustion, Highlights.* International Energy Agency.

International Energy Agency. (2016). *20 Years of Carbon Capture and Storage-Accelerating Future Developments.* Paris: International Energy Agency.

IPCC. (2007). *Contribution of Working Group III to the Fourth Assessment Report of the Intergovernmental Panel on Climate Change, 2007*. Cambridge: IPPC. Retrieved March 5, 2017, from IPCC Fourth Assessment Report: Climate Change 2007: http://www.ipcc.ch/publications_and_data/ar4/wg3/en/ch4s4-3-6.html

IUPAC. (2002, September 5). *Chemiosorption and Physisorption*. Retrieved March 5, 2017, from http://old.iupac.org/reports/2001/colloid_2001/manual_of_s_and_t/node16.html

JECFA. (1992). *Food and Agriculture Organization of the United Nations*. Retrieved March 5, 2017, from www.fao.org/ag/agn/jecfa-additives/specs/.../Additive-006.pdf

Keller, J. U., & Staudt, R. (2005). *Gas Adsorption Equilibria*. Boston: Springer Science.

Kiruba , A., Uthayakumar , V., Munirasu , S., & Ramasubramanian , V. (2013). Extraction, Characterization and Physico Chemical Properties of Chitin and Chitosan from Mud Crab Shell (Scylla Serrata). *Indian Journal of Applied Recearch, 3*(8), 44 - 46.

Kucukgulmez, A., Celik, M., Yanar, Y., Sen, D., Polat, H., & Kadak, A. E. (2011). Physiochemical Characterisation of Chitosan Extracted from Metpeneaus Stebbingi Shells. *Food Chemistry, 126*(1), 1144-1148.

Laubach , S. E., Marrett, R. A., Olson, J. E., & Scott, A. R. (1998). Characteristics and origins of coal cleat: A review. *International Journal of Coal Geology, 35*(1-4), 175-207.

Lazic, Z. R. (2004). *Design of Experiments in Chemical Engineering*. Germany: Wiley - VCH.

Lee, M., & Park, S. (2015). Silica-Coated Multi-Walled Carbon Nanotubes Impregnated with polyethyleneimine for Carbon Dioxide Capture under Flue Gas Condition. *Journal of Solid State Chemistry, 226*(2015), 17-23.

Liebscher, A., & Munch, U. (2015). *Geological Storage of CO_2 - Long term Security Aspects*. Switzerland: Springer International Publishing AG .

Lurgi. (2010, July 12). The Rectisol Process. *The Rectisol Process-Lurgi's Leading Technology for the Purification of Synthesis Gas*. Frankfurt: Lurgi.

Maroto-Valer, M. M. (2010). Developments And Innovation In Carbon Dioxide (CO_2) Capture And Storage Technology. In *Overview of carbon dioxide capture and storage technology* (pp. 1-24). Boca Raton: CRC Press.

Millward, A. R., & Yaghi, O. M. (2005). Metal-Organic Frameworks with Exceptionally High Capacity for Storage of Carbon Dioxide at Room Temperature. *Journal of American Chemical Society, 127*(51), 17998-17999.

Minitab. (2015). *Minitab 17 Support*. Retrieved November 28, 2015, from http://support.minitab.com/en-us/minitab/17/topic-library/modeling-statistics/doe/basics/orthogonal-designs/

Monoj, K., & Mondal, H. (2012). Progress and trends in CO_2 capture/ seperation technologies: A review. *Energy, 46*(1), 431-441.

Monthioux, M., Serp, P., Flahaut, E., Razafinimanana, M., Laurent, C., Peigney, A., . Bacsa, W. and Broto, J.-M. (2010). Introduction to Carbon Nanotubes. In P. B. Bhushan (Ed.), *Springer Handbook of Nanotechnology: Part A* (pp. 47-118). Springer Berlin Heidelberg.

Mosher, K. (2011). *The Impact of Pore Size on Methane and CO_2 Adsorption in Carbon*. Stanford: Department of Energy Resources and the Committee of Graduate Studies of Stanford University.

NANOCYL. (2014). *NANOCYL, The Carbon Nanotube Specialist*. Retrieved June 2014, from http://www.nanocyl.com/en/CNT-Expertise-Centre/Carbon-Nanotubes/Single-wall-Nanotubes-SWNT

Nanoscience Instruments. (2014). *Nanoscience Instruments, Inc*. Retrieved June 2014, from http://www.nanoscience.com/products/carbon-nanotube-synthesis/technology-overview/

NASA. (2016). *NASA: Climate Change and Global Warming*. Retrieved February, 2017, from http://climate.nasa.gov/

National Geographic. (2016). *Sea Level Rise - National Geographic*. Retrieved February, 2017, from http://ocean.nationalgeographic.com/ocean/critical-issues-sea-level-rise/

Ngoy, J. (2016). A CO2 Capture Technology using Carbon Nanotubes with Polyaspartamide Surfactant.(Doctorial Dissertation) Johannesburg: University of the Witwatersrand. Retrieved March 2017 from http://wiredspace.wits.ac.za/jspui/bitstream/10539/20570/2/PhD%20Thesis%20(JM%20Ngoy%2028695).pdf

Ngoy, J., Wagner, N., Riboldi, L., & Bolland, O. (2014). A CO_2 Capture Technology Using Multi-walled Carbon Nanotubes. *Energy Procedia*, 2230 - 2248.

NIST/SEMATECH. (2012, April). *E-Handbook of Statistical Methods*. Retrieved November 28, 2015, from http://www.itl.nist.gov/div898/handbook/

Osler, K., Dheda D., Ngoy J., Wagner N., Daramola M.O. (2017), Synthesis and Evaluation of Carbon Nanotube Composite Adsorbent for CO_2 Capture: A Comparative Study of CO_2 Adsorption Capacity of Single-Walled and Multi-Walled Carbon Nanotubes. *Int. J of Coal Science and Technology*. 4(1), 41 - 49. DOI 10.1007/s40789-017-0157-2

Patkool, C., Chawakitchareon, P., & Anuwattana, R. (2014). Enhancement of Efficiency of Activated Carbon Impregnated Chitosan for Carbon Dioxide Adsorption. *Environmental Engineering Research, 19*(3), 289-292. doi:https://doi.org/10.4491/eer.2014.S1.008

Perry, R. H., & Chilton, C. H. (2008). *Chemical Engineers' Handbook* (8th ed.). McGraw-Hill: New York, Chicago, San Francisco, Lisbon, London, Madrid, Mexico City, Milan, New Delhi, San Juan, Seoul, Singapore, Sydney, Toronto. ISBN: 9780071422949

Pires, J., Martins, F., Alvium-Ferraz, M., & Simoes, M. (2011). Recent Developments on Carbon Capture and Storage: An Overview. *Chemical Engineering Research and Design, 89*(2011), 1446-1460.

Rodrigues, C. F., Laiginhas, C., Fernandes, M., Lemos de Sousa, M. J., & Dinis, M. A. (2014). The coal cleat system: A new approach to its study. *Journal of Rock Mechanics and Geotechnical Engineering, 6*(1), 208-218.

SACCCS. (2010). *Atlas on Geological Storage of Carbon Dioxide in South Africa.* Retrieved March 2017 from http://www.sacccs.org.za/wp-content/uploads/2010/11/Atlas.pdf

SACCCS. (2014). *South African Center For Carbon Capture and Storage-Roadmap/Strategy*. Retrieved March 5, 2017, from https://www.sacccs.org.za/About-Us/SA-CCS-Roadmap/

Saha, S., Chandra, S., & Banerjee, R. (2012). Carbon dioxide capture by metal organic frameworks. *Indian Journal of Chemistry, 51A*, 1223-1230.

Sethi, R., & Barron, A. R. (2009). Characterisation of Single-Walled Carbon Nanotubes by Raman Spectroscopy. Open-Stax CNX. Retrieved March 5, 2017, from file:///C:/Users/USER/Downloads/characterization-of-single-walled-carbon-nanotubes-by-raman-spectroscopy-2.pdf

Shao, R., & Stangeland, A. (2009). *Amines Used in CO_2 Capture - Health and Environmental Impacts* . Oslo, Norway: The Bellona Foundation.

Sneddon, G., Ganin, A. Y. and Yiu, H. H. P. (2015), Sustainable CO_2 Adsorbents Prepared by Coating Chitosan onto Mesoporous Silicas for Large-Scale Carbon Capture Technology. Energy Technology, 3: 249–258. doi:10.1002/ente.201402211

Spigarelli, B. P. (2013). A Novel Approach to Carbon Dioxide Capture and Storage. *A Novel Approach to Carbon Dioxide Capture and Storage*. (Master's Dissertation). Houghton, Michigan, United States of America: Michigan Technological University. Retrieved March 5, 2017, from file:///C:/Users/USER/Desktop/Masters/Papers/A%20Novel%20Approach%20to%20Carbon%20Dioxide%20Capture%20and%20Storage.pdf

Su, F., & Chen, H.-S. (2011). Adsorption, Desorption, and Thermodynamic Studies of CO_2 with High-Amine-Loaded Multiwalled Carbon Nanotubes. *Langmuir*, 8090 - 8098.

The Linde Group. (2014). *CO_2 Separation before Combustion*. Retrieved March 5, 2017, from The Linde Group: http://www.the-linde-group.com/en/clean_technology/clean_technology_portfolio/carbon_capture_storage/precombustion_ccs/index.html

Think Global Green. (2014, March 18). *Carbon Dioxide*. Retrieved March 5, 2017, from https://www.thinkglobalgreen.org/carbondioxide.html

Thomas, W., & Crittenden, B. (1998). *Adsorption Technology and Design*. Butterworth-Heinemann.

UNFCC. (2010). *Cancun Climate Change Conference - November 2010*. Retrieved March 5, 2017, from http://unfccc.int/meetings/cancun_nov_2010/meeting/6266.php

Urban Earth. (2015). *SA's CO2 emissions per capita | Urban Earth*. Retrieved January 6, 2017, from http://www.urbanearth.co.za/articles/sa%25E2%2580%2599s-co2-emissions-capita

Wang, M., Lawal, A., Stephenson, P., & Sidders, J. (2011). Post-combustion CO2 capture with chemical absorption:. *Chemical Engineering Research and Design (89)*, 1609-1624.

White, C. M., Smith, D. H., Kenneth, J. L., Goodman, A. L., Jikich, S. A., LaCount, R. B., DuBose, Stephen B., Ozdemir, Ekrem, Morsi, Badie and Schroeder, K. T. (2005). Sequestration of Carbon Dioxide in Coal with Enhanced Coal Bed Methane Recovery. *Energy and Fuels, 19*(3), 659-724.

Yang, R. (1997). *Gas Separation by Adsorption Processes* (1 ed.). London: London: Imperial College Press.

Yen, M.-T., Yang, J.-H., & Mau, J.-L. (2009). Physicochemical Characterisation of Chitin and Chitosan from Crab Shells. *Carbohydrate Polymers, 75*(1), 15-21.

Younes, I., Rinaudo, M., (2015). Chitin and Chitosan Preparation from Marine Sources. Structure, Properties and Applications. *Marine Drugs*. 13(3), 1133-1174

Zhao , A. (2012). Adsorptive Removal of CO_2 by Amine Functionalized Sorbents: Experimental and Kinetics Study. *Adsorptive Removal of CO2 by Amine Functionalized Sorbents: Experimental and Kinetics Study*. Edmonton, Alberta , Canada: Department of Chemical and Materials Engineering , University of Alberta .

Appendices

Appendix A: Synthesis and Characterisation Information

Appendix A contains additional information on the synthesis and characterization results.

A1: Percentage Yield Calculation - Chitosan

$$\%\,Yield = \frac{total\ mass\ of\ product}{total\ mass\ of\ reactant} \times 100$$ Equation A1-1

Table A1-1: Percentage Yield Calculations

	Total Mass of Reactants	**Total Mass of Products**	**% Mass Lost**	**Yield**	**Average Yield**	**Standard Deviation**
Formula	Mass of Chitin	Mass of Chitosan	(Mass of Chitin - Mass of Chitosan)	Mass of Chitin/Mass of Chitosan *100	(Yield of A + Yield of B)/2	Standard Deviation
1A	10	1.53	84.74	15.26		
1B	2	0.51	74.7	25.3	20.28	7.099352
2A	10	0.92	90.85	9.15		
2B	10	1.73	82.71	17.29	13.22	5.755849
3A	2	0.04	98.15	1.85		
3B	2	0.19	90.55	9.45	5.65	5.374012
4A	4	0.29	92.675	7.325		
4B	2	0.11	94.6	5.4	6.3625	1.361181
5A	10	1.20	87.99	12.01		
5B	2	0.42	79	21	16.505	6.35689
6A	10	0.97	90.28	9.72		
6B	2	0.06	96.95	3.05	6.385	4.716402
7A	10	0.36	96.42	3.58		
7B	10	0.48	95.16	4.84	4.21	0.890955
8A	2	0.14	92.95	7.05		
8B	10	0.65	93.46	6.54	6.795	0.360624
9A	2	0.34	83.15	16.85		
9B	2	0.38	81.1	18.9	17.875	1.449569
10A	10	1.23	87.7	12.3		
10B	2	0.16	92.05	7.95	10.125	3.075914
11A	10	0.57	94.28	5.72		
11B	10	1.19	88.06	11.94	8.83	4.398204
12A	10	1.78	82.16	17.84		
12B	2	0.53	73.35	26.65	22.245	6.229611
13A	2	0.11	94.75	5.25		
13B	2	0.16	91.85	8.15	6.7	2.05
14A	10	0.65	93.48	6.52		
14B	2	0.09	96.2	3.8	5.16	1.92
15A	10	0.51	94.93	5.07		
15B	2	0.19	90.5	9.5	7.285	3.13

A2: Thermal Stability Analysis – Chitosan

Table A2-1: TGA Raw Data for Thermal Stability Analysis for Sample 1A – Before Adsorption

Time (min)	Temperature (°C)	Weight (%)	Time (min)	Temperature (°C)	Weight (%)
0	53.02	99.98	70	401.83	26.98
5	79.92	90.97	75	426.64	24.23
10	99.51	90.12	80	451.56	21.11
15	124.55	89.89	85	476.47	17.55
20	148.94	89.82	90	501.15	13.86
25	174.6	89.66	95	525.93	10.37
30	200.26	89.38	100	550.69	7.238
35	225.44	89.03	105	575.42	4.445
40	250.7	87.88	110	600.24	1.945
45	276.07	84.84	115	623.9	1.553
50	302.12	77.23	120	648.77	1.523
55	334.14	48.24	125	673.64	1.486
60	354.83	32.75	130	695.16	1.466
65	377.42	29.57			

Table A2-2: TGA Raw Data for Thermal Stability Analysis for Sample 1A – After Adsorption

Time (min)	Temperature (°C)	Weight (%)	Time (min)	Temperature (°C)	Weight (%)
0	14.08	100	75	389.99	29.43
5	35.21	99.09	80	414.49	26.71
10	59.96	96.71	85	439.28	23.65
15	85.18	94.08	90	464.09	20.17
20	110.37	93.06	95	488.71	16.43
25	135.78	92.81	100	513.12	12.83
30	161.78	92.59	105	537.58	9.71
35	186.97	92.43	110	562.98	6.927
40	212.16	92.17	115	587.91	4.08
45	237.45	91.47	120	612.33	1.301
50	262.88	89.52	125	635.45	1.11
55	288.75	84.5	130	660.31	1.086
60	318.41	68.17	135	685.19	1.067
65	348.06	38.33	140	695.53	1.059
70	366.9	32.14			

Table A2-3: TGA Raw Data for Thermal Stability Analysis for Sample 2A – Before Adsorption

Time (min)	Temperature (°C)	Weight (%)	Time (min)	Temperature (°C)	Weight (%)
0	31.97	100	70	382.52	34.41
5	52.66	98.77	75	407.54	32.03
10	77.49	96.29	80	432.61	29.37
15	102.96	94.39	85	458.66	26.23
20	127.94	93.78	90	489.9	18.49
25	153.46	93.59	95	513.74	11.17
30	179.46	93.26	100	535.22	5.752
35	204.89	92.42	105	555.55	3.28
40	230.43	90.12	110	578.76	2.837
45	256.07	85.84	115	603.52	2.77
50	282.51	79.63	120	628.38	2.712
55	312.36	63.52	125	653.24	2.675
60	335.4	46.29	130	678.12	2.634
65	358.54	37.66	135	695.48	2.6

A3: FTIR Graphs - Chitosan

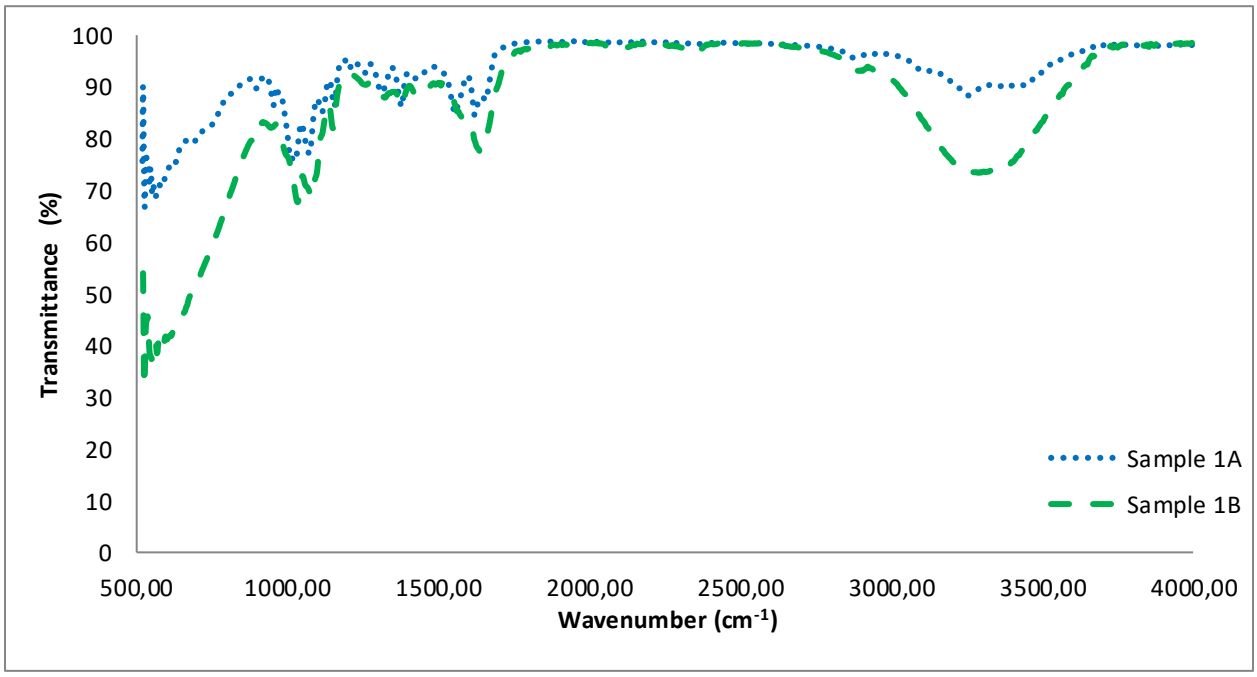

Figure A3-1: FTIR Graph for Sample 1A and 1B

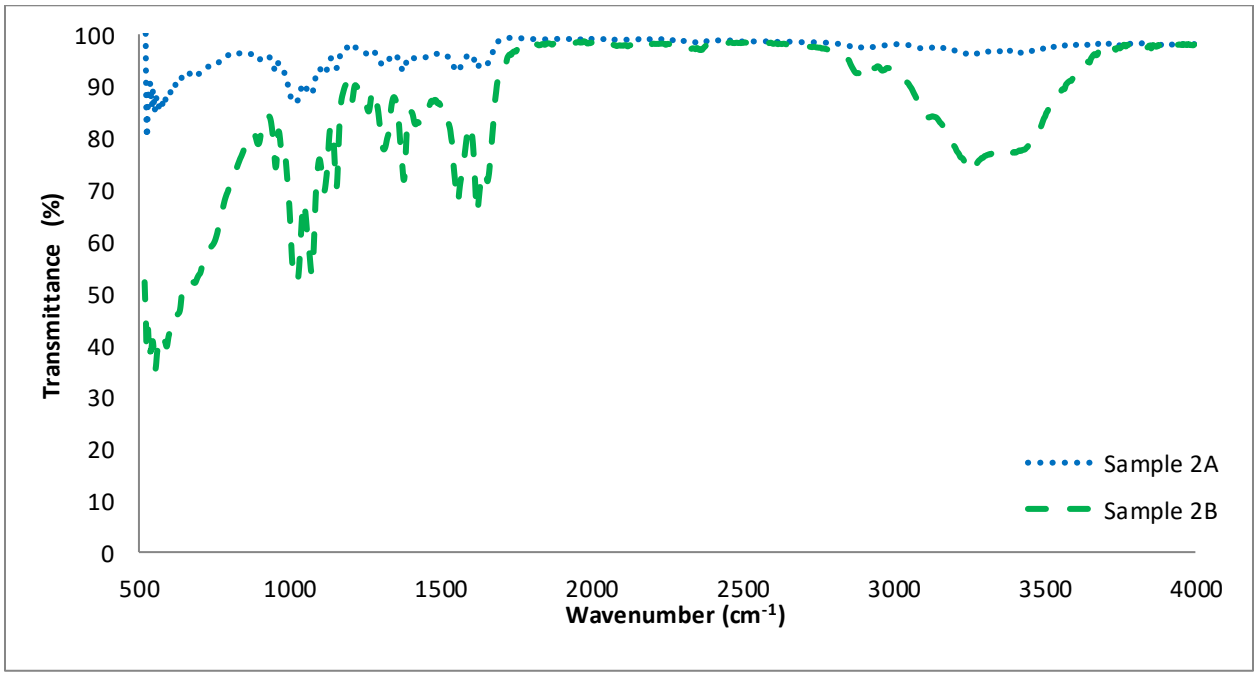

Figure A3-2: FTIR Graph for Sample 2A and 2B

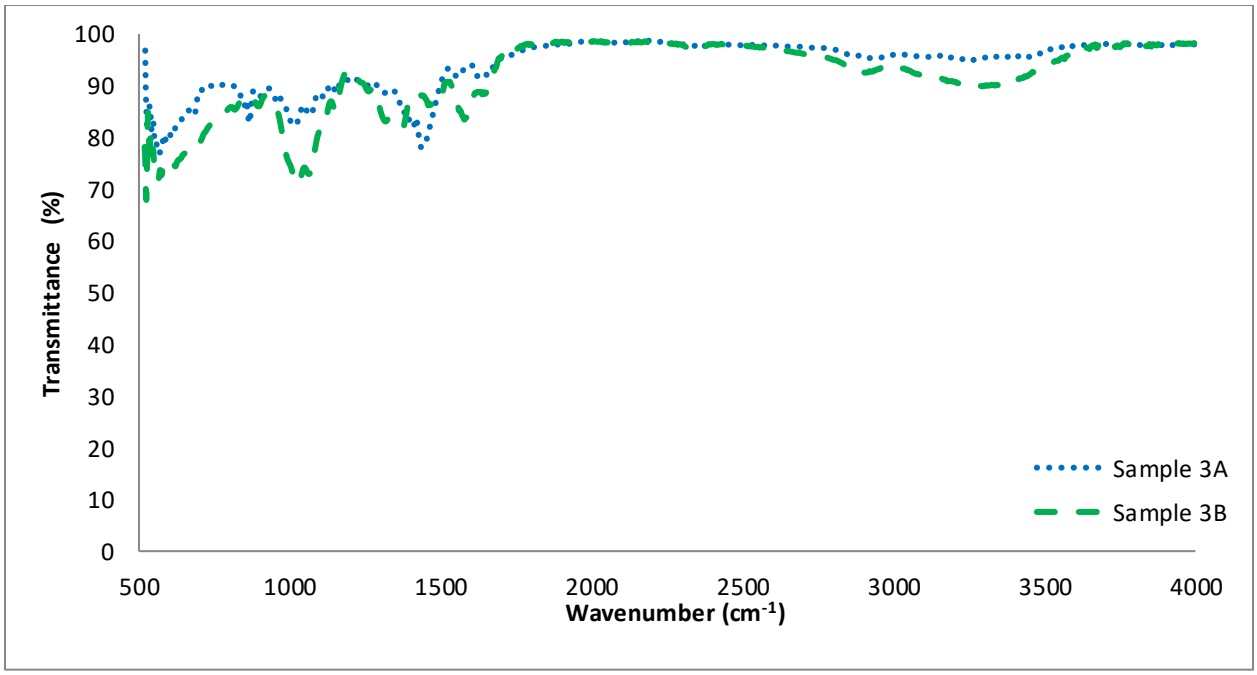

Figure A3-3: FTIR Graph for Sample 3A and 3B

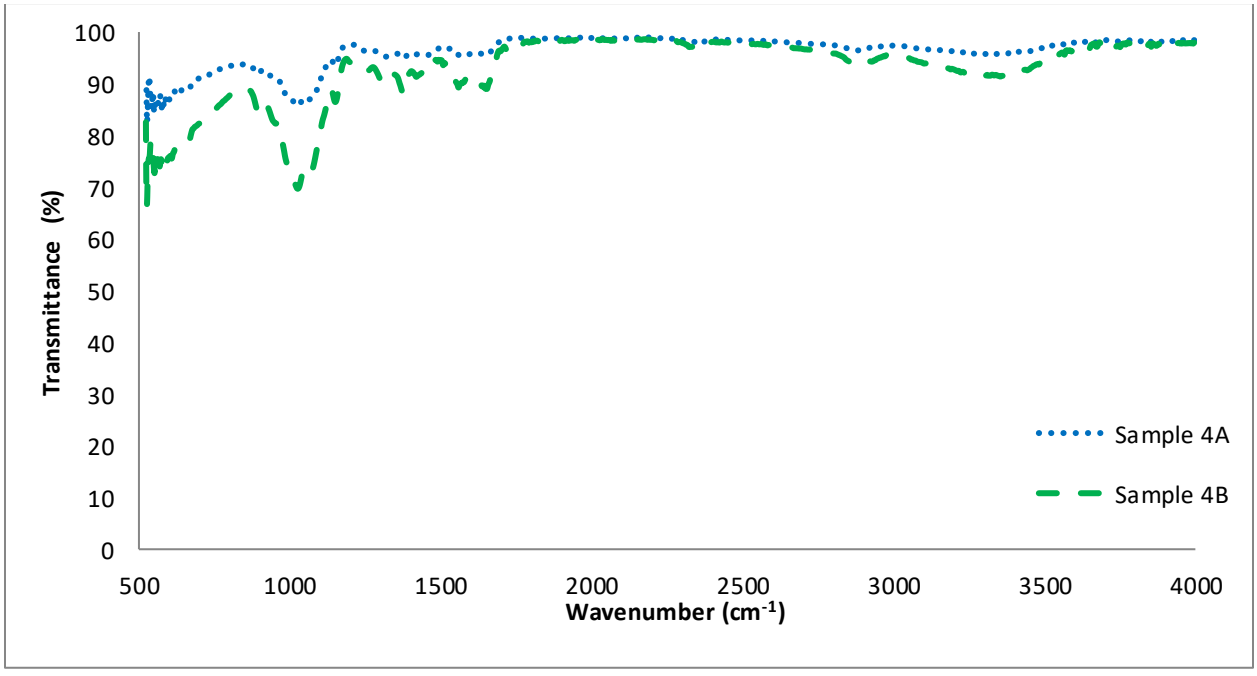

Figure A3-4: FTIR Graph for Sample 4A and 4B

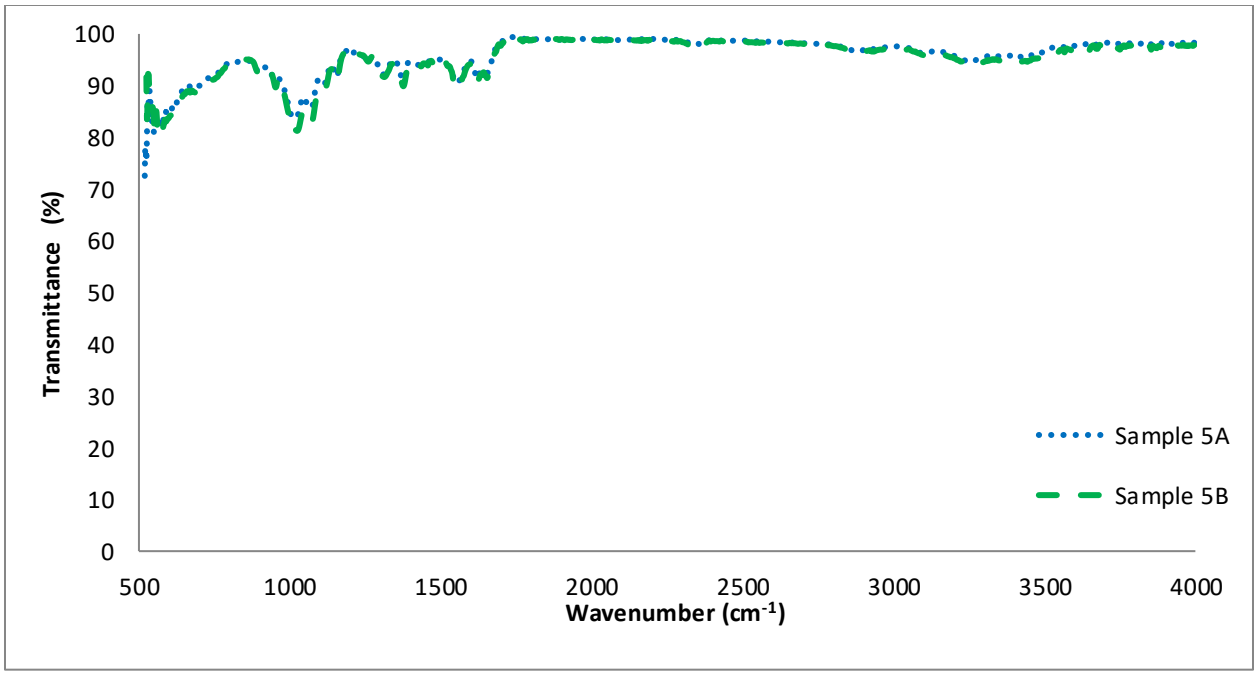

Figure A3-5: FTIR Graph for Sample 5A and 5B

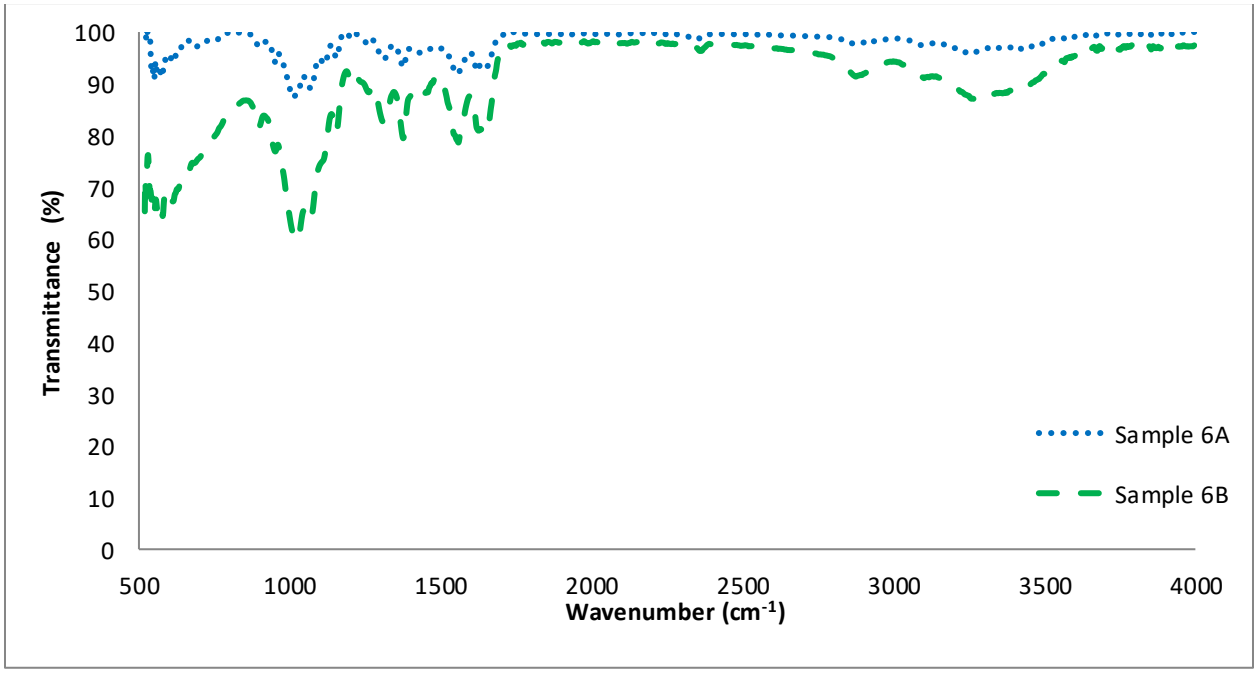

Figure A3-6: FTIR Graph for Sample 6A and 6B

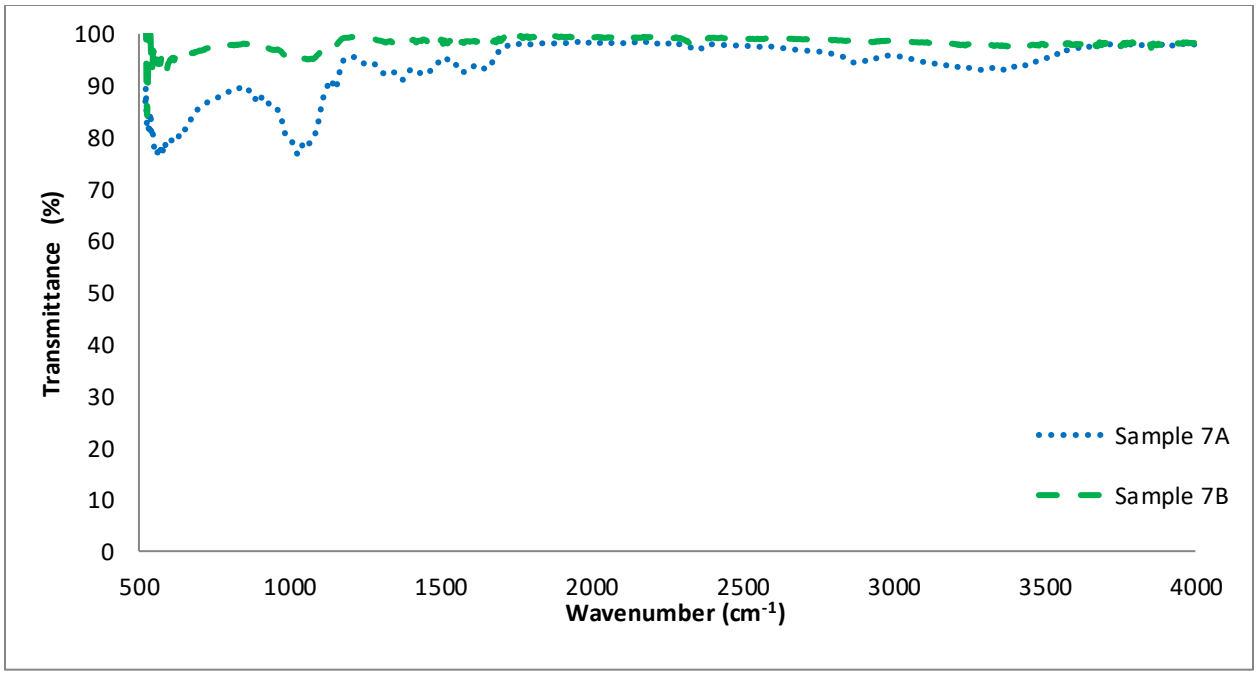

Figure A3-7: FTIR Graph for Sample 7A and 7B

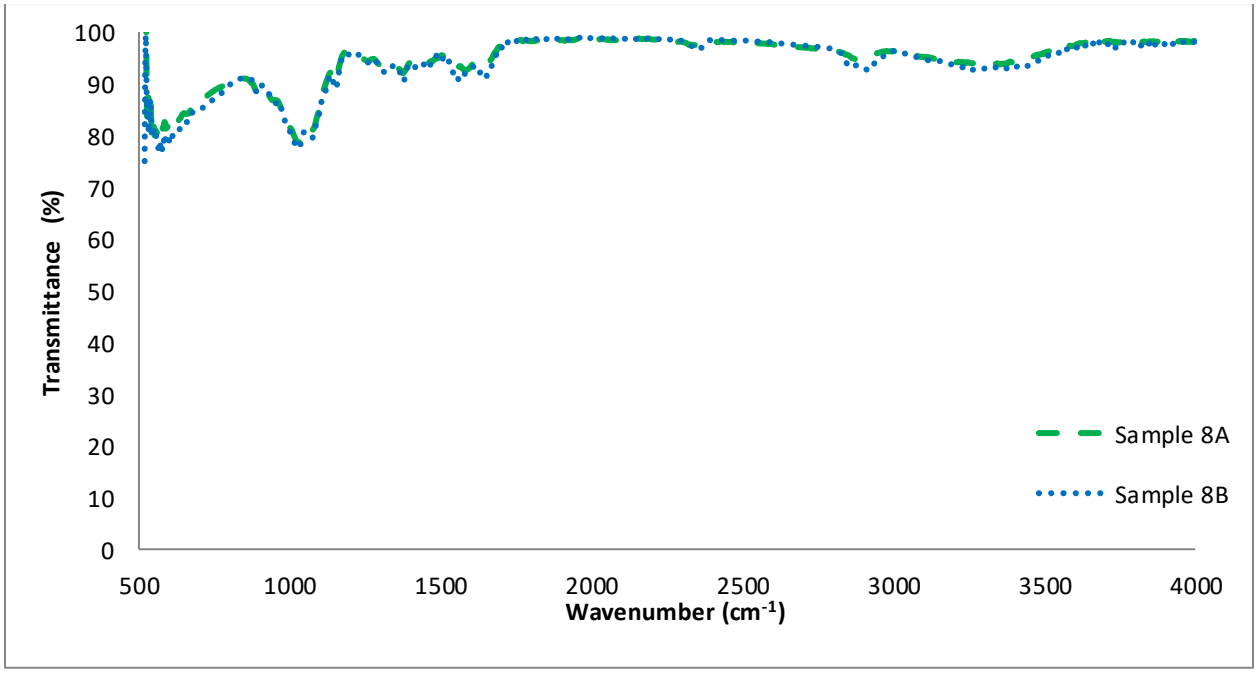

Figure A3-8: FTIR Graph for Sample 8A and 8B

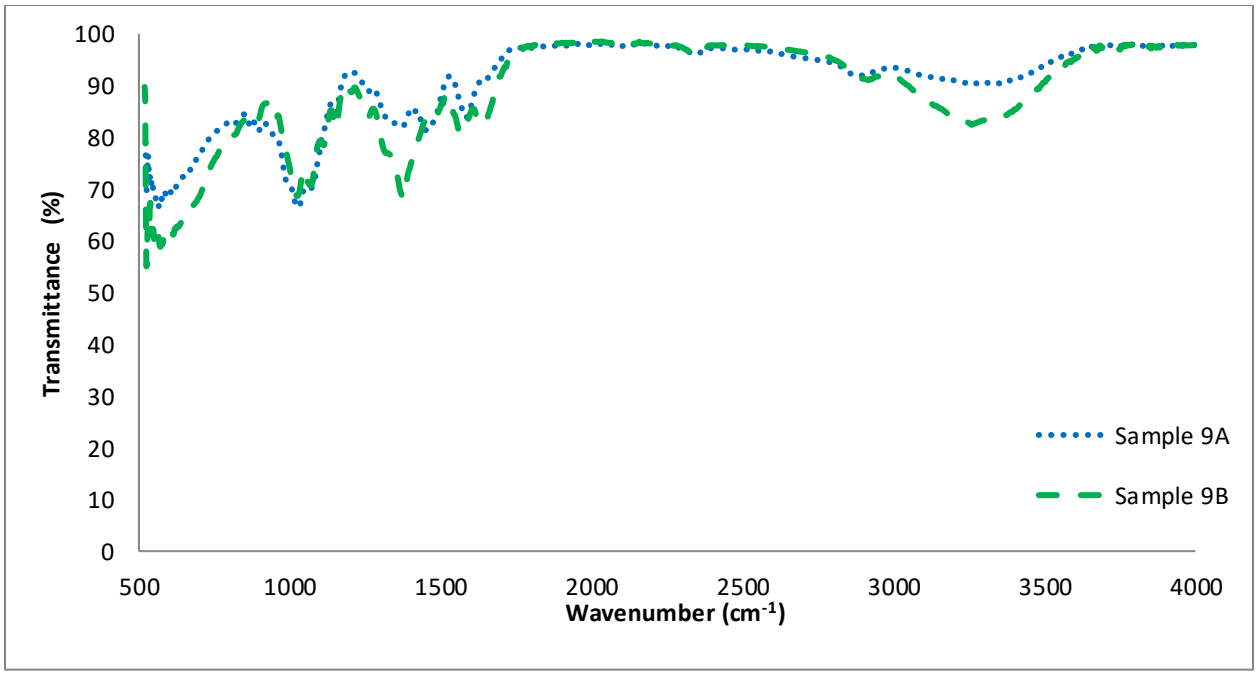

Figure A3-9: FTIR Graph for Sample 9A and 9B

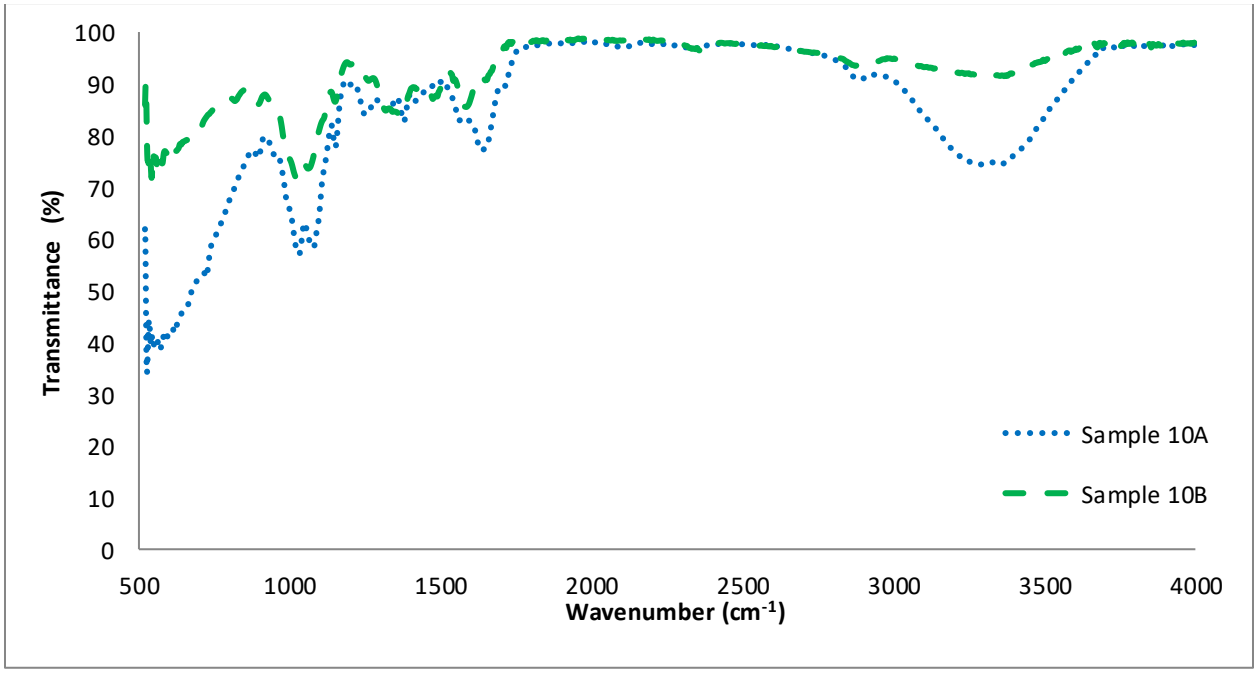

Figure A3-10: FTIR Graph for Sample 10A and 10B

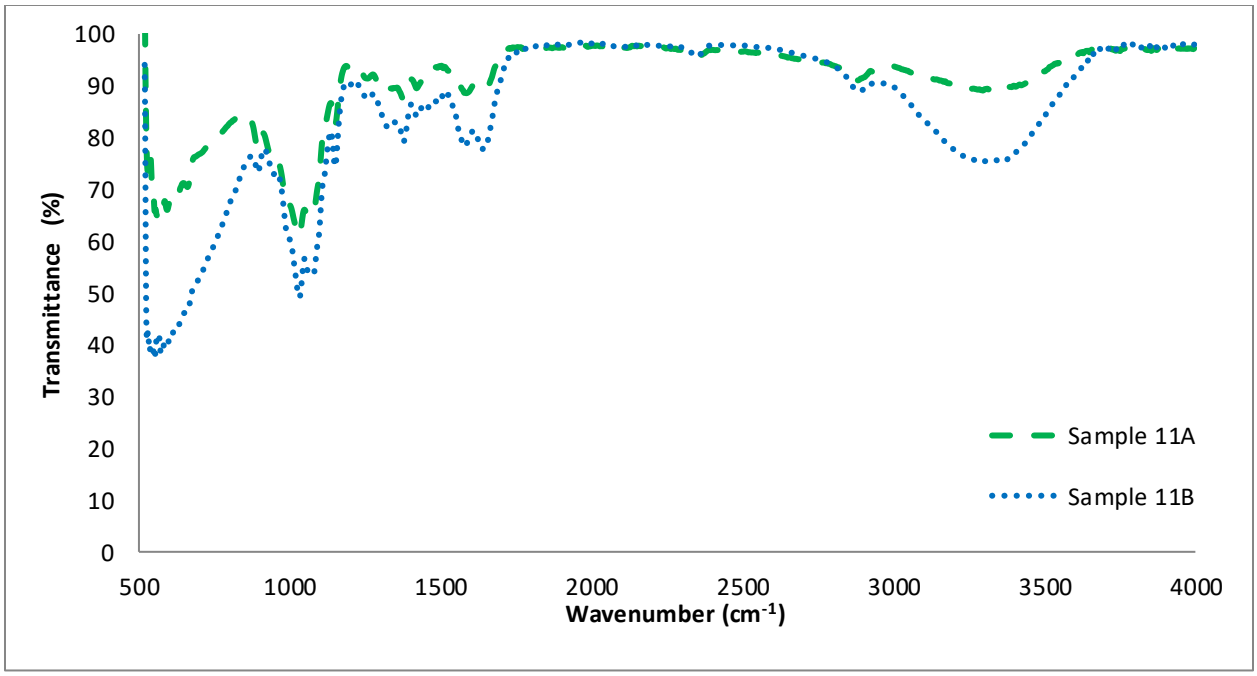

Figure A3-11: FTIR Graph for Sample 11A and 11B

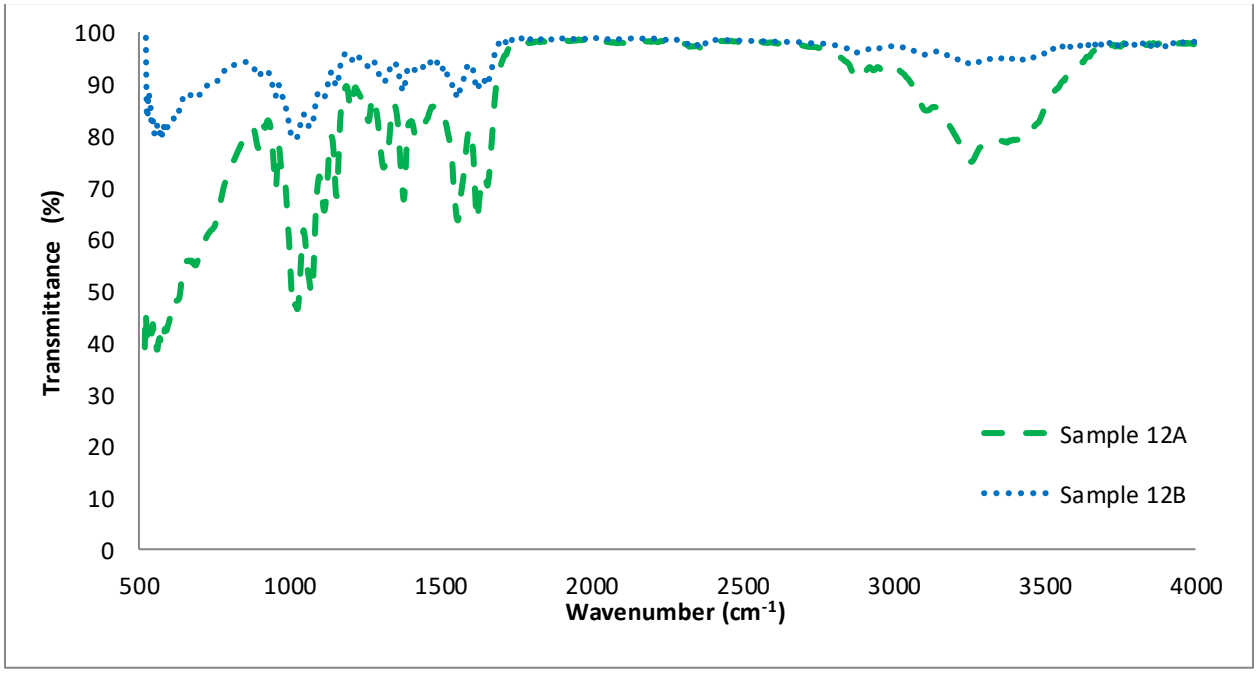

Figure A3-12: FTIR Graph for Sample 12A and 12B

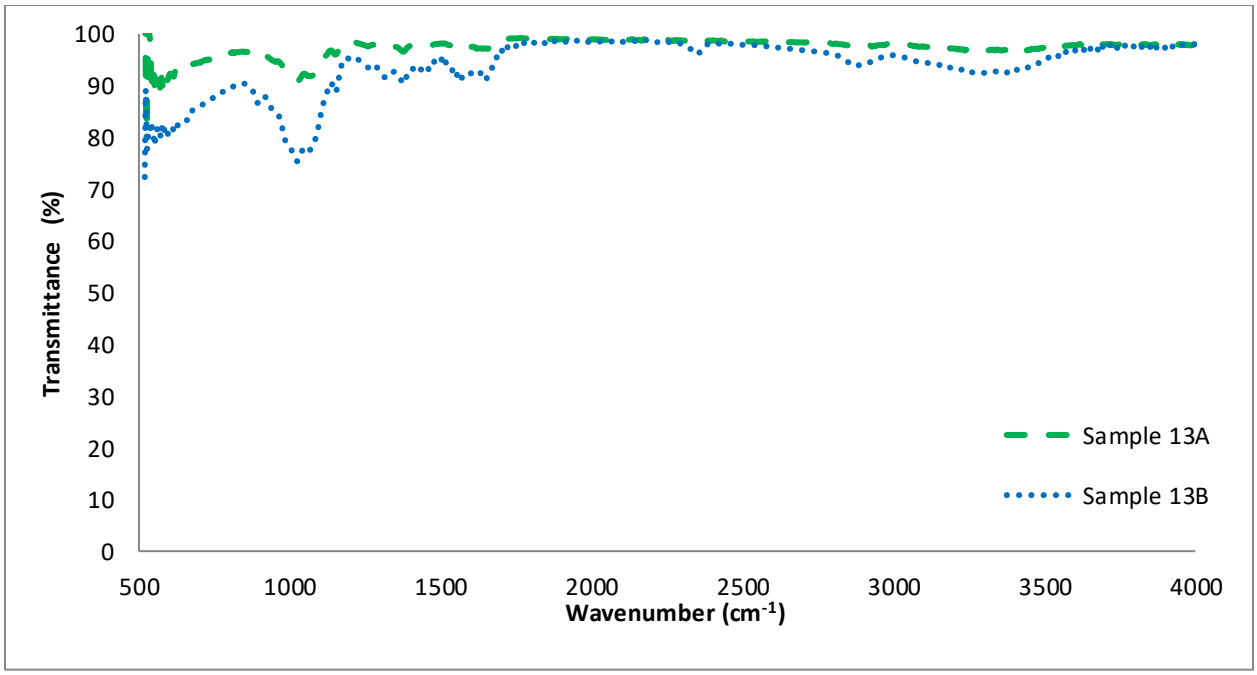

Figure A3-13: FTIR Graph for Sample 13A and 13B

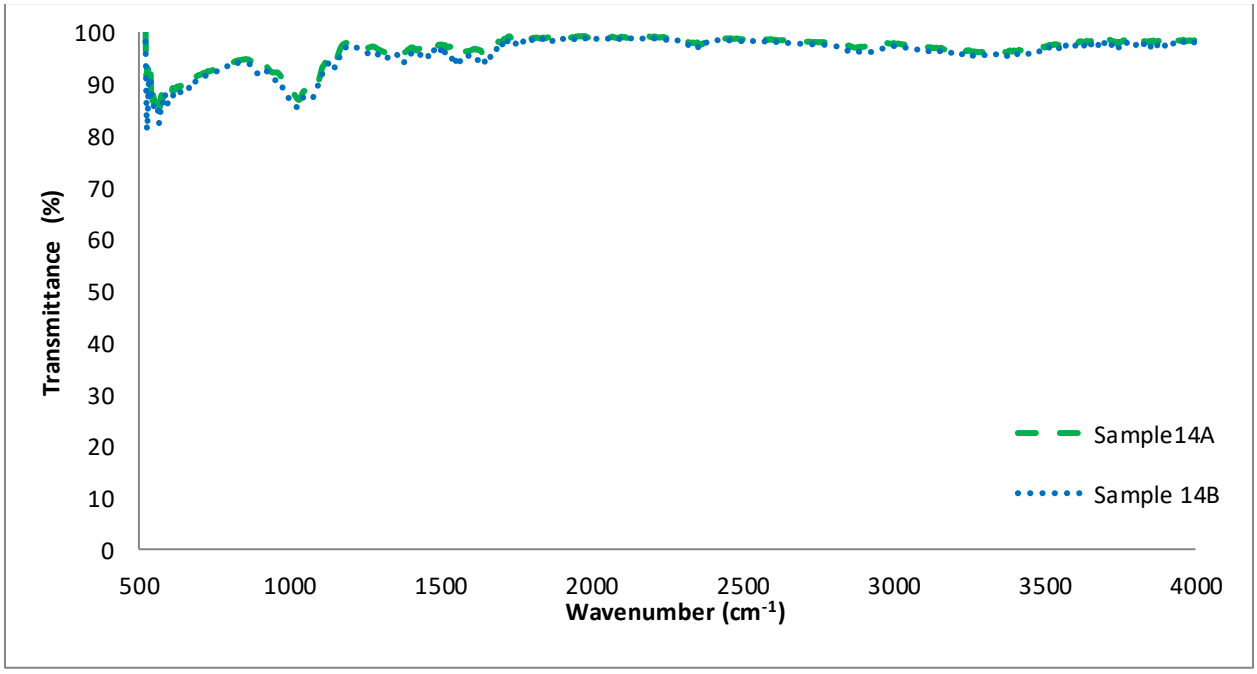

Figure A3-14: FTIR Graph for Sample 14A and 14B

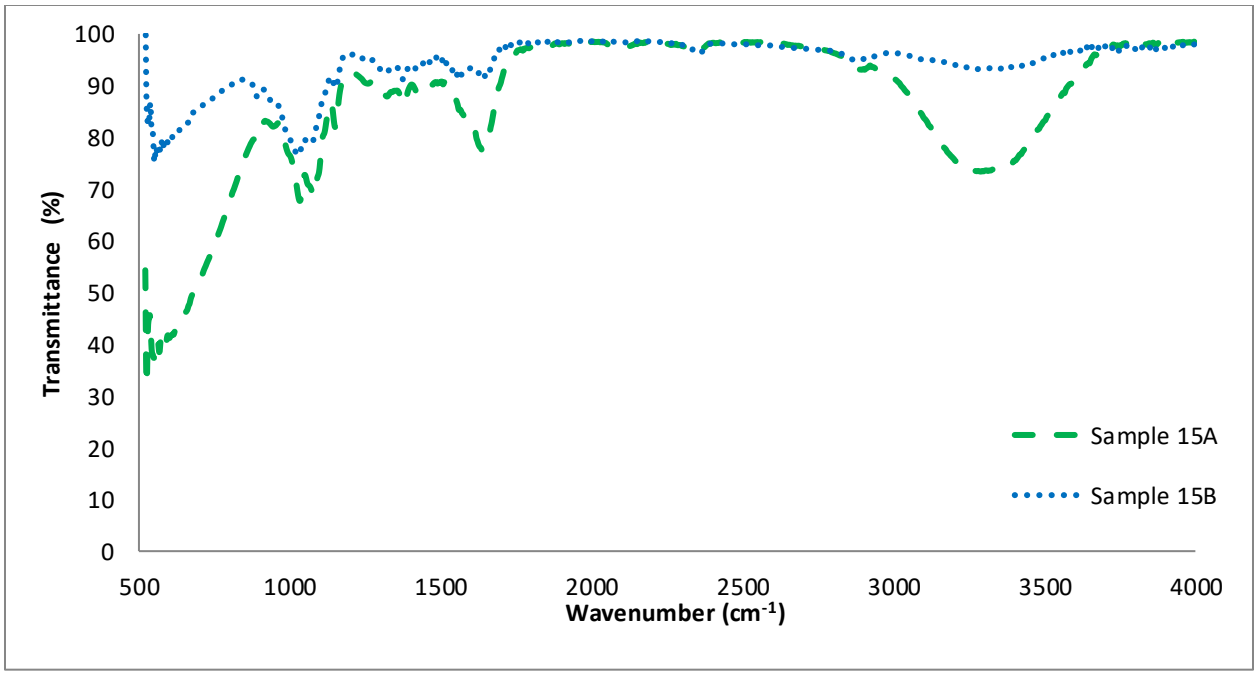

Figure A3-15: FTIR Graph for Sample 15A and 15B

Appendix B: Chitosan Adsorption Results

B1: Preliminary TGA CO_2 Adsorption Raw Data

Table B1-1: TGA Raw Data for CO_2 Adsorption of Sample 1A

Adsorption Time (min)	**Temperature (°C)**	**Weight %**	**Cumulative Adsorption Capacity (gCO2/kg Ads)**
0	71.17	80.28	0.00
5	59.53	80.36	1.00
10	50.80	80.43	1.87
15	44.17	80.49	2.61
20	39.09	80.55	3.36
25	35.27	80.61	4.10
30	34.83	80.67	4.85
35	34.81	80.73	5.59
40	34.81	80.77	6.09
45	34.80	80.81	6.58
50	34.80	80.84	6.95
55	34.81	80.87	7.32
60	34.82	80.89	7.57
65	34.81	80.91	7.82
70	34.81	80.93	8.06
75	34.82	80.95	8.31
80	34.83	80.97	8.56
85	34.83	80.99	8.81
90	34.85	81.00	8.93
95	34.87	81.01	9.05
100	34.88	81.02	9.18
105	34.89	81.03	9.30
110	34.89	81.04	9.42
115	34.89	81.04	9.42
120	34.90	81.05	9.55
125	34.89	81.06	9.67
130	34.91	81.06	9.67
135	34.90	81.07	9.79
140	34.90	81.08	9.92
145	34.90	81.09	9.92

Table B1-2: TGA Raw Data for CO_2 Adsorption of Sample 1B

Adsorption Time (min)	**Temperature (ºC)**	**Weight %**	**Cumulative Adsorption Capacity (gCO_2/kg Ads)**
0	73.37	63.91	0.00
5	61.39	63.96	0.78
10	52.39	64.01	1.56
15	45.59	64.06	2.34
20	40.37	64.10	2.97
25	36.32	64.14	3.59
30	34.73	64.19	4.37
35	34.74	64.23	4.99
40	34.72	64.26	5.46
45	34.70	64.29	5.93
50	34.70	64.32	6.40
55	34.71	64.34	6.71
60	34.71	64.35	6.86
65	34.70	64.37	7.17
70	34.71	64.38	7.33
75	34.71	64.40	7.64
80	34.72	64.41	7.79
85	34.72	64.42	7.95
90	34.74	64.42	7.95
95	34.74	64.43	8.10
100	34.76	64.44	8.26
105	34.76	64.44	8.26
110	34.78	64.45	8.41
115	34.77	64.45	8.41
120	34.78	64.46	8.57
125	34.78	64.46	8.57
130	34.78	64.46	8.57
135	34.78	64.47	8.73
140	34.78	64.47	8.73
145	34.78	64.48	8.88

Table B1-3: TGA Raw Data for CO_2 Adsorption of Sample 2A

Adsorption Time (min)	Temperature (°C)	Weight %	Cumulative Adsorption Capacity (gCO2/kg Ads)
0	80.64	91.87	0.00
5	66.41	91.93	0.65
10	55.89	91.98	1.20
15	47.96	92.03	1.74
20	41.92	92.08	2.28
25	37.28	92.12	2.72
30	34.68	92.16	3.15
35	34.83	92.20	3.59
40	34.82	92.23	3.91
45	34.81	92.25	4.13
50	34.81	92.27	4.34
55	34.81	92.29	4.56
60	34.82	92.31	4.78
65	34.82	92.33	4.99
70	34.82	92.34	5.10
75	34.82	92.35	5.21
80	34.83	92.37	5.43
85	34.83	92.38	5.54
90	34.84	92.39	5.64
95	34.85	92.40	5.75
100	34.87	92.40	5.75
105	34.87	92.41	5.86
110	34.87	92.42	5.97
115	34.89	92.43	6.08
120	34.89	92.43	6.08
125	34.89	92.44	6.19
130	34.90	92.45	6.29
135	34.90	92.45	6.29
140	34.90	92.46	6.40
145	34.89	92.47	6.51

Table B1-4: TGA Raw Data for CO_2 Adsorption of Sample 2B

Adsorption Time (min)	Temperature (ºC)	Weight %	Cumulative Adsorption Capacity (gCO2/kg Ads)
0	76.76	67.08	0.00
5	64.08	67.12	0.60
10	54.63	67.15	1.04
15	47.51	67.18	1.49
20	42.05	67.21	1.94
25	37.84	67.24	2.38
30	34.70	67.26	2.68
35	34.66	67.29	3.13
40	34.68	67.32	3.57
45	34.67	67.34	3.87
50	34.66	67.36	4.17
55	34.67	67.38	4.46
60	34.67	67.39	4.61
65	34.67	67.41	4.91
70	34.67	67.42	5.06
75	34.69	67.44	5.35
80	34.69	67.45	5.50
85	34.70	67.46	5.65
90	34.70	67.47	5.80
95	34.71	67.48	5.95
100	34.73	67.49	6.09
105	34.73	67.49	6.09
110	34.75	67.50	6.24
115	34.76	67.51	6.39
120	34.76	67.51	6.39
125	34.76	67.52	6.54
130	34.76	67.53	6.69
135	34.77	67.53	6.69
140	34.76	67.54	6.83
145	34.77	67.54	6.83
150	34.76	67.55	7.00

Table B1-5: TGA Raw Data for CO_2 Adsorption of Sample 3A

Adsorption Time (min)	Temperature (°C)	Weight %	Cumulative Adsorption Capacity (gCO2/kg Ads)
0	87.36	87.29	0.00
5	71.76	87.34	0.57
10	60.31	87.38	1.03
15	51.74	87.42	1.49
20	45.26	87.46	1.95
25	40.31	87.50	2.40
30	36.45	87.53	2.75
35	34.65	87.57	3.20
40	34.73	87.59	3.43
45	34.73	87.61	3.66
50	34.72	87.62	3.77
55	34.71	87.64	4.00
60	34.71	87.64	4.00
65	34.72	87.65	4.12
70	34.73	87.66	4.23
75	34.73	87.66	4.23
80	34.73	87.66	4.23
85	34.75	87.67	4.34
90	34.75	87.67	4.34
95	34.75	87.67	4.34
100	34.77	87.67	4.34
105	34.79	87.67	4.34
110	34.80	87.66	4.23
115	34.81	87.66	4.23
120	34.82	87.66	4.23
125	34.81	87.66	4.23
130	34.83	87.66	4.23
135	34.81	87.67	4.35
140	34.82	87.67	4.35
145	34.82	87.67	4.35
150	34.82	87.67	4.35

Table B1-6: TGA Raw Data for CO_2 Adsorption of Sample 3B

Adsorption Time (min)	Temperature (°C)	Weight %	Cumulative Adsorption Capacity (gCO2/kg Ads)
0	67.34	91.03	0.00
5	56.65	91.03	0.00
10	48.65	91.03	0.00
15	42.53	91.03	0.00
20	37.82	91.03	0.00
25	34.56	91.03	0.00
30	34.74	91.03	0.00
35	34.75	91.02	-0.11
40	34.75	91.02	-0.11
45	34.74	91.02	-0.11
50	34.74	91.02	-0.11
55	34.74	91.02	-0.11
60	34.75	91.02	-0.11
65	34.75	91.02	-0.11
70	34.75	91.02	-0.11
75	34.77	91.02	-0.11
80	34.76	91.02	-0.11
85	34.77	91.02	-0.11
90	34.79	91.02	-0.11
95	34.81	91.01	-0.22
100	34.82	91.01	-0.22
105	34.83	91.01	-0.22
110	34.82	91.01	-0.22
115	34.84	91.01	-0.22
120	34.83	91.01	-0.22
125	34.84	91.00	-0.33
130	34.84	91.00	-0.33
135	34.83	91.00	-0.33
140	34.84	91.00	-0.33
145	34.83	91.00	-0.33

Table B1-7: TGA Raw Data for CO_2 Adsorption of Sample 4A

Adsorption Time (min)	Temperature (°C)	Weight %	Cumulative Adsorption Capacity (gCO2/kg Ads)
0	47.04	95.02	0.00
5	41.89	95.04	0.21
10	37.90	95.04	0.21
15	34.89	95.04	0.21
20	34.64	95.04	0.21
25	34.66	95.05	0.32
30	34.67	95.05	0.32
35	34.66	95.05	0.32
40	34.66	95.05	0.32
45	34.67	95.05	0.32
50	34.67	95.05	0.32
55	34.68	95.05	0.32
60	34.69	95.05	0.32
65	34.70	95.05	0.32
70	34.70	95.05	0.32
75	34.71	95.05	0.32
80	34.72	95.05	0.32
85	34.72	95.05	0.32
90	34.74	95.05	0.32
95	34.75	95.05	0.32
100	34.75	95.05	0.32
105	34.74	95.05	0.32
110	34.75	95.05	0.32
115	34.76	95.05	0.32
120	34.76	95.05	0.32
125	34.75	95.05	0.32
130	34.76	95.05	0.32
135	34.76	95.05	0.32
140	34.76	95.05	0.32
145	34.76	95.05	0.32

Table B1-8: TGA Raw Data for CO_2 Adsorption of Sample 4B

Adsorption Time (min)	Temperature (ºC)	Weight %	Cumulative Adsorption Capacity (gCO2/kg Ads)
0	54.86	90.14	0.00
5	47.48	90.15	0.11
10	41.83	90.16	0.22
15	37.48	90.16	0.22
20	34.51	90.16	0.22
25	34.70	90.17	0.33
30	34.72	90.17	0.33
35	34.71	90.17	0.33
40	34.70	90.17	0.33
45	34.70	90.18	0.44
50	34.70	90.18	0.44
55	34.71	90.18	0.44
60	34.71	90.18	0.44
65	34.72	90.18	0.44
70	34.72	90.18	0.44
75	34.73	90.18	0.44
80	34.73	90.18	0.44
85	34.73	90.18	0.44
90	34.75	90.18	0.44
95	34.76	90.18	0.44
100	34.77	90.18	0.44
105	34.77	90.18	0.44
110	34.78	90.18	0.44
115	34.78	90.18	0.44
120	34.78	90.18	0.44
125	34.78	90.18	0.44
130	34.78	90.18	0.44
135	34.78	90.18	0.44

Table B1-9: TGA Raw Data for CO_2 Adsorption of Sample 5A

Adsorption Time (min)	Temperature (ºC)	Weight %	Cumulative Adsorption Capacity (gCO2/kg Ads)
0	82.43	91.93	0.00
5	68.49	91.97	0.44
10	58.18	92.01	0.87
15	50.39	92.04	1.20
20	44.46	92.07	1.52
25	39.88	92.09	1.74
30	36.29	92.12	2.06
35	34.62	92.14	2.28
40	34.70	92.16	2.50
45	34.69	92.18	2.72
50	34.69	92.19	2.82
55	34.68	92.21	3.04
60	34.68	92.22	3.15
65	34.69	92.23	3.26
70	34.70	92.25	3.48
75	34.70	92.25	3.48
80	34.70	92.26	3.58
85	34.71	92.27	3.69
90	34.72	92.28	3.80
95	34.73	92.29	3.91
100	34.74	92.30	4.02
105	34.75	92.30	4.02
110	34.75	92.31	4.13
115	34.76	92.31	4.13
120	34.77	92.32	4.23
125	34.76	92.32	4.23
130	34.77	92.33	4.34
135	34.77	92.34	4.45
140	34.78	92.34	4.45
145	34.78	92.35	4.56
150	34.78	92.35	4.56

Table B1-10: TGA Raw Data for CO_2 Adsorption of Sample 5B

Adsorption Time (min)	Temperature (ºC)	Weight %	Cumulative Adsorption Capacity (gCO2/kg Ads)
0	49.06	93.53	0.00
5	43.23	93.54	0.11
10	38.71	93.54	0.11
15	35.26	93.54	0.11
20	34.69	93.54	0.11
25	34.68	93.55	0.21
30	34.67	93.55	0.21
35	34.67	93.55	0.21
40	34.67	93.55	0.21
45	34.67	93.55	0.21
50	34.67	93.55	0.21
55	34.68	93.55	0.21
60	34.68	93.55	0.21
65	34.68	93.55	0.21
70	34.69	93.55	0.21
75	34.70	93.55	0.21
80	34.71	93.55	0.21
85	34.72	93.55	0.21
90	34.73	93.55	0.21
95	34.74	93.55	0.21
100	34.73	93.55	0.21
105	34.74	93.55	0.21
110	34.74	93.55	0.21
115	34.75	93.55	0.21
120	34.75	93.55	0.21
125	34.75	93.55	0.21
130	34.76	93.55	0.21

Table B1-11: TGA Raw Data for CO_2 Adsorption of Sample 6A

Adsorption Time (min)	Temperature (°C)	Weight %	Cumulative Adsorption Capacity (gCO_2/kg Ads)
0	78.26	92.04	0.00
5	64.76	92.08	0.43
10	54.75	92.10	0.65
15	47.18	92.13	0.98
20	41.42	92.15	1.19
25	36.97	92.17	1.41
30	34.71	92.19	1.63
35	34.82	92.21	1.85
40	34.81	92.22	1.95
45	34.80	92.24	2.17
50	34.80	92.25	2.28
55	34.80	92.26	2.39
60	34.80	92.27	2.50
65	34.82	92.28	2.60
70	34.81	92.29	2.71
75	34.81	92.30	2.82
80	34.82	92.31	2.93
85	34.83	92.32	3.04
90	34.83	92.32	3.04
95	34.85	92.33	3.15
100	34.88	92.33	3.15
105	34.88	92.34	3.25
110	34.89	92.34	3.25
115	34.89	92.35	3.36
120	34.89	92.36	3.47
125	34.90	92.36	3.47
130	34.90	92.37	3.58
135	34.90	92.37	3.58
140	34.90	92.38	3.69
145	34.89	92.38	3.69

Table B1-12: TGA Raw Data for CO_2 Adsorption of Sample 6B

Adsorption Time (min)	Temperature (°C)	Weight %	Cumulative Adsorption Capacity (gCO_2/kg Ads)
0	62.58	90.06	0.00
5	52.97	90.08	0.22
10	45.74	90.09	0.33
15	40.21	90.10	0.44
20	35.94	90.12	0.67
25	34.84	90.12	0.67
30	34.79	90.13	0.78
35	34.79	90.13	0.78
40	34.77	90.14	0.89
45	34.78	90.15	1.00
50	34.77	90.15	1.00
55	34.78	90.16	1.11
60	34.78	90.16	1.11
65	34.78	90.17	1.22
70	34.78	90.17	1.22
75	34.79	90.17	1.22
80	34.79	90.18	1.33
85	34.80	90.18	1.33
90	34.82	90.18	1.33
95	34.83	90.18	1.33
100	34.84	90.19	1.44
105	34.85	90.19	1.44
110	34.84	90.19	1.44
115	34.85	90.19	1.44
120	34.85	90.20	1.55
125	34.85	90.20	1.55
130	34.86	90.20	1.55
135	34.85	90.20	1.55
140	34.85	90.21	1.66

Table B1-13: TGA Raw Data for CO_2 Adsorption of Sample 7A

Adsorption Time (min)	Temperature (°C)	Weight %	Cumulative Adsorption Capacity (gCO_2/kg Ads)
0	78.91	86.98	0.00
5	65.45	87.00	0.23
10	55.48	87.02	0.46
15	47.98	87.03	0.57
20	42.27	87.04	0.69
25	37.87	87.05	0.80
30	34.66	87.05	0.80
35	34.75	87.06	0.92
40	34.77	87.06	0.92
45	34.76	87.07	1.03
50	34.76	87.07	1.03
55	34.76	87.07	1.03
60	34.76	87.08	1.15
65	34.77	87.08	1.15
70	34.76	87.08	1.15
75	34.77	87.09	1.26
80	34.77	87.09	1.26
85	34.78	87.09	1.26
90	34.79	87.09	1.26
95	34.80	87.10	1.38
100	34.81	87.10	1.38
105	34.82	87.10	1.38
110	34.84	87.10	1.38
115	34.83	87.10	1.38
120	34.84	87.10	1.38
125	34.84	87.10	1.38
130	34.84	87.10	1.38
135	34.84	87.10	1.38
140	34.84	87.10	1.38
145	34.84	87.10	1.38
150	34.85	87.11	1.49

Table B1-14: TGA Raw Data for CO_2 Adsorption of Sample 7B

Adsorption Time (min)	Temperature (ºC)	Weight %	Cumulative Adsorption Capacity (gCO_2/kg Ads)
0	59.19	88.19	0.00
5	50.52	88.20	0.11
10	43.96	88.21	0.23
15	38.94	88.22	0.34
20	35.16	88.22	0.34
25	34.75	88.22	0.34
30	34.76	88.22	0.34
35	34.76	88.22	0.34
40	34.75	88.23	0.45
45	34.75	88.23	0.45
50	34.75	88.23	0.45
55	34.76	88.23	0.45
60	34.77	88.23	0.45
65	34.77	88.23	0.45
70	34.77	88.24	0.57
75	34.77	88.24	0.57
80	34.78	88.24	0.57
85	34.79	88.24	0.57
90	34.80	88.24	0.57
95	34.81	88.24	0.57
100	34.82	88.24	0.57
105	34.83	88.24	0.57
110	34.83	88.24	0.57
115	34.83	88.24	0.57
120	34.83	88.24	0.57
125	34.84	88.24	0.57
130	34,84	88,24	0,57
135	34,84	88,24	0,57
140	34,84	88,25	0,68

Table B1-15: TGA Raw Data for CO_2 Adsorption of Sample 8A

Adsorption Time (min)	Temperature (°C)	Weight %	Cumulative Adsorption Capacity (gCO_2/kg Ads)
0	64.10	87.95	0.00
5	54.68	87.96	0.11
10	47.55	87.98	0.34
15	42.09	87.99	0.45
20	37.88	88.00	0.57
25	34.75	88.00	0.57
30	34.69	88.00	0.57
35	34.72	88.01	0.68
40	34.72	88.01	0.68
45	34.71	88.02	0.80
50	34.71	88.02	0.80
55	34.71	88.02	0.80
60	34.71	88.02	0.80
65	34.72	88.03	0.91
70	34.72	88.03	0.91
75	34.73	88.03	0.91
80	34.75	88.03	0.91
85	34.76	88.03	0.91
90	34.76	88.04	1.02
95	34.77	88.03	0.91
100	34.78	88.03	0.91
105	34.80	88.03	0.91
110	34.80	88.03	0.91
115	34.81	88.03	0.91
120	34.80	88.04	1.02
125	34.81	88.04	1.02
130	34.81	88.04	1.02
135	34.81	88.04	1.02
140	34.82	88.04	1.02
145	34.82	88.04	1.02

Table B1-16: TGA Raw Data for CO_2 Adsorption of Sample 8B

Adsorption Time (min)	Temperature (°C)	Weight %	Cumulative Adsorption Capacity (gCO_2/kg Ads)
0	79.92	88.72	0.00
5	66.21	88.74	0.23
10	56.05	88.76	0.45
15	48.38	88.78	0.68
20	42.53	88.80	0.90
25	38.03	88.81	1.01
30	34.70	88.82	1.13
35	34.70	88.83	1.24
40	34.72	88.84	1.35
45	34.72	88.85	1.46
50	34.71	88.86	1.58
55	34.70	88.87	1.69
60	34.72	88.87	1.69
65	34.71	88.88	1.80
70	34.72	88.88	1.80
75	34.73	88.89	1.91
80	34.73	88.89	1.91
85	34.75	88.90	2.03
90	34.75	88.90	2.03
95	34.75	88.90	2.03
100	34.78	88.90	2.03
105	34.79	88.90	2.03
110	34.79	88.91	2.14
115	34.78	88.91	2.14
120	34.79	88.91	2.14
125	34.79	88.91	2.14
130	34.80	88.92	2.25
135	34.80	88.92	2.25
140	34.81	88.92	2.25
145	34.80	88.92	2.25

Table B1-17: TGA Raw Data for CO_2 Adsorption of Sample 9A

Adsorption Time (min)	Temperature (°C)	Weight %	Cumulative Adsorption Capacity (gCO_2/kg Ads)
0	61.44	87.13	0.00
5	52.36	87.13	0.00
10	45.51	87.13	0.00
15	40.25	87.13	0.00
20	36.20	87.14	0.11
25	34.83	87.13	0.00
30	34.79	87.13	0.00
35	34.78	87.13	0.00
40	34.77	87.13	0.00
45	34.77	87.13	0.00
50	34.76	87.13	0.00
55	34.77	87.13	0.00
60	34.77	87.13	0.00
65	34.78	87.13	0.00
70	34.78	87.13	0.00
75	34.79	87.13	0.00
80	34.79	87.13	0.00
85	34.80	87.13	0.00
90	34.82	87.13	0.00
95	34.83	87.12	-0.11
100	34.85	87.12	-0.11
105	34.84	87.12	-0.11
110	34.84	87.12	-0.11
115	34.85	87.12	-0.11
120	34.84	87.12	-0.11
125	34.85	87.12	-0.11
130	34.85	87.12	-0.11
135	34.86	87.12	-0.11
140	34.85	87.12	-0.11

Table B1-18: TGA Raw Data for CO_2 Adsorption of Sample 9B

Adsorption Time (min)	Temperature (°C)	Weight %	Cumulative Adsorption Capacity (gCO_2/kg Ads)
0	54.69	87.26	0.00
5	45.97	87.26	0.00
10	39.36	87.26	0.00
15	34.77	87.27	0.11
20	35.01	87.27	0.11
25	35.04	87.27	0.11
30	35.05	87.26	0.00
35	35.03	87.26	0.00
40	35.04	87.26	0.00
45	35.03	87.26	0.00
50	35.02	87.26	0.00
55	35.00	87.26	0.00
60	34.99	87.27	0.11
65	34.95	87.27	0.11
70	34.96	87.27	0.11
75	35.01	87.26	0.00
80	35.02	87.26	0.00
85	35.03	87.26	0.00
90	35.04	87.26	0.00
95	35.05	87.26	0.00
100	35.05	87.26	0.00
105	35.05	87.26	0.00
110	35.04	87.26	0.00
115	35.04	87.26	0.00
120	35.03	87.26	0.00
125	35.04	87.26	0.00
130	35.03	87.25	-0.11

Table B1-19: TGA Raw Data for CO_2 Adsorption of Sample 10A

Adsorption Time (min)	Temperature (°C)	Weight %	Cumulative Adsorption Capacity (gCO_2/kg Ads)
0	94.14	62.75	0.00
5	75.99	62.77	0.32
10	62.86	62.79	0.64
15	53.12	62.80	0.80
20	45.76	62.82	1.12
25	40.13	62.83	1.27
30	35.79	62.85	1.59
35	34.89	62.86	1.75
40	34.84	62.87	1.91
45	34.84	62.88	2.07
50	34.83	62.88	2.07
55	34.84	62.89	2.23
60	34.83	62.90	2.39
65	34.84	62.90	2.39
70	34.85	62.91	2.55
75	34.85	62.91	2.55
80	34.85	62.91	2.55
85	34.85	62.92	2.71
90	34.86	62.92	2.71
95	34.88	62.93	2.87
100	34.90	62.92	2.71
105	34.91	62.92	2.71
110	34.92	62.93	2.87
115	34.91	62.93	2.87
120	34.92	62.93	2.87
125	34.92	62.93	2.87
130	34.93	62.93	2.87
135	34.93	62.93	2.87
140	34.92	62.93	2.87
145	34.93	62.94	3.02
150	34.93	62.94	3.02

Table B1-20: TGA Raw Data for CO_2 Adsorption of Sample 10B

Adsorption Time (min)	Temperature (°C)	Weight %	Cumulative Adsorption Capacity (gCO_2/kg Ads)
0	54.27	91.91	0.00
5	46.77	91.91	0.00
10	41.06	91.91	0.00
15	36.65	91.91	0.00
20	34.75	91.91	0.00
25	34.77	91.90	-0.11
30	34.76	91.90	-0.11
35	34.75	91.90	-0.11
40	34.75	91.90	-0.11
45	34.75	91.90	-0.11
50	34.76	91.90	-0.11
55	34.76	91.90	-0.11
60	34.77	91.90	-0.11
65	34.76	91.89	-0.22
70	34.77	91.89	-0.22
75	34.78	91.89	-0.22
80	34.78	91.89	-0.22
85	34.80	91.89	-0.22
90	34.81	91.89	-0.22
95	34.82	91.89	-0.22
100	34.82	91.88	-0.33
105	34.83	91.88	-0.33
110	34.83	91.88	-0.33
115	34.83	91.88	-0.33
120	34.83	91.88	-0.33
125	34.84	91.88	-0.33
130	34.83	91.88	-0.33
135	34.83	91.88	-0.33

Table B1-21: TGA Raw Data for CO_2 Adsorption of Sample 11A

Adsorption Time (min)	Temperature (°C)	Weight %	Cumulative Adsorption Capacity (gCO_2/kg Ads)
0	83.79	87.37	0.00
5	68.83	87.40	0.34
10	57.85	87.42	0.57
15	49.59	87.44	0.80
20	43.31	87.45	0.92
25	38.51	87.47	1.14
30	34.89	87.48	1.26
35	34.78	87.49	1.37
40	34.80	87.50	1.49
45	34.79	87.50	1.49
50	34.79	87.51	1.60
55	34.79	87.51	1.60
60	34.80	87.52	1.72
65	34.79	87.52	1.72
70	34.80	87.53	1.83
75	34.81	87.53	1.83
80	34.80	87.54	1.94
85	34.82	87.54	1.94
90	34.82	87.54	1.94
95	34.83	87.54	1.94
100	34.85	87.54	1.94
105	34.87	87.54	1.94
110	34.87	87.54	1.94
115	34.87	87.55	2.06
120	34.87	87.55	2.06
125	34.88	87.55	2.06
130	34.89	87.55	2.06
135	34.88	87.55	2.06
140	34.89	87.55	2.06
145	34.89	87.56	2.17
150	34.88	87.56	2.17

Table B1-22: TGA Raw Data for CO_2 Adsorption of Sample 11B

Adsorption Time (min)	Temperature (°C)	Weight %	Cumulative Adsorption Capacity (gCO_2/kg Ads)
0	97.44	77.09	0.00
5	78.94	77.27	2.33
10	65.46	77.32	2.98
15	55.50	77.27	2.33
20	47.97	77.29	2.59
25	42.23	77.29	2.59
30	37.79	77.30	2.72
35	34.60	77.30	2.72
40	34.71	77.20	1.43
45	34.74	77.20	1.43
50	34.72	77.20	1.43
55	34.71	77.19	1.30
60	34.71	77.35	3.37
65	34.72	77.27	2.34
70	34.72	77.29	2.60
75	34.72	77.34	3.24
80	34.73	77.21	1.56
85	34.74	77.21	1.56
90	34.75	77.15	0.78
95	34.75	77.24	1.95
100	34.76	77.24	1.95
105	34.78	77.24	1.95
110	34.79	77.24	1.95
115	34.80	77.24	1.95
120	34.80	77.24	1.95
125	34.80	77.24	1.95
130	34.80	77.24	1.95
135	34.80	77.24	1.95
140	34.80	77.24	1.95
145	34.80	77.24	1.95
150	34.81	77.24	1.95

Table B1-23 TGA Raw Data for CO_2 Adsorption of Sample 12A

Adsorption Time (min)	Temperature (ºC)	Weight %	Cumulative Adsorption Capacity (gCO_2/kg Ads)
0	100.44	77.66	0.00
5	81.28	77.72	0.77
10	67.33	77.78	1.54
15	57.00	77.84	2.32
20	49.22	77.89	2.96
25	43.28	77.95	3.73
30	38.71	77.99	4.24
35	35.24	78.04	4.88
40	34.77	78.10	5.65
45	34.76	78.14	6.16
50	34.75	78.18	6.67
55	34.75	78.22	7.19
60	34.75	78.25	7.57
65	34.74	78.27	7.82
70	34.75	78.30	8.21
75	34.76	78.32	8.46
80	34.76	78.34	8.72
85	34.76	78.35	8.85
90	34.78	78.37	9.10
95	34.78	78.38	9.23
100	34.79	78.39	9.36
105	34.80	78.40	9.48
110	34.81	78.41	9.61
115	34.82	78.42	9.74
120	34.83	78.43	9.87
125	34.83	78.43	9.87
130	34.83	78.44	9.99
135	34.83	78.45	10.12
140	34.84	78.46	10.25
145	34.83	78.46	10.25
150	34.85	78.47	10.38
155	34.84	78.47	10.38

Table B1-24 TGA Raw Data for CO_2 Adsorption of Sample 12B

Adsorption Time (min)	Temperature (°C)	Weight %	Cumulative Adsorption Capacity (gCO_2/kg Ads)
0	81.05	93.38	0.00
5	67.40	93.41	0.32
10	57.28	93.43	0.54
15	49.67	93.45	0.75
20	43.83	93.47	0.96
25	39.35	93.49	1.18
30	35.85	93.51	1.39
35	34.70	93.53	1.61
40	34.67	93.55	1.82
45	34.67	93.56	1.93
50	34.65	93.58	2.14
55	34.66	93.59	2.25
60	34.66	93.60	2.35
65	34.66	93.61	2.46
70	34.66	93.62	2.57
75	34.68	93.62	2.57
80	34.67	93.63	2.67
85	34.68	93.64	2.78
90	34.68	93.64	2.78
95	34.69	93.65	2.89
100	34.70	93.65	2.89
105	34.71	93.66	2.99
110	34.70	93.66	2.99
115	34.71	93.67	3.10
120	34.72	93.67	3.10
125	34.72	93.68	3.21
130	34.72	93.68	3.21
135	34.72	93.68	3.21
140	34.72	93.69	3.31
145	34.73	93.69	3.31
150	34.73	93.69	3.31

Table B1-25 TGA Raw Data for CO_2 Adsorption of Sample 13A

Adsorption Time (min)	Temperature (°C)	Weight %	Cumulative Adsorption Capacity (gCO_2/kg Ads)
0	89.79	89.65	0.00
5	73.22	89.68	0.33
10	61.11	89.71	0.67
15	52.04	89.74	1.00
20	45.17	89.76	1.23
25	39.91	89.79	1.56
30	35.85	89.81	1.78
35	34.87	89.82	1.89
40	34.82	89.84	2.12
45	34.80	89.85	2.23
50	34.79	89.86	2.34
55	34.79	89.87	2.45
60	34.80	89.88	2.56
65	34.81	89.89	2.67
70	34.81	89.90	2.79
75	34.80	89.91	2.90
80	34.82	89.91	2.90
85	34.82	89.92	3.01
90	34.83	89.92	3.01
95	34.84	89.93	3.12
100	34.86	89.93	3.12
105	34.87	89.93	3.12
110	34.89	89.93	3.12
115	34.89	89.98	3.67
120	34.90	89.99	3.79
125	34.88	89.99	3.79
130	34.89	89.99	3.79
135	34.89	89.99	3.79
140	34.90	89.99	3.79
145	34.90	90.00	3.90
150	34.90	90.00	3.90

Table B1-26 TGA Raw Data for CO_2 Adsorption of Sample 13B

Adsorption Time (min)	Temperature (°C)	Weight %	Cumulative Adsorption Capacity (gCO_2/kg Ads)
0	91.29	89.01	0.00
5	73.91	89.01	0.00
10	61.28	89.03	0.23
15	51.84	89.06	0.56
20	44.69	89.08	0.79
25	39.23	89.11	1.12
30	35.14	89.12	1.24
35	34.83	89.15	1.57
40	34.84	89.16	1.69
45	34.84	89.17	1.80
50	34.83	89.18	1.91
55	34.84	89.18	1.91
60	34.84	89.19	2.02
65	34.84	89.20	2.13
70	34.85	89.21	2.25
75	34.85	89.22	2.36
80	34.85	89.23	2.47
85	34.85	89.24	2.58
90	34.87	89.26	2.81
95	34.88	89.25	2.70
100	34.90	89.24	2.58
105	34.90	89.23	2.47
110	34.91	89.23	2.47
115	34.92	89.23	2.47
120	34.91	89.22	2.36
125	34.92	89.21	2.25
130	34.93	89.20	2.14
135	34.91	89.22	2.36
140	34.92	89.22	2.36
145	34.92	89.23	2.47
150	34.93	89.23	2.47

Table B1-27 TGA Raw Data for CO_2 Adsorption of Sample 14A

Adsorption Time (min)	Temperature (°C)	Weight %	Cumulative Adsorption Capacity (gCO_2/kg Ads)
0	88.38	86.41	0.00
5	72.47	86.43	0.23
10	60.86	86.44	0.35
15	52.16	86.44	0.35
20	45.54	86.45	0.46
25	40.45	86.47	0.69
30	36.49	86.48	0.81
35	34.69	86.48	0.81
40	34.76	86.48	0.81
45	34.75	86.48	0.81
50	34.73	86.49	0.93
55	34.72	86.49	0.93
60	34.72	86.49	0.93
65	34.73	86.49	0.93
70	34.73	86.50	1.04
75	34.74	86.50	1.04
80	34.74	86.50	1.04
85	34.74	86.50	1.04
90	34.75	86.50	1.04
95	34.76	86.51	1.16
100	34.77	86.51	1.16
105	34.78	86.51	1.16
110	34.79	86.50	1.04
115	34.80	86.50	1.04
120	34.80	86.50	1.04
125	34.80	86.50	1.04
130	34.80	86.51	1.16
135	34.81	86.51	1.16
140	34.81	86.51	1.16
145	34.81	86.51	1.16
150	34.80	86.51	1.16

Table B1-28 TGA Raw Data for CO_2 Adsorption of Sample 14B

Adsorption Time (min)	Temperature (°C)	Weight %	Cumulative Adsorption Capacity (gCO_2/kg Ads)
0	75.14	89.15	0.00
5	61.87	89.19	0.45
10	52.03	89.23	0.90
15	44.56	89.26	1.23
20	38.89	89.29	1.57
25	34.76	89.31	1.79
30	34.86	89.33	2.02
35	34.89	89.35	2.24
40	34.90	89.36	2.35
45	34.89	89.37	2.47
50	34.89	89.38	2.58
55	34.89	89.39	2.69
60	34.90	89.39	2.69
65	34.89	89.40	2.80
70	34.89	89.41	2.91
75	34.89	89.42	3.02
80	34.90	89.43	3.14
85	34.91	89.44	3.25
90	34.93	89.44	3.25
95	34.94	89.43	3.14
100	34.95	89.43	3.14
105	34.96	89.44	3.25
110	34.96	89.44	3.25
115	34.96	89.43	3.14
120	34.97	89.44	3.25
125	34.96	89.45	3.36
130	34.97	89.45	3.36
135	34.96	89.45	3.36
140	34.96	89.45	3.36
145	34.96	89.46	3.47

Table B1-29 TGA Raw Data for CO_2 Adsorption of Sample 15A

Adsorption Time (min)	Temperature (°C)	Weight %	Cumulative Adsorption Capacity (gCO_2/kg Ads)
0	61.26	48.90	0.00
5	52.04	48.90	0.00
10	45.06	48.91	0.20
15	39.75	48.91	0.20
20	35.65	48.91	0.20
25	34.81	48.91	0.20
30	34.76	48.91	0.20
35	34.76	48.92	0.41
40	34.74	48.92	0.41
45	34.75	48.92	0.41
50	34.75	48.92	0.41
55	34.75	48.92	0.41
60	34.75	48.92	0.41
65	34.75	48.92	0.41
70	34.77	48.92	0.41
75	34.77	48.92	0.41
80	34.77	48.92	0.41
85	34.79	48.92	0.41
90	34.81	48.92	0.41
95	34.82	48.92	0.41
100	34.82	48.92	0.41
105	34.83	48.92	0.41
110	34.83	48.92	0.41
115	34.83	48.92	0.41

Table B1-30 TGA Raw Data for CO_2 Adsorption of Sample 15B

Adsorption Time (min)	Temperature (°C)	Weight %	Cumulative Adsorption Capacity (gCO_2/kg Ads)
0	95.39	88.77	0.00
5	77.30	88.79	0.23
10	64.14	88.80	0.34
15	54.37	88.82	0.56
20	47.00	88.83	0.68
25	41.38	88.85	0.90
30	37.07	88.86	1.01
35	34.59	88.87	1.13
40	34.75	88.88	1.24
45	34.74	88.89	1.35
50	34.73	88.89	1.35
55	34.73	88.90	1.46
60	34.72	88.90	1.46
65	34.74	88.91	1.58
70	34.73	88.91	1.58
75	34.74	88.91	1.58
80	34.74	88.92	1.69
85	34.74	88.92	1.69
90	34.74	88.92	1.69
95	34.76	88.92	1.69
100	34.76	88.93	1.80
105	34.77	88.93	1.80
110	34.78	88.92	1.69
115	34.78	88.92	1.69
120	34.78	88.93	1.80
125	34.79	88.93	1.80
130	34.80	88.93	1.80
135	34.78	88.93	1.80
140	34.79	88.93	1.80
145	34.80	88.93	1.80
150	34.78	88.93	1.80

B2: Sample 12 TGA CO_2 Adsorption Raw Data

Table B2-1: TGA Raw Data for CO_2 Adsorption of Sample 12A, 25 ºC and 60 mL/min

Adsorption Time (min)	Temperature (ºC)	Weight %	Cumulative Adsorption Capacity (gCO_2/kg Ads)
0	96.35	83.03	0.00
5	77.87	83.10	0.84
10	64.48	83.16	1.56
15	54.52	83.23	2.41
20	46.99	83.30	3.25
25	41.27	83.36	3.97
30	36.84	83.41	4.57
35	33.38	83.46	5.17
40	30.66	83.51	5.76
45	28.49	83.55	6.24
50	26.76	83.59	6.72
55	25.46	83.62	7.08
60	24.82	83.67	7.68
65	24.84	83.71	8.28
70	24.84	83.70	8.04
75	24.83	83.78	8.99
80	24.83	83.81	9.35
85	24.82	83.83	9.59
90	24.82	83.85	9.83
95	24.83	83.87	10.07
100	24.81	83.89	10.31
105	24.82	83.91	10.55
110	24.82	83.92	10.67
115	24.82	83.94	10.90
120	24.82	83.95	11.02
125	24.82	83.96	11.14
130	24.83	83.97	11.26
135	24.83	83.98	11.38
140	24.83	83.98	11.38
145	24.83	83.99	11.50
150	24.83	84.00	11.62
155	24.83	84.01	11.74
160	24.83	84.01	11.74
165	24.83	84.02	11.86
170	24.84	84.02	11.86

Table B2-2: TGA Raw Data for CO_2 Adsorption of Sample 12A, 35 ºC and 45 mL/min

Adsorption Time (min)	Temperature (ºC)	Weight %	Cumulative Adsorption Capacity (gCO_2/kg Ads)
0	102.09	83.11	0.00
5	82.83	83.16	0.60
10	68.62	83.23	1.44
15	57.95	83.28	2.04
20	49.81	83.34	2.76
25	43.55	83.40	3.36
30	38.71	83.45	4.08
35	35.01	83.48	4.44
40	34.80	83.55	5.28
45	34.83	83.60	5.88
50	34.83	83.64	6.36
55	34.82	83.67	6.72
60	34.81	83.71	7.19
65	34.81	83.73	7.43
70	34.79	83.76	7.79
75	34.79	83.78	8.03
80	34.78	83.80	8.27
85	34.78	83.82	8.51
90	34.77	83.83	8.63
95	34.75	83.85	8.87
100	34.74	83.86	8.99
105	34.74	83.88	9.22
110	34.71	83.83	8.63
115	34.72	83.84	8.75
120	34.73	83.85	8.87
125	34.73	83.85	8.87
130	34.74	83.86	8.99
135	34.75	83.86	8.99
140	34.75	83.86	8.99
145	34.75	83.87	9.10
150	34.75	83.87	9.10
155	34.76	83.87	9.10

Table B2-3: TGA Raw Data for CO_2 Adsorption of Sample 12A, 45 ºC and 60 mL/min

Adsorption Time (min)	Temperature (ºC)	Weight %	Cumulative Adsorption Capacity (gCO_2/kg Ads)
0	88.63	83.98	0.00
5	72.77	84.06	0.95
10	61.16	84.13	1.78
15	52.46	84.20	2.62
20	45.88	84.26	3.33
25	44.62	84.34	4.28
30	44.61	84.40	4.99
35	44.63	84.44	5.46
40	44.64	84.48	5.94
45	44.63	84.51	6.29
50	44.61	84.54	6.65
55	44.59	84.56	6.88
60	44.56	84.59	7.24
65	44.51	84.62	7.59
70	44.50	84.63	7.71
75	44.56	84.62	7.59
80	44.60	84.62	7.59
85	44.61	84.62	7.59
90	44.62	84.62	7.59
95	44.65	84.61	7.47
100	44.63	84.63	7.71
105	44.63	84.64	7.83
110	44.63	84.64	7.83
115	44.63	84.64	7.83
120	44.63	84.65	7.95
125	44.63	84.65	7.95
130	44.63	84.65	7.95
135	44.63	84.66	7.95
140	44.63	84.66	8.07

Table B2-4: TGA Raw Data for CO_2 Adsorption of Sample 12A, 35 ºC and 75 mL/min

Adsorption Time (min)	Temperature (ºC)	Weight %	Cumulative Adsorption Capacity (gCO_2/kg Ads)
0	90.30	82.75	0.00
5	73.64	82.82	0.85
10	61.52	82.89	1.69
15	52.48	82.97	2.66
20	45.60	83.05	3.62
25	40.26	83.10	4.22
30	36.08	83.15	4.82
35	34.82	83.20	5.42
40	34.81	83.24	5.90
45	34.82	83.28	6.39
50	34.83	83.31	6.75
55	34.84	83.33	6.99
60	34.84	83.36	7.35
65	34.85	83.37	7.47
70	34.85	83.38	7.59
75	34.86	83.39	7.71
80	34.85	83.40	7.83
85	34.84	83.40	7.83
90	34.83	83.40	7.83
95	34.82	83.41	7.95
100	34.83	83.42	8.07
105	34.83	83.43	8.19
110	34.84	83.44	8.19
115	34.85	83.44	8.31
120	34.84	83.45	8.43
125	34.85	83.45	8.43
130	34.84	83.45	8.43
135	34.84	83.46	8.55
140	34.84	83.46	8.55
145	34.84	83.47	8.67
150	34.84	83.47	8.67

B3: Sample 12 Custom Built CO_2 Adsorption Raw Data

Table B3-1: Custom Built CO_2 Equipment Raw Data for CO_2 Adsorption of Chitosan, 25 ºC and 50 mL/min

Adsorption Time (s)	**Y, CO_2 out**	**Q, CO_2 ads (ml/min)**	**m, CO_2 ads (g/min)**	**CO_2 adsorbed (g/g ads)**
0	0.15	0.00	0.00	0.00
5	0.15	0.18	0.00	0.00
10	0.14	0.70	0.00	0.01
15	0.13	1.38	0.00	0.03
20	0.11	2.26	0.00	0.07
25	0.10	3.05	0.01	0.11
30	0.08	3.92	0.01	0.17
35	0.08	4.27	0.01	0.22
40	0.07	4.32	0.01	0.26
45	0.08	4.07	0.01	0.27
50	0.09	3.72	0.01	0.28
55	0.10	3.16	0.01	0.26
60	0.11	2.74	0.00	0.24
65	0.12	2.10	0.00	0.20
70	0.13	1.66	0.00	0.17
75	0.13	1.38	0.00	0.15
80	0.14	1.04	0.00	0.12
85	0.14	0.81	0.00	0.10
90	0.14	0.64	0.00	0.09
95	0.15	0.47	0.00	0.07
100	0.15	0.35	0.00	0.05
105	0.15	0.24	0.00	0.04
110	0.15	0.18	0.00	0.03
115	0.15	0.18	0.00	0.03
120	0.15	0.12	0.00	0.02
125	0.15	0.12	0.00	0.02
130	0.15	0.06	0.00	0.01
135	0.15	0.06	0.00	0.01
140	0.15	0.06	0.00	0.01
145	0.15	0.06	0.00	0.01
150	0.15	0.00	0.00	0.00

Appendix C: Chitosan/MWCNTs Adsorption Results

C1: Preliminary TGA CO_2 Adsorption Raw Data

Table C1-1: TGA Raw Data for CO_2 Adsorption of MWCNTs, 45 ºC and 60 mL/min

Adsorption Time (min)	**Temperature (ºC)**	**Weight %**	**Cumulative Adsorption Capacity (gCO_2/kg Ads)**
0	49.41	99.83	0.00
1	48.50	99.84	0.10
2	47.61	99.85	0.20
3	46.78	99.85	0.20
4	45.98	99.85	0.20
5	45.24	99.85	0.20
6	44.63	99.84	0.10
7	44.10	99.85	0.20
8	44.09	99.85	0.20
9	44.32	99.85	0.20
10	44.35	99.85	0.20
11	44.28	99.85	0.20
12	44.27	99.86	0.30
13	44.31	99.86	0.30
14	44.32	99.86	0.30
15	44.30	99.86	0.30
16	44.30	99.86	0.30
17	44.31	99.86	0.30
18	44.30	99.86	0.30
19	44.30	99.86	0.30
20	44.30	99.86	0.30
21	44.30	99.87	0.40

Table C1-2: TGA Raw Data for CO_2 Adsorption of Chitosan/MWCNTs, 45 ºC and 60 mL/min

Adsorption Time (min)	Temperature (ºC)	Weight %	Cumulative Adsorption Capacity (gCO_2/kg Ads)
0	90.98	98.56	0.00
5	76.03	98.59	0.30
10	65.17	98.63	0.71
15	57.03	98.66	1.01
20	50.84	98.69	1.32
25	46.05	98.72	1.62
30	44.40	98.76	2.03
35	44.37	98.79	2.33
40	44.36	98.80	2.43
45	44.35	98.81	2.53
50	44.35	98.82	2.64
55	44.35	98.83	2.74
60	44.35	98.83	2.74
65	44.35	98.84	2.84
70	44.36	98.85	2.94
75	44.36	98.85	2.94
80	44.36	98.85	2.94
85	44.37	98.86	3.04
90	44.39	98.88	3.24
95	44.41	98.85	2.94
100	44.41	98.85	2.94
105	44.43	98.85	2.94
110	44.42	98.85	2.94
115	44.43	98.85	2.94
120	44.44	98.85	2.94
125	44.44	98.85	2.94
130	44.44	98.84	2.84
135	44.44	98.84	2.84
140	44.43	98.84	2.84
145	44.43	98.85	2.94
150	44.44	98.85	2.94

C2: Custom Built CO_2 Adsorption Equipment Raw Data

Table C2-1: Custom Built CO_2 Equipment Raw Data for CO_2 Adsorption of MWCNTs, 25 ºC and 50 mL/min

Adsorption Time (s)	**Y, CO_2 out**	**Q, CO_2 ads (ml/min)**	**m, CO_2 ads (g/min)**	**CO_2 adsorbed (g/g ads)**
0	0.16	0.00	0.00	0.00
5	0.15	0.24	0.00	0.00
10	0.14	0.87	0.00	0.03
15	0.12	2.10	0.00	0.09
20	0.10	3.21	0.01	0.19
25	0.08	3.93	0.01	0.29
30	0.08	3.93	0.01	0.35
35	0.09	3.52	0.01	0.37
40	0.10	3.00	0.01	0.36
45	0.11	2.37	0.00	0.32
50	0.12	1.77	0.00	0.26
55	0.13	1.27	0.00	0.21
60	0.14	0.93	0.00	0.17
65	0.14	0.64	0.00	0.12
70	0.15	0.47	0.00	0.10
75	0.15	0.35	0.00	0.08
80	0.15	0.29	0.00	0.07
85	0.15	0.18	0.00	0.04
90	0.15	0.12	0.00	0.03
95	0.15	0.12	0.00	0.03
100	0.15	0.12	0.00	0.04
105	0.15	0.06	0.00	0.02
110	0.15	0.06	0.00	0.02
115	0.15	0.06	0.00	0.02
120	0.15	0.06	0.00	0.02
125	0.15	0.06	0.00	0.02
130	0.15	0.06	0.00	0.02
135	0.15	0.06	0.00	0.02
140	0.15	0.06	0.00	0.02
145	0.15	0.06	0.00	0.02
150	0.16	0.00	0.00	0.00

Table C2-2: Custom Built CO_2 Equipment Raw Data for CO_2 Adsorption of Chitosan/MWCNTs, 25 ºC and 50 mL/min – Run 1

Adsorption Time (s)	Y, CO_2 out	Q, CO_2 ads (ml/min)	m, CO_2 ads (g/min)	CO_2 adsorbed (g/g ads)
0	0.15	0.00	0.00	0.00
5	0.15	0.00	0.00	0.00
10	0.15	0.00	0.00	0.00
15	0.15	0.00	0.00	0.00
20	0.15	0.00	0.00	0.00
25	0.15	0.00	0.00	0.00
30	0.15	0.00	0.00	0.00
35	0.15	0.00	0.00	0.00
40	0.15	0.00	0.00	0.00
45	0.15	0.00	0.00	0.00
50	0.15	0.00	0.00	0.00
55	0.15	0.00	0.00	0.00
60	0.15	0.00	0.00	0.00
65	0.15	0.00	0.00	0.00
70	0.15	0.00	0.00	0.00
75	0.15	0.18	0.00	0.00
80	0.14	0.70	0.00	0.02
85	0.12	1.71	0.00	0.08
90	0.11	2.58	0.00	0.15
95	0.09	3.47	0.01	0.26
100	0.08	4.07	0.01	0.36
105	0.08	4.27	0.01	0.44
110	0.08	4.12	0.01	0.49
115	0.09	3.72	0.01	0.50
120	0.10	3.16	0.01	0.47
125	0.11	2.63	0.00	0.43
130	0.12	2.04	0.00	0.36
135	0.13	1.60	0.00	0.31
140	0.13	1.21	0.00	0.25
145	0.14	0.93	0.00	0.21
150	0.14	0.70	0.00	0.17
155	0.15	0.53	0.00	0.13
160	0.15	0.35	0.00	0.09
165	0.15	0.29	0.00	0.08
170	0.15	0.18	0.00	0.05

175	0.15	0.18	0.00	0.06
180	0.15	0.12	0.00	0.04
185	0.15	0.06	0.00	0.02
190	0.15	0.06	0.00	0.02
195	0.15	0.06	0.00	0.02
200	0.15	0.06	0.00	0.02
205	0.15	0.00	0.00	0.00

Table C2-2: Custom Built CO_2 Equipment Raw Data for CO_2 Adsorption of Chitosan/MWCNTs, 25 ºC and 50 mL/min – Run 2

Adsorption Time (s)	**Y, CO_2 out**	**Q, CO_2 ads (ml/min)**	**m, CO_2 ads (g/min)**	**CO_2 adsorbed (g/g ads)**
0	0.15	0.00	0.00	0.00
5	0.15	0.00	0.00	0.00
10	0.15	0.00	0.00	0.00
15	0.15	0.00	0.00	0.00
20	0.15	0.00	0.00	0.00
25	0.15	0.00	0.00	0.00
30	0.15	0.00	0.00	0.00
35	0.15	0.00	0.00	0.00
40	0.15	0.00	0.00	0.00
45	0.15	0.00	0.00	0.00
50	0.15	0.00	0.00	0.00
55	0.15	0.00	0.00	0.00
60	0.15	0.00	0.00	0.00
65	0.15	0.12	0.00	0.00
70	0.14	0.58	0.00	0.00
75	0.13	1.27	0.00	0.02
80	0.12	2.15	0.00	0.06
85	0.10	2.89	0.01	0.13
90	0.09	3.72	0.01	0.22
95	0.07	4.27	0.01	0.32
100	0.07	4.41	0.01	0.39
105	0.07	4.36	0.01	0.45
110	0.08	4.12	0.01	0.49
115	0.09	3.72	0.01	0.50
120	0.09	3.26	0.01	0.48

125	0.11	2.68	0.00	0.44
130	0.11	2.20	0.00	0.39
135	0.12	1.88	0.00	0.36
140	0.13	1.49	0.00	0.31
145	0.13	1.10	0.00	0.24
150	0.14	0.93	0.00	0.22
155	0.14	0.70	0.00	0.18
160	0.14	0.53	0.00	0.14
165	0.15	0.41	0.00	0.12
170	0.15	0.35	0.00	0.10
175	0.15	0.24	0.00	0.07
180	0.15	0.18	0.00	0.06
185	0.15	0.18	0.00	0.06
190	0.15	0.12	0.00	0.04
195	0.15	0.12	0.00	0.04
200	0.15	0.06	0.00	0.02
205	0.15	0.06	0.00	0.02
210	0.15	0.06	0.00	0.02
215	0.15	0.06	0.00	0.03
220	0.15	0.06	0.00	0.03
225	0.15	0.00	0.00	0.00

Appendix D: Plagiarism Report

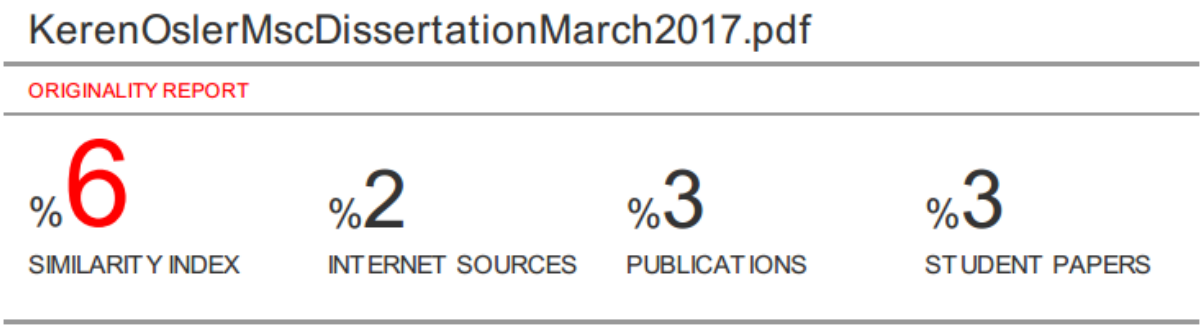

KerenOslerMscDissertationMarch2017.pdf

ORIGINALITY REPORT

%6	%2	%3	%3
SIMILARITY INDEX	INTERNET SOURCES	PUBLICATIONS	STUDENT PAPERS

Appendix E: Publication

The publications are attached on the next page.